博士論文

Quantum Approaches to the Modeling of Stock Markets

The Recovery of Stylized Facts with Quantum Oscillators

（株式市場のモデル化に対する量子的アプローチ

- 量子振動子による定型化された事実の再現 - ）

高　婷婷

Quantum Approaches to the Modeling of Stock Markets

The Recovery of Stylized Facts with Quantum Oscillators

(株式市場のモデル化に対する量子的アプローチ -量子振動子による定型化された事実の再現-)

TINGTING GAO
高　婷婷

Department of Human and Engineered Environmental Studies
Graduate School of Frontier Sciences
The University of Tokyo
東京大学大学院　新領域創成科学研究科　人間環境学専攻

July 2017

Abstract

This doctoral dissertation presents my work in the past three years as a PhD student. It describes the motivation, objectives, methods, results and enlightenment of my research about quantum approaches to the modeling of stock markets.

Physical modeling, as well as mathematical analysis, has become a indispensable tool in financial studies. When the mathematical methods pay attention to the phenomenological behaviors of historical economic data, the physical models shed more light on the microscopic mechanics of the economic systems. The coin of the word "econophysics" in the mid-1990s started the official union of physics and economics. The major tool for the modeling of financial markets in econophysics, including stock markets, is stochastic processes from statistical physics. Although large number of differently developed stochastic models have succeeded in describing the market variables such as stock price, return volatility and trading volume, the underlying mechanics was rarely discussed. Agent-based models (ABMs) simulate the markets on the basis of some microscopic rules predefined, has also become popular with the development of computational technology. Both of these two methods are time-consuming due to thousands of steps of simulation. On the other hand, quantum mechanics has been becoming a novel alternate for financial study with the expectation to overcome the before mentioned defects. In this dissertation, we propose quantum approaches to explain two of the most important stylized facts of the stock markets: leptokurtic distributions of price return and volatility clustering, as well as some discussions about another one - volume/volatility correlation.

In quantum models, the stock price is described wave functions instead of a series of numbers. The uncertainty in the stock price makes it possible to apply squared wave function as the probability density function (PDF) of price return. The dynamics of wave function is described by Schrodinger equation (SE), which can be reduced to a time-independent version as the eigen equation of energy for the stationary markets with invariant Hamiltonian. Different from the previous quantum studies that applied a quantum harmonic oscillator potential directly, we proposed a financially interpretable Hamiltonian of a harmonic or anharmonic oscillator for stationary market, by analyzing the instantaneous order excess in the market. It is demonstrated that the introduction of

a quartic term in the potential as a measurement of the risk aversion brought PDF with sharper peak and heavier tails. The concept of energy levels can convincingly explain the different shapes of PDFs for the data with different frequencies. In addition, the generality of the potential which is derived from the mechanics of the stock price makes the model applicable to illiquid markets such as trend following dominant market (TFDM). In order to verify the theoretical results of the quantum model for TFDM, we suggest a simplified method to filter data for the moments when the the market is dominated by trend followers. The statistics of the filtered data can be well modeled by the quantum model.

In the study of the dynamics of stock price, we use expected time series of price return and volatility to study the certainty in the stock. It is firstly confirmed that the autocorrelation of volatility in price return is retained in the expected time series, which makes the study of expected time series reasonable. Taking trading volume as a measurement of the energy for stock price, we can successfully recover volatility clustering by modeling the dynamics of energy level or potential respectively. GARCH model is included as a special case in our quantum model. A quantitative correlation between volatility and volume is obtained as a by-product.

The content of this dissertation is organized as follows. In Chapter 1, the background including fundamental knowledge of stock markets and quantum mechanics is introduced, followed by the objectives of this thesis. Chapter 2 proposes a stationary quantum oscillator model to describe the stock price with reasonable financial interpretation. It is demonstrated that this model can recover the leptokurtic distributions of price return without noise term that is indispensable in classical models. The parameters of the model are adjusted to the real market data in Chapter 3, where an original data filtering method is proposed for illiquid market that is unstable and rarely observed in reality. In Chapter 4, the stationary model is extended to a dynamical one, in order to study the stylized facts - the zero autocorrelations of price return and the positive autocorrelation of volatility. Conclusions and future plans are addressed in Chapter 5. I hope this work can be a contribution to the quantum modeling of stock markets.

Acknowledgements

I would like firstly to express my sincere gratitude to my supervisor Professor Yu Chen for his continuous support through my Ph.D studies. Finance and economics was a brand new field to me when I started this work. I have had to overcome the disappointment at the slow process of my research in the first few months. Some of my thinking and working patterns do not fit the new interdisciplinary field of nature and social science. Thanks to Prof. Chen' patience, kindness and encouragement. I was always inspirited by his illuminating advices on my research. He was always glad to share the brilliant tips on doing research.

Thanks to all the members in Chen Lab. They gave me some valuable suggestions on my research. Moreover, they were kindly enough to provide me a relaxed and homelike atmosphere in the office.

Thanks to the thesis defense committee, Prof. Ohashi, Prof. Izumi, Prof. Sasaki, Prof. Hashimoto, and Prof. Chen. Thanks to their time to read the manuscript of my thesis and listen to my presentation, as well as their kind and valuable advice.

I must greatly appreciate the financial support from China Scholarship Council.

Last but not the least, I would like to thank my parents for their support financially and morally in the past years of my life.

Contents

List of Tables

List of Figures

Chapter 1

Introduction

1.1 Econophysics

Financial market, as a consisting part of the modern financial system, is not only related to the operations of the governments, organizations, companies, etc, but also concerned to individuals. More and more individuals have began to take part into the financial market in different kinds of ways. In order to make a profit or at least to prevent from losing money, the market participants have been pursuing the patterns of the market, if they are existed, for over a hundred years. However, the pursuit itself, as well as the complex internal structure of the market, makes the market more complicated and more indeterminate.

Although there is a lack of a general theory, a large number of well established methods have been applied to the study of financial markets for different purposes [*Bachelier*, 1964; *Challet et al.*, 2005; *Cont*, 2001; *Johnson et al.*, 2003; *Francq and Zakoian*, 2010]. Those methods can be briefly classified into two types - phenomenological modeling and structural modeling. The phenomenological modeling focuses on the statistical behaviors of the financial variables such as stock price, return volatility and trading volume [*Gopikrishnan et al.*, 1999; *Plerou et al.*, 1999; *Liu et al.*, 1999; *Preis et al.*, 2011]. The historical time series of these variables provide all the information that is needed for the

study of past and the prediction of future. Based on the idea that the market is too complex to be modeled precisely, the phenomenological analysis is practical in trading. On the other hand, the structural modeling, specially meaning ABMs, concentrates itself on the microscopic structures of the market [*Challet and Zhang*, 1997, 1998; *Challet and Marsili*, 1999; *Challet et al.*, 2001; *Challet and Marsili*, 2003]. It predefines the structure and some trading rules of the market, leaving the rest things to the computer.

Mathematics has been the major tool in dealing with mass of financial data since the 17th century. Statistical methods help the economists to describe the historical behaviors of financial variables, assist the government and financial organization to draft economic plans, and help the investors to make decisions. Physical methods have become another alternative for economic studies since the born of Econophysics in the mid-1990s [*Mantegna and Stanley*, 1999, 1995]. Different from the statistical methods that devoted themselves to the phenomenological behaviors of the economy, physical methods concerns more about the mechanics of financial markets [*Takayasu et al.*, 2006; *Mizuno et al.*, 2007; *Huang*, 2015]. In the past decades, econophysics has highly developed with continuous emergence of inspiring works. Universal power law was quantitatively confirmed with in different markets [*Mantegna and Stanley*, 1995; *Ohnishi et al.*, 2004; *Zhang et al.*, 2007]. Random walk models [*Scalas*, 2006], random matrix theory [*Sharifi et al.*, 2004; *Daly et al.*, 2008] and path integral method [*Linetsky*, 1998; *Cassagnes et al.*, 2014] that originated from physics have been applied to modeling economic systems. Novel experimental methods were introduced by some econophysicists for market modeling [*Huang*, 2015]. Some of the physically modeling method have been successfully realized in practice, such predicting the trend of market price [*Takayasu et al.*, 2006; *Mizuno et al.*, 2007; *Takayasu et al.*, 2007] and managing portfolios [*Sharifi et al.*, 2004; *Daly et al.*, 2008].

Although there is some criticism from traditional economists, it is acknowledged that economy has benefited quite a lot from the works of the econophysicists [*Buchanan*, 2013]. Some of the contributions are listed below.

- Stylized facts [*Farmer et al.*, 2005] of financial markets were quantitatively estab-

lished.

- ABMs as visualized simulation demonstrated the internal mechanics in the formation of the heavy tails, and can even be realized by experiments [*Huang*, 2015].
- Similarity between the dynamics of markets and the behavior of other natural phenomena such as earthquake was discovered [*Lillo and Mantegna*, 2003].
- The relationship of market efficiency and stability were deeply studied by the analysis of leverage [*Thurner et al.*, 2010] and information completeness [*Caccioli and Marsili*, 2010].
- Econophysicists tried to develop networks, which has been popular in modeling complex systems, to uncover the mystery of the complex financial markets.

1.2 Quantum finance

1.2.1 Overview of quantum mechanics

Quantum mechanics, as one of the two greatest discoveries of physics in the 20th century, is founded on the basis of a series of experimental and theoretical studies on the fundamental particles. In 1900, Max Planck proposed a formula for the blackbody radiation, i.e. Planck's Law, which fitted the experimental results perfectly. However, this formula can only be obtained under the assumption that the energy of light is quantized, which is contradicted with our intuition and even our mastered physical logic. Inspired by the idea of quantized energy, Albert Einstein successfully explained the photoelectric effect in 1905. Then in 1913, Niels Bohr discovered the quantized structure of hydrogen atom. The unprecedented theory grew explosively in the first 30 years of the 20th century attributed to the effort of dozens of genius physicists, such as Louis de Broglie and Erwin Schrodinger as the founders of wave mechanics, Werner Heisenberg, Max Born and Pascual Jordan who developed matrix mechanics.

Quantum mechanics was started from the problem of blackbody radiation and photoelectric effect. One of the fundamental hypotheses is thus introduced, i.e. the quantization of the photon energy. The energy quantum is scaled by a constant, saying Planck's constant denoted as $h \approx 6.626 \times 10^{-34} J \cdot s$ (reduced Planck's constant is more widely used as $\hbar = h/2\pi$). This constant is the key in de Broglie's hypothesis that all matter has a wave-like nature with a wavelength as $\lambda = h/p$, where p is the momentum of the matter and h is the Planck's constant. The macroscopic matter seems no wavy because its momentum is quite large, which together with the small value of h makes the wavelength much smaller than the size of the matter. However, the case is different for fundamental particles such as electron. Electron behaves like a wave similarly to photon. Thus the classical Newtonian description becomes useless in the atoms. We have to describe a microscopic matter in a wave frame. Schrodinger discovered the equation for the dynamics of those waves (Schrodinger equation). But the physical nature of these waves is obviously different from the waves in ocean. Born interpreted this kind wave as probability wave. More specifically, a wave function whose dynamics is described by SE is denoted as wave function $\Psi(x,t)$, and the probability to find the corresponding particle between x and $x+dx$ at time t is $|\Psi(x,t)|^2 dx$. Based on these hypotheses, the building of quantum physics was constructed in the last century.

Although the theory of quantum physics is still under development due to its complexity and inscrutability, it has been playing an important role in not only various physical studies but also different kinds of disciplines such as chemistry, biology and even social science.

1.2.2 Application of quantum mechanics into finance

Statistical physics became the major resource for the methodologies of econophysics because that it deals with physical systems of high complexity which can be considered similar to the economic systems. With the development of econophysics, physical theories other than statistical physics have attracted the attention of econophysicists in the

past decades. Among those theories, quantum mechanics, born to study the microscopic physical world, has attracted our attention due to its novel wave-particle consideration of the world where the financial market is obviously included. For example, B. Baaquie systematically explained the path integral method for option pricing in his book [*Baaquie*, 2004], while M. Schaden tried to use wave functions of cash and security to describe the state of a financial market [*Schaden*, 2002].

The feasibility of applying quantum mechanics into finance and other social science has been discussed a lot. One of the universally accepted argument is that we consider all the complex systems no matter physical systems or social ones as just quantum-like [*Khrennikov*, 2010; *Haven and Khrennikov*, 2013], which means their collective behaviors can be described by quantum theory. It does not intend to debate on the nature of these different kinds of problems, but just to apply the same set of mathematical formula to help find out the truth underlying. This can not be blamed since not only quantum models but also the classical ones have been developed on the basis of similar assumptions. However, with the development of the quantum biology and quantum social science, it is recognized that there may be some essential links between the social science and quantum mechanics. Physicist Ettore Majorana coined similar idea in the early developing stage of quantum mechanics [*Mantegna*, 2005], which was not uncovered until 1942 and have been rarely mentioned since its publication. Based on the view that the statistical laws are shared in physics and social science, Majorana considered philosophical aspects related to the nature and value of deterministic and statistical laws in science. Here comes the thinking that quantum mechanics may be more appropriate for social science than the classical mechanics because the former two are naturally related.

1.3 Stylized facts of stock markets

A stock market, as well as other financial markets, provides a great number of information every day. Besides, there exist different markets all around the world. Millions of shares

for thousands of stocks are traded by different individuals, agents and companies. For general analysis, market index is proposed for a global view of the market. A market index is designed to reflect the main behavior of the corresponding market by synthesizing the shares of prominent companies in the stock exchange market. For example, Nikkei 225 is a stock index based on the trading shares of the most important companies in Tokyo Stock Exchange (TSE), and SSE Composite Index is for all stocks traded in Shanghai Stock Exchange while S&P 500 is an American one.

1.3.1 Time series of stock price and price return

For global understanding, we focus on the universal stylized facts of the stock markets in this dissertation.

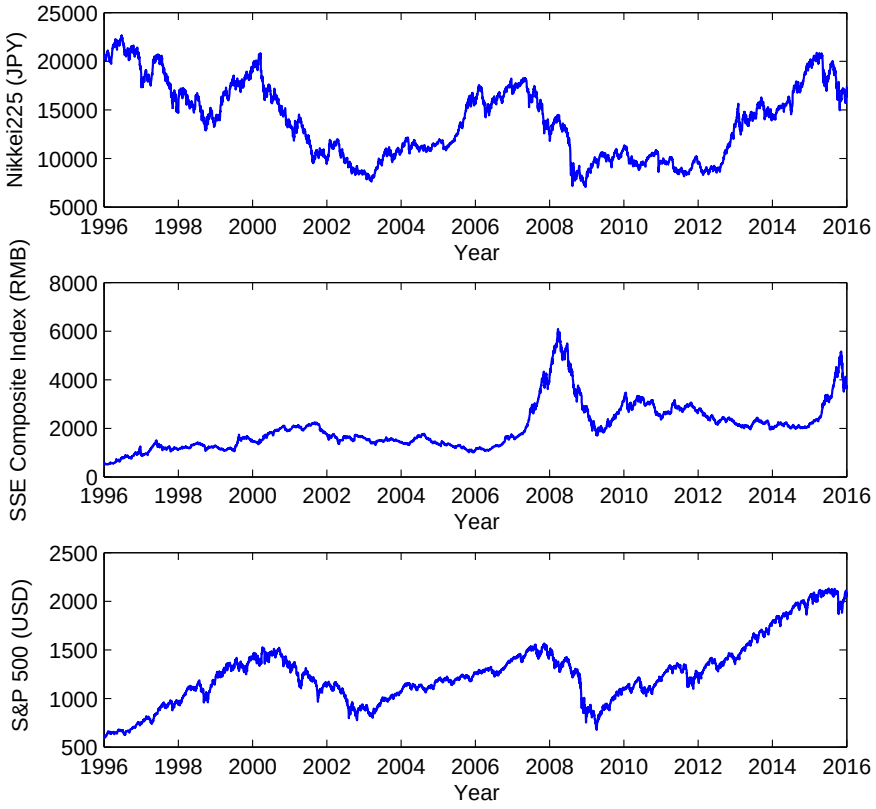

Figure 1.1: Daily series of Nikkei225, SSE Composite Index and S&P 500 respectively, from the year of 1996 to 2016.

Our studies are based on the numerous recorded data of stock markets, among which the trading price is one of the most important and the most widely studied item. Figure 1.1 plots the time series of index price for Nikkei 225, SSE Composite Index and S&P 500 respectively. It seems that the moving patterns are completely different for the three different indices. During the twenty years from 1996 to 2016, Nikkei 225 experienced two distinct periods of rising and two periods of declining, SSE Composite Index has going up gradually except for a hump around 2008, while S&P 500 behaves like waves. Further observation indicates some similarity among those price series of different markets. It is shown that the declining trends from 2000 to 2002 appears both in Nikkei 225 and S&P 500, which can be attributed to the IT bubble. In addition, the American subprime mortgage crisis caused the crashes in all the three markets around 2008.

In order to quantify this kind of similarities, price return (1.1) or log-return (1.2) is defined for the analysis of stock or index price [*Johnson et al.*, 2003],

$$r(t, \Delta t) = \frac{p(t) - p(t - \Delta t)}{p(t - \Delta t)}, \tag{1.1}$$

$$z(t, \Delta t) = \lg p(t) - \lg p(t - \Delta t), \tag{1.2}$$

where $p(t)$ is the stock price at time t and Δt is the time interval. Although log-return is more frequently used in practice, the price return (1.1) will be applied in this dissertation for the convenience of introducing the financial interpretation of our model.

The index price series in Figure 1.1 are transformed into return series and plotted in Figure 1.2. It is shown that although the price series of Nikkei 225 and S&P 500 are much different, the corresponding price return series share the similar pattern. Consistently with the crashes in the price series, the price return fluctuates frequently from the year 2000 to 2002 and violently around 2008. On the other hand, the fluctuating pattern for SSE Composite seems quite different from the other two. It seems that the Japanese and American markets may have similar structure while the Chinese market is still in its early age.

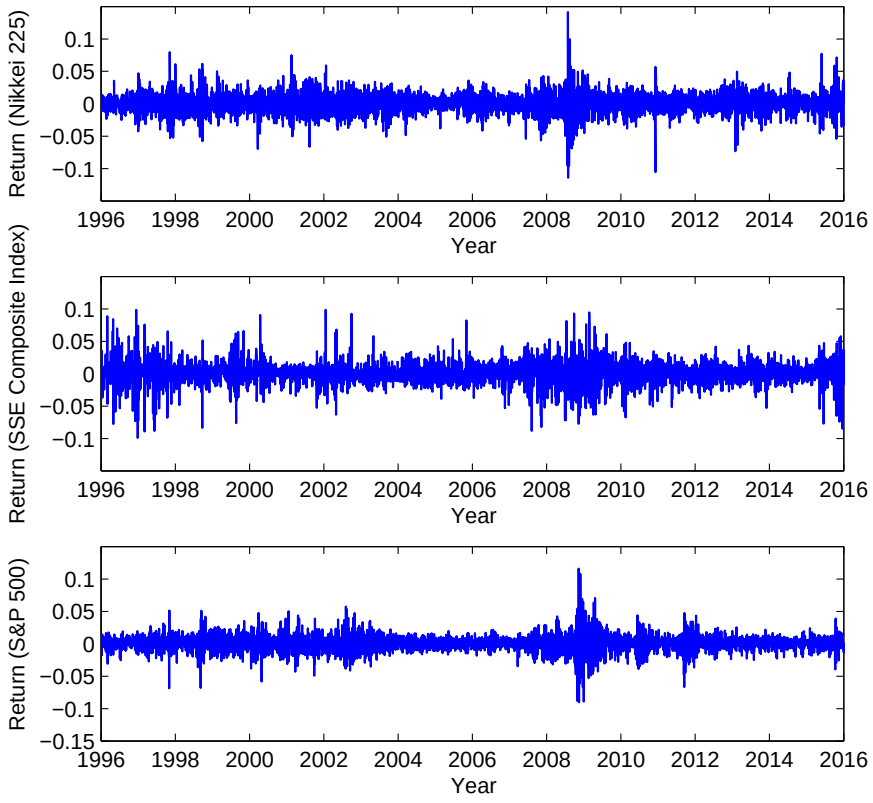

Figure 1.2: Daily series of index return for Nikkei 225, SSE Composite Index and S&P 500 from 1996 to 2016 respectively. The fluctuations for Nikkei 225 and S&P 500 behave similar while that for SSE Composite Index is of different pattern.

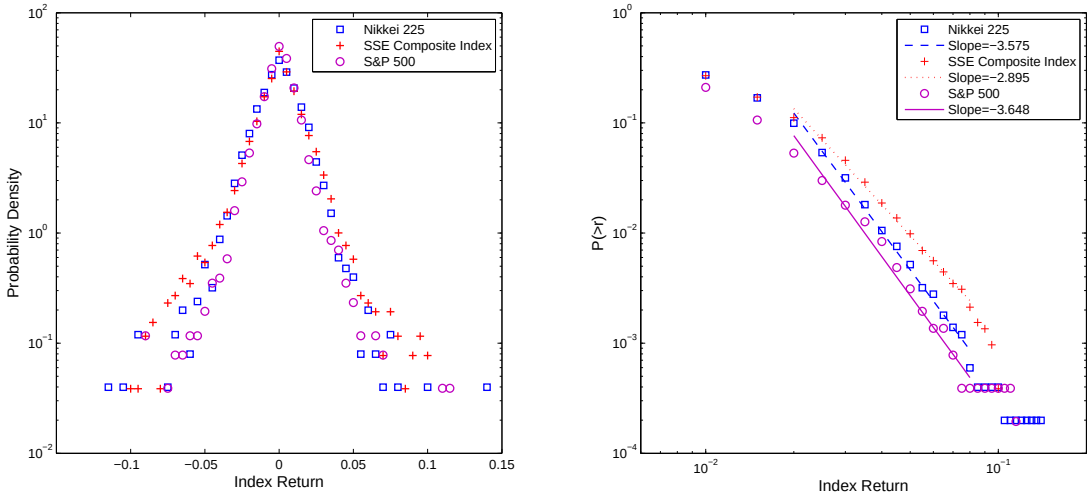

Figure 1.3: Statistically obtained probability distributions of price return for Nikkei 225 , SSE Composite Index and S&P 500.

1.3.2 Leptokurtic distributions of price return

Although the fluctuations of price return seem random for all the indices (and also single stocks), the statistical results of the return series share the characters in common. Figure 1.3 shows the statistical probability densities of price return for different market indices. Although there seems no general pattern in the time series of price return, their statistical results can be described by a Gaussian-like distribution, which is the basis of the standard random walk model. Moreover, all the cumulative probabilities exhibit power laws. The leptokurtic distribution with sharper peak and heavier tails than Gaussian distribution exists not only in the daily market indices, but also in single stocks and the data of different frequencies, i.e. price return calculated from different time intervals such as minute, day and month. As leptokurtic distributions can be observed regardless of the markets or time windows, it is accounted as one of the stylized facts of stock markets (and also financial markets).

1.3.3 Volatility clustering

Another important stylized fact which will be studied in this dissertation is volatility clustering. The concrete meaning of the term volatility clustering is that "large changes tend to be followed by large changes, of either sign, and small changes tend to be followed by small changes" [*Mandelbrot*, 1963]. The average of price change, either positive or negative, representing volatility here, is usually defined by the standard deviation as

$$\sigma = \sqrt{\frac{1}{T-1}\sum_{t=1}^{T}(r(t)-\mu)^2}, \tag{1.3}$$

where μ is the average price return over the time period T. It is common to consider variance σ^2 as a measurement of the volatility. As shown in Figure 1.3, the price series

have mean return around $\mu = 0$. Thus the variance can be reduced to

$$\sigma^2 = \frac{1}{T-1}\sum_{t=1}^{T}|r(t)|^2. \tag{1.4}$$

And we usually study on the instant volatility of the price return as $\sigma_t^2 = |r(t)|^2$.

This stylized fact can be quantitatively described as the fact that the autocorrelations of the squared return (or absolute return) are positive and decaying slowly, while the return itself is uncorrelated. The autocorrelations for time series of price return with increasing time lag are shown in Figure 1.4, where the autocorrelation is calculated by

$$\rho\left[\{x[t]\},\{x[t-\Delta t]\}\right] = \langle (x[t]-\overline{x[t]})(x[t-\Delta t]-\overline{x[t-\Delta t]})\rangle/\sigma^2, \tag{1.5}$$

where $x[t]$ is the value of data sample such as the price return or squared return at time t, σ^2 is the variance of the whole data sample, and $\langle\cdot\rangle$ represents calculation of average.

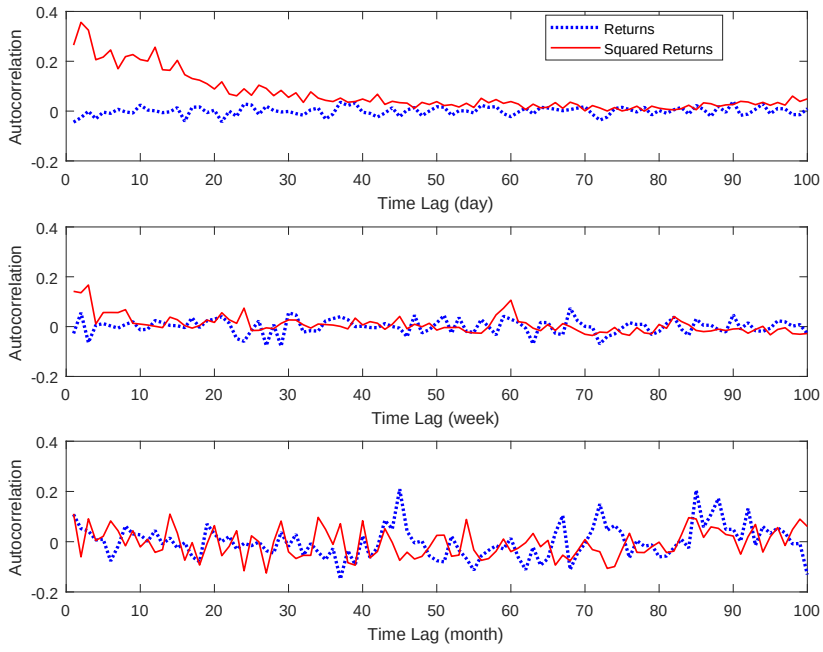

Figure 1.4: Autocorrelation of returns and squared returns for Nikkei 225 in Figure 1.2 with different time lags.

It is found that the autocorrelations of price return are zero, which is the basis for

the utilization of random walk models. The highly frequent data demonstrated that the autocorrelation of asset return decays to insignificance with about 20 minutes [*Cont*, 2001] - short memory that can be neglected for the study of daily data or data with larger time scales. On the other hand, the autocorrelations of squared return (volatility) for daily Nikkei 225 are positive and decay to insignificance until about 1 month. As we study the index data with time scale of one day or longer, we can neglect the autocorrelation of price return and have to take the positive autocorrelation of squared return into account.

There remain other stylized facts besides leptokurtic distributions and volatility clustering, such as leverage effect, gain/loss asymmetry and asymmetry in time scales [*Cont*, 2001], which will not be discussed in this dissertation. But another facts concerning the correlation of volume and volatility will be involved in the quantum modeling of volatility clustering.

1.3.4 Volume/volatility correlation

Trading volume is another key reference for the participants to make decisions. Figure 1.5 shows the trading volume of Nikkei 225 from 2004 to 2017.

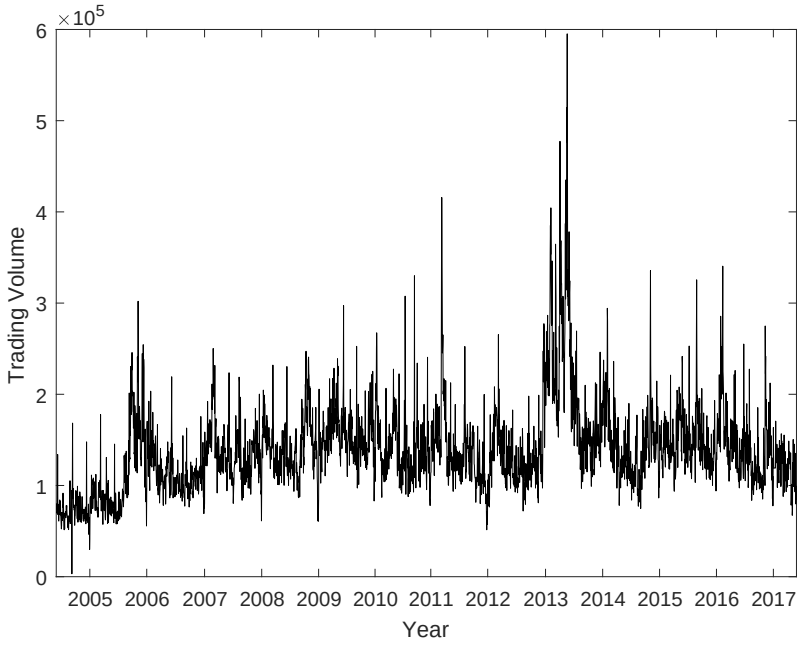

Figure 1.5: Trading volume of Nikkei225 from June 2004 to June 2017.

It is shown that there are consistent fluctuations in the time series just like price return. There are also some universal characters of its statistics, such as pow law in its cumulative distribution and long memory of its series. These characters will not be involved in this dissertation as we focus on price return.

However, the correlation between volume and volatility[*Gallant et al.*, 1992; *Cont*, 2007] as another stylized fact of stock markets, will be discussed. This facts has been much less discussed than leptokurtic distributions or volatility clustering because 1) available data for trading volume is much less than the stock price, which makes the empirical analysis difficult, and 2)there has been no reliable model for the study of volume. In our study, as we will give a physical correspondence of trading volume, the correlation of volume and volatility can be quantitatively modeled in the quantum model.

1.4 Motivation and objectives

It is known that the real markets tend to deviate from the standard random-walk paradigm. The empirical deviations are called the stylized facts of stock markets (financial markets). Two of the most fundamental stylized facts of stock market are the leptokurtosis of price return distributions and volatility clustering, which are the main issues of this dissertation.

The leptokurtic distributions of the price return means that the although the probability distributions of price return can be scaled close to a general distribution, the deviation of them from Gaussian distribution always exists and can not be neglected sometimes.

Based on the previous works on quantum finance and the consideration that quantum mechanics may be closer to the nature of financial markets, we intend to find out whether the uncertainty included in quantum mechanics can be efficiently applied to stock markets and hope to find some hints for the nature of finance.

We will take use of the concept of wave function as the fundamental tool to study the stylized facts (leptokurtic distributions and volatility clustering) in the stock markets.

This study is encouraged by some achievements of previous quantum modeling [*Ye and Huang*, 2008; *Zhang and Huang*, 2010; *Cotfas*, 2013; *Meng et al.*, 2015]. For instance, Ye et al. proposed a quantum harmonic oscillator model in 2008 to explain the persistent fluctuations in stock markets, where the squared modulus of ground state wave function was used as a probability measure of the stock price in stationary market [*Ye and Huang*, 2008]. As the study focused on the dynamics of the stock price under sudden information, no convincible financial interpretation of its Hamiltonian was addressed and one could deplore a lack of comparison between the derived probability distributions and that of the classical models. Zhang et al. explained the financial meaning of the wave function and gave a financial form of the uncertainty principle in 2010 [*Zhang and Huang*, 2010], and Cotfas proposed its discrete version [*Cotfas*, 2013]. Although they demonstrated the feasibility of quantum model by proposing a cosine formed potential, the model did not show any advantage over the quantum harmonic oscillator or the classical random walk.

Thus we list the main objectives of this dissertation.

- Propose a new financially interpretable quantum Hamiltonian for stationary market.
- Describe the stock price with the help of wave functions obtained from the above proposed Hamiltonian and verify it with the analysis of historical time series.
- Extend the stationary model into a dynamical one to recover volatility clustering.
- Discuss the correlation between volume and volatility.

Chapter 2

A Quantum Oscillator Model for Stationary Markets

We propose a quantum model for stationary markets that can be used for the study of the probability distributions of stock price return. As the state of stock price is described by the wave functions of quantum oscillator (both harmonic oscillator and anharmonic one are discussed), we call it the quantum oscillator model for stock markets. This model can be extended into a dynamical one for the study of volatility clustering whose details will be demonstrated in Chapter 4.

In this chapter, we firstly give a overview of the classical modeling results. Then a quantum description of stock price is introduced, followed by financial derivation of the Hamiltonian for the stock price. Finally, the main theoretical results of the quantum model are addressed and summarized.

2.1 Classical modeling of stock price

It is known that the Gaussian-like distribution of price return is a global stylized fact of the stock markets (or financial markets). In addition with the fact that the price returns for different times can be approximately considered uncorrelated, random walk was proposed as the most simple but efficient model for the dynamics of price return. Then Gaussian

distribution (normal distribution) was used to describe the probability distributions of long time scale price series. However, it does not work well for the short time scale series attributed to the leptokurtic characters of the data. Then more complicated models such as Levy stable non-Gaussian model and Student's t-distribution [*Mantegna and Stanley*, 1999] were developed to explains this phenomenon.

Making use of the probability theory of quantum mechanics, it is believed that the probability distribution of stock price can be modeled without the time-consuming random walks. As the wave function itself in quantum mechanics is something closely related to probability, we analogize the motion of stock price to the dynamics of wave function of a quantum particle.

2.2 Quantum description of stock price

2.2.1 Preliminaries of quantum mechanics

Heisenberg uncertainty principle tells us that the two variables represented by non-commuting operators cannot be simultaneously measured. One of the most well known uncertainty relations is that

$$\Delta x \cdot \Delta p \geq \frac{\hbar}{2}, \tag{2.1}$$

which means that in the quantum frame, the position and momentum cannot be of the precise values at the same time. This principle is guaranteed by the idea of wave-particle duality, saying that everything must have a de Broglie wavelength as $\lambda = h/p$ with Plank constant h and momentum p.

The uncertainty is so insignificant in the macroscopic world that it can be just neglected. Thus the determinate theory, Newtonian mechanics, is applicable and satisfying until the day when the scientists go deep into the atomic world. But we must take the uncertainty into account when referring to the microscopic world, where there is no precise trajectory for the particle anymore. Erwin Schrodinger introduced a brand new mechan-

ical equation to describe the dynamics of a microscopic object which is both particle and wave

$$i\hbar\frac{\partial}{\partial t}\Psi\left(\boldsymbol{r},t\right)=\hat{H}(t)\Psi\left(\boldsymbol{r},t\right), \tag{2.2}$$

where $\hat{H}(t)$ is Hamiltonian representing the total energy, $\Psi\left(\boldsymbol{r},t\right)$ is the wave function describing the state of the microscopic object with the position vector $\boldsymbol{r}$ at time t, i is imaginary unit, and $\hbar$ is the reduced Planck constant. Max Born interpreted the wave function as probability amplitude, saying the squared modulus of wave function $\rho(\boldsymbol{r},t)=|\Psi(\boldsymbol{r},t)|^2$ is the probability density of the microscopic object.

For the 1-dimension (1D) situation, the Schrodinger equation can be put as

$$i\hbar\frac{\partial}{\partial t}\Psi\left(x,t\right)=\left(-\frac{\hbar^2}{2m}\nabla^2+\hat{V}(x,t)\right)\Psi\left(x,t\right), \tag{2.3}$$

where ∇^2 is Laplace operator and $\hat{V}(x,t)$ is the potential operator. According to Born's probability wave theory, the probability of finding the object around position x among the small volume element ε at time t is represented by

$$P\left(x-\frac{\varepsilon}{2}\sim x+\frac{\varepsilon}{2}\right)=\rho\left(x,t\right)\cdot\varepsilon=|\Psi\left(x,t\right)|^2\cdot\varepsilon. \tag{2.4}$$

Given an initial state, the 1D partial differential Eq. (2.3) can fully determine the dynamics of wave function. However, the partial differential equations are difficult to be solved. A commonly used method is to reduce it into a time-independent form for stationary Hamiltonian, where the potential operator is not time dependent explicitly. Then the variables x and t can be separated in the wave function as

$$\Psi(x,t)=f(t)\psi(x), \tag{2.5}$$

which can be substituted into Eq. (2.3) to obtain

$$i\hbar\frac{1}{f(t)}\frac{df(t)}{dt}=\frac{1}{\psi(x)}\left[-\frac{\hbar^2}{2m}\nabla^2+V(x)\right]\psi(x)=E, \tag{2.6}$$

where E is a constant. The above equation can then be reduced into

$$\left[-\frac{\hbar^2}{2m}\nabla^2 + V(x)\right]\psi(x) = E\psi(x), \tag{2.7}$$

with

$$\Psi(x,t) = \exp\left(-iEt/\hbar\right)\psi(x). \tag{2.8}$$

Eq. (2.7) is in fact the energy eigen equation of the quantum particle (system). The corresponding solutions are eigen vectors $\{\psi_n(x)\}$ with eigen values $\{E_n\}$. In quantum mechanics, they are named eigen wave function and eigen energy respectively. It is proved that the state of a quantum particle can be fully described by the set of eigen vectors for energy, i.e. represented by the superposition of the eigen wave functions of different energy levels:

$$\Psi(x,t) = \sum_n c_n(t)\psi_n(x), \tag{2.9}$$

where $c_n(t)$ is a time dependent number representing the probability amplitude of nth energy state.

Further more, in quantum mechanics, the observables are represented by operators, such as position operator $\hat{x}$, momentum operator $\hat{p}$ and energy operator $\hat{H}$. The measurement of a observable can then be described by the corresponding operator acting on a quantum state. For example, the measurement of the position of a particle in quantum state $\Psi(x,t)$ results in $\Psi(x,t+\varepsilon) = \hat{x}\Psi(x,t)$.

2.2.2 Wave functions for stock price

Supposing the state of stock price can be analogically described by a wave function instead of absolute price values, we can define a "wave function" for stock price as $\Psi(r,t)$. Here, r is the price return. The dynamics of $\Psi(r,t)$ is similarly determined by SE as

$$i\hbar\frac{\partial}{\partial t}\Psi(r,t) = \hat{H}(r,t)\Psi(r,t). \tag{2.10}$$

In order to obtain the wave functions for stock price, we must figure out the Hamiltonian $\hat{H}(r,t)$. Again we take use the Hamiltonian form from physics

$$\hat{H}(r,t) = -\frac{\hbar^2}{2m}\nabla^2 + \hat{V}(r,t), \tag{2.11}$$

which can be regarded as the "energy operator" of stock price and consists of a kinetic energy operator $-\frac{\hbar^2}{2m}\nabla^2$ and potential energy operator $\hat{V}(r,t)$. Here the price return r can be considered a correspondence of position in physics. $\hbar$ can be regarded as the uncertainty of irrational transaction and m represents the intrinsic properties of the stock such as the capital [*Zhang and Huang*, 2010; *Meng et al.*, 2015]. It is obviously these two variables have different meanings from that in physics. For a stock in a certain market, for example the stock issued by Mitsubishi Corporation at Tokyo Stock Exchange, $\hbar$ and m can be considered constant. Without losing generality, we assume both $\hbar$ and m of unit value in the following context.

Once the form of the Hamiltonian operator is known, the state of the stock price that is fully described by the wave function can be acquired. According to the Hamiltonian operator in Eq. (2.11), the potential part $\hat{V}(r,t)$ is the only variable part in this model, which describes the interaction between the stock and the corresponding markets and even the external information. In our model, it is assumed that the changes of potential is relatively small compared to the internal kinetic energy and the invariant part of the potential when we concern long time horizons. Hence the first step and simplified model is studying the stationary stock market with time-independent potential operator. Then we only need to deal with the time-independent SE for stock price as

$$\left[-\frac{\hbar^2}{2m}\frac{d^2}{dr^2} + V(r)\right]\psi(r) = E\psi(r), \tag{2.12}$$

where E is a real number that can be interpreted as the "energy" of stock (price). The time-dependent wave function is $\Psi(r,t) = \exp(-iEt)\psi(r)$.

In the stock market, before the stock price is measured, we do not know its value in

the next time step even though we have its long history in hand. The classical models have regarded the movement of stock price as stochastic processes. However, no process could predict its movement precisely. An appropriate probability description based on history data is quite satisfying. In our quantum description, the stock price is essentially indeterminate until it is measured (the finish of a deal). Before the "measurement", the stock price return is described by a wave packet whose dynamics is described by SE. Although the price value is uncertain, its probability density function (PDF) is determinate as

$$\rho(r,t) = |\Psi(r,t)|^2. \tag{2.13}$$

For the stationary markets,

$$\rho(r,t) = |\Psi(r,t)|^2 = |e^{(-iEt)}\psi(r)|^2 = |\psi(r)|^2. \tag{2.14}$$

It indicates that the probability distribution of price return for a stock in the stationary market is time independent, which is consistent with the stable processes for classical modeling.

2.3 Hamiltonian of stock price

Several pieces of work concerning the wave function for stock price have been achieved [*Ye and Huang*, 2008; *Ataullah et al.*, 2009; *Zhang and Huang*, 2010; *Cotfas*, 2013; *Meng et al.*, 2015]. Briefly speaking, three types of potentials, i.e. harmonic oscillator, finite well and a cosine formed potential, were applied directly for the Hamiltonian of stock price. However, none of them explained the financial meaning of the Hamiltonians. For instance, Ye et al. considered the probability distributions of stock price as a Gaussian wave packet to explain the persistent fluctuations in stock markets [*Ye and Huang*, 2008]. Moreover, the PDFs they obtained can go no further than Gaussian which itself is not perfect enough for the stock price.

In this section, we will propose a financially interpretable Hamiltonian for the stock price. We analyze the microscopic dynamics of order excess and the macroscopic dynamics of price return respectively. The combination of these two descriptions lead us to the classical potential. It is assumed that the classical potential energy can be corresponded to the quantum potential operator.

2.3.1 Microscopic dynamics of order excess

Order excess is the difference between the number of demand ϕ_+ and supply ϕ_- orders, i.e. $\Delta\phi = \phi_+ - \phi_-$. The dependence of price return on order excess is widely utilized as

$$r = \Delta\phi/\lambda, \tag{2.15}$$

where λ is the measurement of market depth [*Bouchaud and Cont*, 1998]. Although the price return is discrete according to every deal, we can considered it as continuous since we focus on the dynamics of stock price on a long time scales. Thus we will use instantaneous price return instead of the discrete one addressed in Chapter 1. The definition of instantaneous price return is

$$r(t) = \frac{1}{p(t)}\frac{dp(t)}{dt}, \tag{2.16}$$

where $p(t)$ has also been considered continuous approximately. Correspondingly, order excess can be replaced by instantaneous order excess $\Delta\phi(t)$.

It is obviously the order excess is determined by the behaviors of market participants. When the participants place orders the number of demand or supply will change. In our model, we consider a simplified market structure where the dynamics of order excess is determined by three types of participants: market maker (MM), contrarian (CT) and trend follower (TF), where the latter two can be put together as chartists. Figure 2.1 demonstrates the change of order excess caused by these market participants. MMs absorb the existing orders by using their storage of stocks and money. They have contributions to the decrease of instantaneous orders in the market. On the other hand, CTs and TFs place

new orders based on their judgement of future price return. CTs will put supply orders for anticipated positive return and put demand ones for anticipated negative return. TFs behave conversely to CTs, i.e. demand for positive return and supply for negative return. We assume their anticipation is based on historical return with the instantaneous memory, which can thus approximated as instantaneous price return.

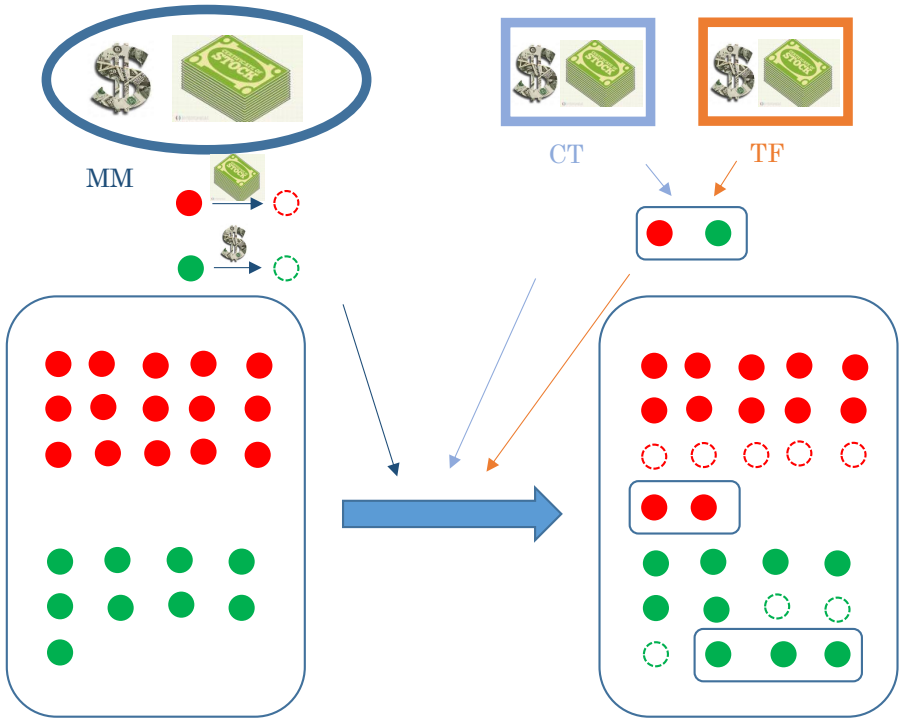

Figure 2.1: Change of order excess caused by the behavior of market makers (MMs), contrarians (CTs) and trend followers (TFs). A red circle represents a unit of demand order, and the green ones represent supply orders. MM can absorb the existing demand and supply orders using the stocks and money they hold, respectively. CT and TF place new orders as a result of their evaluation of the stock based on its history. In this figure, the MMs absorbed 1/3 of the existing orders while 2 new units of demand and 3 new units of supply orders were placed by CTs and TFs.

It is obvious that the market makers can do nothing when there is no instantaneous orders, and they can work more efficiently when there is larger number of orders. In other words, the decreasing of the orders caused by the market makers is positively related to the number of instantaneous buy or sell orders, i.e.

$$\begin{aligned} \frac{d\phi_+}{dt}|_{MM} &= -\Gamma(\phi_+, \{u\})\phi_+; \\ \frac{d\phi_-}{dt}|_{MM} &= -\Gamma(\phi_-, \{u\})\phi_-. \end{aligned} \tag{2.17}$$

The minus sign indicates that the market makers's operation decreases the number of orders by clearing the market. $\Gamma(\phi_\pm, \{u\})$, which should be constrained positive, represents the collective absorbing ability of MMs in the market. It is a function of the instantaneous orders $\phi_\pm$, as well as other factors $\{u\}$ such as the stocks and money hold by MMs. In this dissertation, we neglect the heterogeneity among the MMs and assume the available stocks and money for each MM are infinite, then $\Gamma(\phi_\pm, \{u\})$ can be reduced to $\Gamma(\phi_\pm)$ with the only variable $\phi_\pm$.

Taylor expansion of $\Gamma(\phi_\pm)$ is

$$\Gamma(\phi_\pm) = \gamma_\pm + \gamma_\pm^{'}\phi_\pm + \gamma_\pm^{''}\phi_\pm^2 + \ldots, \tag{2.18}$$

where for most of the market the constant term $\gamma_\pm$ is the dominant factor, thus we have

$$\Gamma(\phi_\pm) = \gamma_\pm \qquad (\gamma_\pm > 0). \tag{2.19}$$

Based on the approximately symmetric empirical probability distributions of price return, we assume the MMs' absorbing ability of demand and supply orders are the same, $\gamma_+ = \gamma_= \gamma$. Substituting the above relations into Eq. (2.17), we obtain the change of order excess in unit time caused by MMs:

$$\frac{d\Delta\phi}{dt}|_{MM} = -\gamma\Delta\phi, \tag{2.20}$$

where γ is a positive parameter measuring their collective absorbing ability, which has been assumed symmetric for demand and supply. For example, we have $\gamma = 1/3$ in Figure 2.1.

At the same time, new orders will be placed by the contrarians and trend followers. Both of them make their decisions based on the anticipated price return, approximated as instantaneous price return in this dissertation.

When the stock price is increasing (positive instantaneous price return), the contrarians are willing to sell their holdings (place supply orders) while trend followers will buy (play demand orders):

$$\begin{aligned} \frac{d\phi_-}{dt}|_{CT} &= \alpha_-^{CT}(r,\{u\})r; \\ \frac{d\phi_+}{dt}|_{TF} &= \alpha_+^{TF}(r,\{u\})r. \end{aligned} \tag{2.21}$$

Here $r \geq 0$, and $\alpha_\pm^i(r,\{u\}) > 0$ with $\{i = CT, TF\}$ are positive coefficients reflecting the influence of the instantaneous price return r and other factors $\{u\}$ on the behavior of chartists. We neglect the factors $\{u\}$, then $\alpha_\pm^i(r,\{u\}) > 0$ can be rewritten as $\alpha_\pm^i(r) > 0$ as a function of r alone.

Similarly when the stock price is decreasing (negative instantaneous price return), the contrarians will place demand orders and trend followers will place supply orders, which can be represented as:

$$\begin{aligned} \frac{d\phi_-}{dt}|_{TF} &= -\alpha_-^{TF}(r)r; \\ \frac{d\phi_+}{dt}|_{CT} &= -\alpha_+^{CT}(r)r, \end{aligned} \tag{2.22}$$

with $r < 0$. The minus signs are introduced to offset the negative sign, ensuring the positivity of the right hand of the equations.

The combination of Eqs. (2.21) and (2.22) gives the dynamics of order excess for CTs and TFs respectively as

$$\begin{aligned} \frac{d\Delta\phi}{dt}|_{CT} &= -\frac{d\phi_-}{dt}|_{CT} = -\alpha_-^{CT}(r)r, \ (r \geq 0) \\ \frac{d\Delta\phi}{dt}|_{CT} &= \frac{d\phi_+}{dt}|_{CT} = -\alpha_+^{CT}(r)r; \ (r < 0) \end{aligned} \tag{2.23}$$

and

$$\begin{aligned}\frac{d\Delta\phi}{dt}|_{TF} &= \frac{d\phi_+}{dt}|_{TF} = \alpha_+^{TF}(r)r,\ (r \geq 0)\\ \frac{d\Delta\phi}{dt}|_{TF} &= -\frac{d\phi_-}{dt}|_{TF} = \alpha_-^{TF}(r)r.\ (r < 0)\end{aligned} \tag{2.24}$$

Assuming the behavior of chartists is symmetric for positive and negative returns, i.e. $\alpha_+^i(r) = \alpha_-^i(r) \equiv \beta_i(r)$ with $\{i = CT, TF\}$, Eqs. (2.23) and (2.24) can be written as

$$\begin{aligned}\frac{d\Delta\phi}{dt}|_{TF} &= \beta_{TF}(r)r;\\ \frac{d\Delta\phi}{dt}|_{CT} &= -\beta_{CT}(r)r,\end{aligned} \tag{2.25}$$

with $\beta_i(r) \geq 0$.

The chartists believe that high profit always followed by high risk, which can be measured by the volatility of price return. Take the instantaneous squared price return r^2 as the measurement of volatility, the function $\beta_i(r) = a_i - b_i r^2$ $(i = TF, CT)$ with $\{a_i \geq 0, b_i \geq 0, \beta_i \geq 0\}$ is a reasonable description of the risk averse behavior of the chartists. In this function, a_i is positive parameter representing the fundamental dependency of the chartists' behaviors on the anticipated price return, and $-b_i r^2$ indicates that the chartists are more hesitated to place orders when the volatility of the price return becomes larger. Moreover, the risk aversion terms should not be too negative as to reverse the sign of $\beta_i(r)$, therefore we request $a_i - b_i r^2 \geq 0$.

The change of order excess caused by contrarians and trend followers can then be represented as

$$\begin{aligned}\frac{d\Delta\phi}{dt}|_{CT} &= -(a_{CT} - b_{CT}r^2)r;\\ \frac{d\Delta\phi}{dt}|_{TF} &= (a_{TF} - b_{TF}r^2)r,\end{aligned} \tag{2.26}$$

with $a_i > 0$, $b_i > 0$ and $a_i - b_i r^2 \geq 0$. Figure 2.2 plots the dynamical function of order excess caused by chartists. It is indicated that positive price return encourages the demand for trend followers while negative price return encourages the demand for

contrarians. The consideration of risk aversion makes the relation some different from a simple linear one.

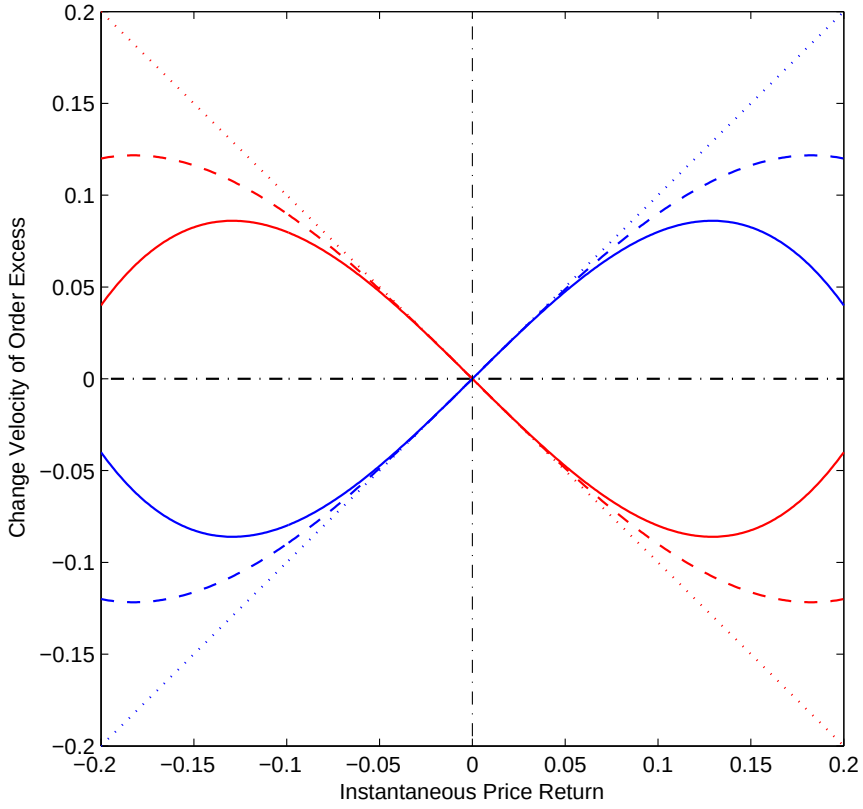

Figure 2.2: The relation of change velocity of order excess and instantaneous price return caused by chartists according to Eq. (2.26), where the parameters have been set as $a_i = 1$ and $b_i = 0, 10, 20$ for the dotted, dashed and solid line respectively. The red lines correspond to CTs and the blue ones for TFs.

It should be noted that ll the parameters reflect the collective behaviors of the market participants, including the information of both the population and the activeness per participant.

The combination of Eqs. (2.20) and (2.26) gives the full change of $\Delta\phi$ over time with r:

$$\frac{d\Delta\phi}{dt} = -\gamma\Delta\phi - (a_{CT} - b_{CT}r^2)r + (a_{TF} - b_{TF}r^2)r. \tag{2.27}$$

Taking the relation of $\Delta\phi$ and r represented by Eq.(2.15) into account, the dynamics of

instantaneous price return in the stock market can be expressed as

$$\frac{dr}{dt} = -(\gamma + \frac{a_{CT} - a_{TF}}{\lambda})r + \frac{b_{CT} - b_{TF}}{\lambda}r^3. \tag{2.28}$$

We consider the contrarians and trend followers evaluating the risk associated with volatility identically as $b_{CT}/a_{CT} = b_{TF}/a_{TF} = k$ $(k \geq 0)$, then Eq.(2.28) is reduced to

$$\frac{dr}{dt} = -(\gamma + c)r + kcr^3, \tag{2.29}$$

where $c = (a_{CT} - a_{TF})/\lambda$, representing the competition between contrarians and trend-followers without the concern of risk aversion ($c > 0$ means more orders placed by the contrarians while $c < 0$ means more orders from the trend followers, which will be described as stronger contrary trading and stronger trend following respectively in the following text); the risk aversion effect is assumed to be identical for the contrarians and the trend followers, i.e. $k = b_{TF}/a_{TF} = b_{CT}/a_{CT}$ with $k \in [0, 1/r^2]$. The risk aversion effect here is measured by the parameter k, which together with the instantaneous volatility r^2 determines the shrinkage percentage of the new orders.

2.3.2 Macroscopic dynamics of price return

In microscopic analysis of order excess, we have simplified the market structure by neglecting the heterogeneity among the same type of market participants and external information. Thus it is not reasonable to use Eq. (2.29) alone for the quantum potential operator of our model. Instead, we will correspond the potential energy from the classical mechanical model to quantum potential operator.

The macroscopic dynamics of price return in classical models can be described by a Langevin equation:

$$m_r \frac{d^2r}{dt^2} = -\eta \frac{dr}{dt} - \frac{dV(r)}{dr} + \xi(t), \tag{2.30}$$

where m_r is the mass of the fictitious particle of price return, η is the damping coeffi-

cient, $V(r)$ is a time-independent potential, and $\xi(t)$ is a random force. Bouchaud et al. [*Bouchaud and Cont*, 1998] considered the evolution of price return as a overdamped viscous fictitious particle under potential $V(r)$, where m_r is ignorable and $\eta = 1$. Hence we obtain the first order derivative of price return over time as a function of potential

$$\frac{dr}{dt} = -\frac{dV(r)}{dr} + \xi(t). \tag{2.31}$$

2.3.3 Classification of different market environments

From Eq. (2.29) and Eq. (2.31), we have

$$-\frac{dV(r)}{dr} = -(\gamma + c)r + kcr^3, \tag{2.32}$$

which gives a financially interpretable potential as

$$V(r) = \frac{\gamma + c}{2}r^2 - \frac{kc}{4}r^4. \tag{2.33}$$

In this potential consisting of a quadratic and a quartic term, there are three parameters, i.e. γ, c and k respectively. γ is a positive real number, measuring the effect of the market makers' behavior on the stock price; c represents the total effect of chartists regardless of risk aversion ($c > 0$ corresponds to stronger contrary trading while $c < 0$ to stronger trend following); k is a parameter measuring risk aversion effect, which has been assumed identical for the contrarians and the trend followers with $k \in [0, 1/r^2]$.

It should be stated that the three types of participants are simplified ideal model agents that cannot be mapped into real markets strictly. A trader in the real stock market can behave sometimes as a contrarian and other times as a trend follower. The role of market makers is usually played by organizations instead of individual investors. Based on the assumptions for this modeled structure of stock market, the liquidity of the markets is ensured by the efficiency. The we can classify the market environments into three different types according to different dominant participants.

Figure 2.3 shows the three market environments clearly. According to the relation of γ and c, the market can be named as liquid market and illiquid market. As the liquidity is evaluated by the effect of MMs, we say it is liquid when $\gamma \gg |c|$. On the other hand, when $\gamma < |c|$, it is illiquid. For the latter situation, we call it a contrarian dominant market and trend follower dominant market for $c > 0$ and $c < 0$ respectively.

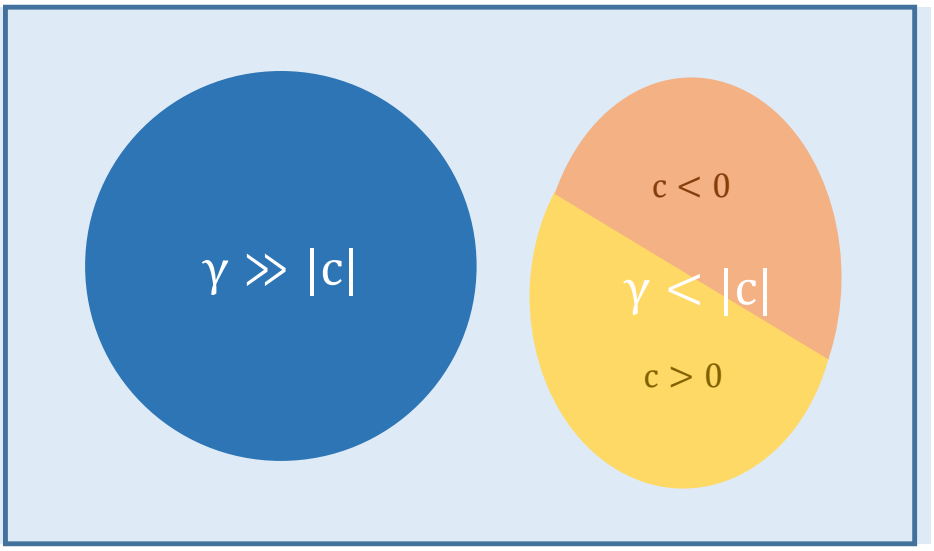

Figure 2.3: The parameter settings for different market environments. The biggest light blue square represents entire market environments which has no been fully covered by our model. The dark blue pie represents MM dominant market, also named liquid market. The yellow one is for CT dominant market and the orange one is for TF dominant market, both of which are illiquid markets.

Figure 2.4 and Figure 2.5 plot the potential shapes with different parameter values. It is shown that when the behaviors of CTs and TFs are balanced, the potential has a form of harmonic oscillator (thick yellow line). Larger c indicating stronger contrarian trading raises the potential uniformly, resulting in potential of an anharmonic oscillator. And finally evolves to CT dominant market (red line). Smaller c (negative) indicating stronger trend following pulls the potential down but with weaker effect near $r = 0$. Thus finally for the TF dominant market (blue line), there is a small hump in the middle. The existence of k can also change the harmonic oscillator into anharmonic, but slightly attributed to the constrain that $0 \leq k \leq 1/r^2$. k has nothing to do with the classification of market environments.

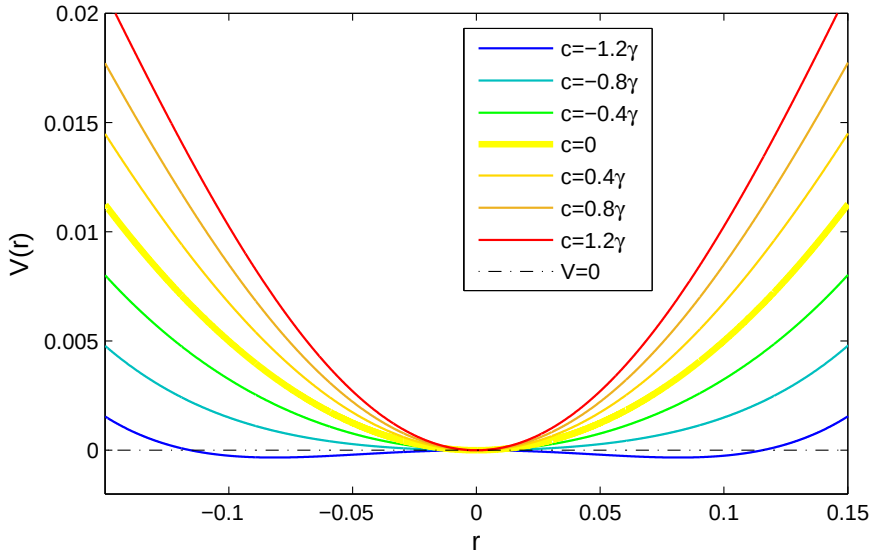

Figure 2.4: Shapes of potential (2.33) according to different c values, where $\gamma = 1$ and $k = 25$ have been assumed.

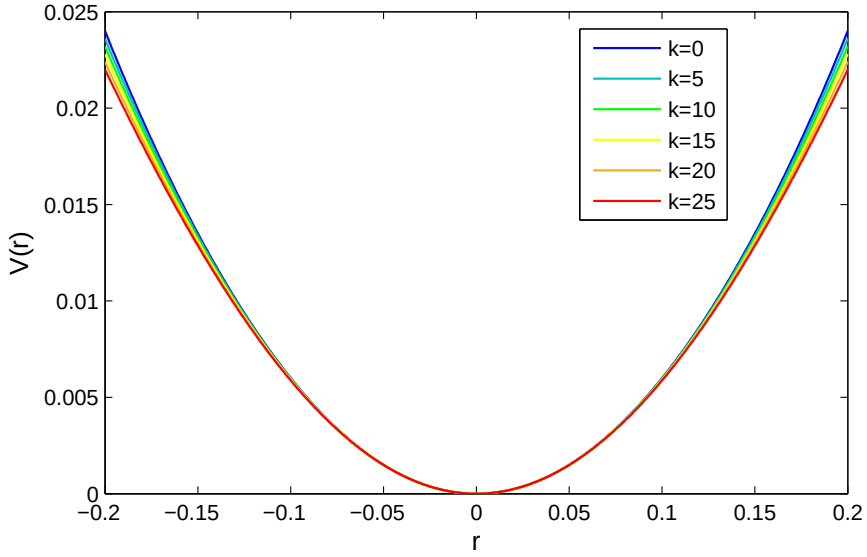

Figure 2.5: Shapes of potential (2.33) according to different k values, where $\gamma = 1$ and $c = 0.2\gamma$ have been assumed.

Adopting the financially deduced potential into the Hamiltonian of "quantum price return", we have to deal with the energy eigen equation for the modeling of stationary markets:

$$\left[-\frac{\hbar^2}{2m}\frac{d^2}{dr^2}+\left(\frac{\gamma+c}{2}r^2-\frac{kc}{4}r^4\right)\right]\psi(r)=E\psi(r). \tag{2.34}$$

2.4 Wave function and probability distribution

The potential proposed in the last section have been constrained, resulting in the potential form of oscillators, anharmonic for most of the situations and harmonic for special situations that neglect risk aversion. Thus the model is named quantum oscillator model in this dissertation. We will discuss the wave functions and probability distributions for these two kinds of potential form respectively in this section.

2.4.1 Harmonic oscillator

The Hamiltonian for harmonic oscillator without consideration of risk aversion is

$$H(r)=-\frac{\hbar^2}{2m}\frac{d^2}{dr^2}+\frac{\gamma+c}{2}r^2. \tag{2.35}$$

Its corresponding eigen energies and eigen vectors has been analytically calculated by physicists as

$$\begin{aligned} E_n &= (n+\frac{1}{2})\hbar\omega, \quad n=0,1,2,\ldots; \\ \psi_n(r) &= N_n\exp(-\frac{1}{2}\alpha^2r^2)H_n(\alpha r) \end{aligned} \tag{2.36}$$

with normalization constant $N_n=[\alpha/(\sqrt{\pi}2^n n!)]^{\frac{1}{2}}$, where $H_n(\alpha r)$ is Hermite polynomial $H_n(\alpha r)$ and $\omega=\sqrt{(\gamma+c)/m}$, $\alpha=\sqrt{m\omega/\hbar}$.

The wave functions and squared modulus of wave functions of the first several energy levels are plotted in Figure 2.6 and Figure 2.7, respectively. It is shown that n is a good quantum number for the 1D harmonic oscillator. The eigenstate of nth energy level can

also be represented by $|n\rangle$, which is the Dirac notation for $\psi_n(r)$.

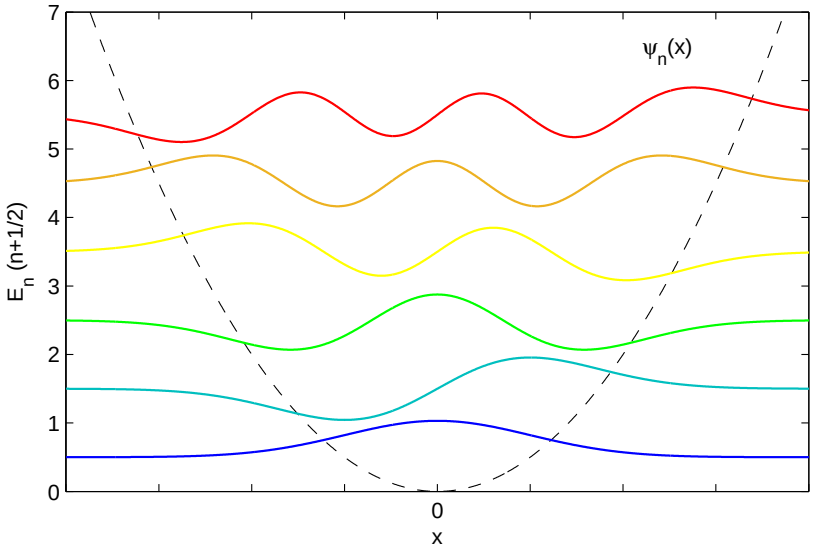

Figure 2.6: Wave functions of the first six energy levels for the 1D harmonic oscillator.

It is shown that the wave function of a harmonic oscillator at the ground state with $n = 0$ gives a rigorous Gaussian distribution for probability density function (PDF). The PDF is consistent with the central limit theorem for stochastic processes in random walk modeling [*Mantegna and Stanley*, 1999]. And it is the basis of those studies that applied quantum harmonic oscillator for stock markets. For example, Ye et al. used the quantum harmonic oscillator to explain the persistent fluctuations in stock markets [*Ye and Huang*, 2008], and Meng et al. extended it to a many-particle models by to study the relationship between the volatility and trading volume [*Meng et al.*, 2015].

Figure 2.8 plots the squared modulus of the ground state wave function of a quantum harmonic oscillator, in comparison with that of a classical one. It is obvious that a classical harmonic oscillator alone can not be used to model the dynamics of stock price, although the potential form is introduced classically. In classical random walk models, in order to produce a Gaussian distribution, a noise term must be considered to manifest the unpredictability of the stock price. But in the quantum modeling, as the wave function, in which the property of uncertainty for the stock price has been included, can itself describe the price return perfectly without any time-consuming stochastic process. It is

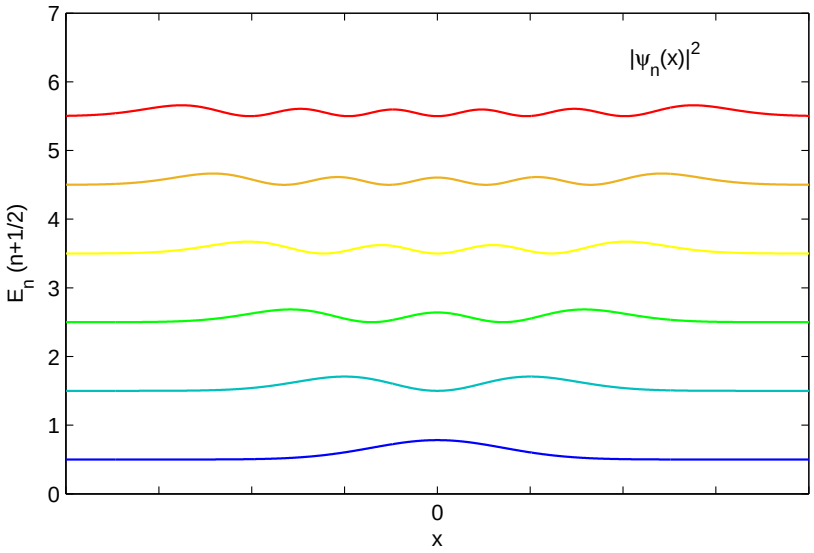

Figure 2.7: Squared modulus (PDF) of wave functions of the first six energy levels for the 1D harmonic oscillator. This figure together with Figure 2.6 is plotted from the numerical solutions of the time-independent SE, where all the constants including $\hbar$, m and ω have been assumed 1.

demonstrated, when studying the statistical properties such as PDF of price return, that the quantum modeling is more convenient and faster than classical stochastic processes.

However, there are other problems have not been solved or explained clearly. One of them is that as the quantum harmonic oscillator has different energy states, why only the ground state is utilized. According to [*Ye and Huang*, 2008], we can explain it as that the excited energy states for stock price are unstable, similarly to physical systems such as hydrogen atom. Although the stock price can sometimes be excited to higher energy states, it would return back to lower energy states and finally ground state in short time. Thus it is satisfying to use the ground states for the analysis of low frequency data. But how about high frequency data? We will discuss this problem in detail in the next chapter.

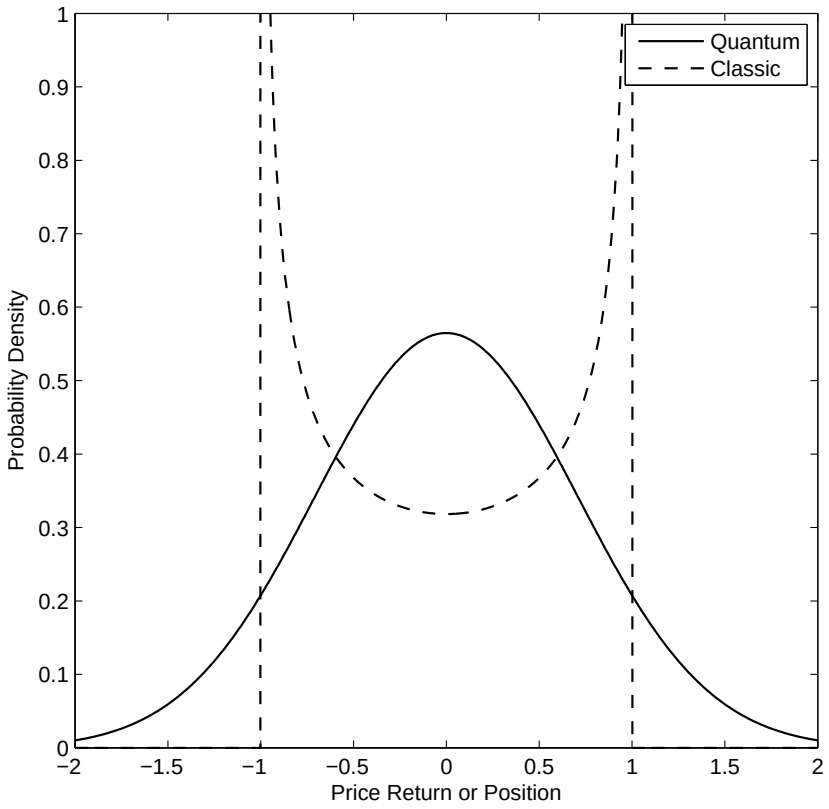

Figure 2.8: The probability density of quantum harmonic oscillator (ground state) and that of a classic harmonic one. The classic harmonic oscillator is of the same energy with the quantum one at the ground state.

2.4.2 Anharmonic oscillator

The full Hamiltonian form including risk aversion term is

$$H(r) = -\frac{\hbar^2}{2m}\frac{d^2}{dr^2} + \frac{\gamma + c}{2}r^2 - \frac{kc}{4}r^4. \tag{2.37}$$

As shown in Figure 2.4 and Figure 2.5 that the potential is deviated from harmonic oscillators but not greatly due to the financial constrains of the parameters. We solve the corresponding time-independent SE numerically with finite difference method (FDM) [*LeVeque*, 2007; *Press et al.*, 2007]. The details and Matlab codes can be found in Appendix A at the end of this dissertation.

The main results, i.e. possible shapes of PDF, which are calculated from the wave functions of the ground state, are shown in Figure 2.9. Corresponding to the left figure which lists the different shapes of potential, the PDFs can generally be considered as two types. The first one is Gaussian-like, i.e. a distribution with a peak in the middle (blue lines). It is shown that when the negative c becomes smaller, the peak will be lower, gradually lower than its neighbor, finally become a distribution with two peaks symmetrically located to the center (red lines). The values of c in the figure corresponds to trend follower dominant market. Although they are not plotted, it is not difficult to understand that for the market maker dominant market (liquid market) and the contrarian dominant one, the PDF is also Gaussian-like and with higher peak than the blue solid line in Figure 2.9(b).

The distributions in red solid line are obviously rarely occur in the real markets. It is reasonable because the real markets are efficient most of the time, ensuring the liquidity of the markets. In our model, c measures the competition between contrarians and trend followers, and that the difference between $|c|$ and γ reflects the effect of the chartists versus the market makers on the market. The efficiency of a market is always guaranteed by the ability of the market makers, indicating that the new orders offered by the chartists (contrarians and trend followers) are much less than that absorbed by the market makers,

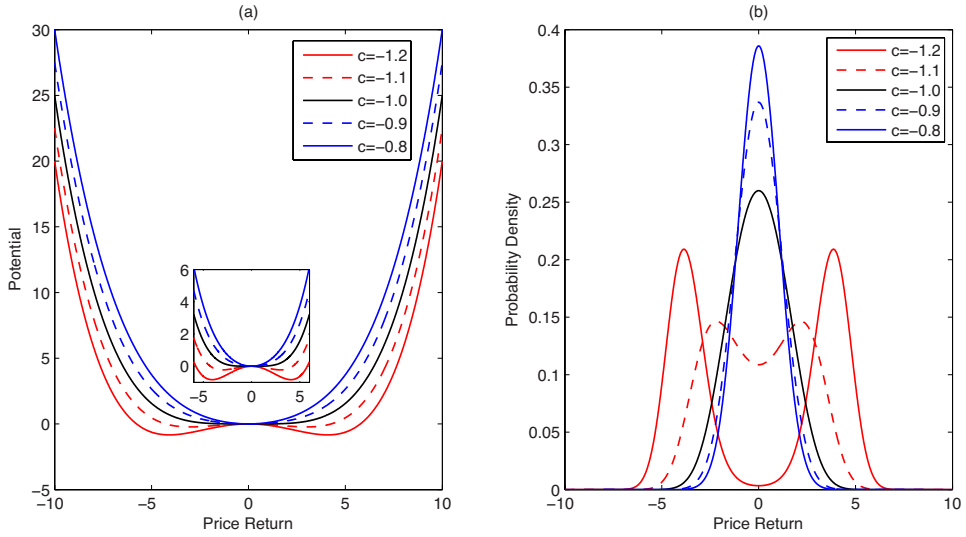

Figure 2.9: (a) The potentials and (b) the corresponding probability distributions of ground states with different c values, where $\gamma = 1$ and $k = 0.01$ are assumed.

which is consistent with our assumption that $|c| \ll \gamma$. We generally use the parameter setting $\gamma = 1$ as it hardly affect the qualitative characters of the modeling results and it can then be adjusted to sample data in the application to different markets.

One of the difference of this quantum model with previous ones is the existence of risk aversion term in potential operator for liquid markets. Thus we compare the Gaussian-like PDF obtained from anharmonic oscillators with that from harmonic oscillator (Gaussian distribution). The PDFs with the value of parameter c around zero, when the market is market maker dominant, are shown in Figure 2.10(a). In the figure, $|c|/\gamma \in [-0.2, 0.2]$ is assumed and $k = 0.01$ is used with $r \in [-10, 10]$ in the numerical calculations. The PDFs have been normalized to that with the unit variance. It is known that when $c = 0$, the anharmonic oscillator reduces to a harmonic one. The distribution for $c = 0$ (solid black line) is a rigorous Gaussian while the others are Gaussian-like. As the quartic part of the potential is largely constrained, the probability distributions are almost the same.

However, the slight differences among the distributions are of significance. The probability distributions with larger c values have sharper peaks and heavier tails. The monotonously positive relation of c value with the corresponding kurtosis in Figure 2.10(b) agrees with the distributions in Figure 2.10(a) that the modeling results of positive c are

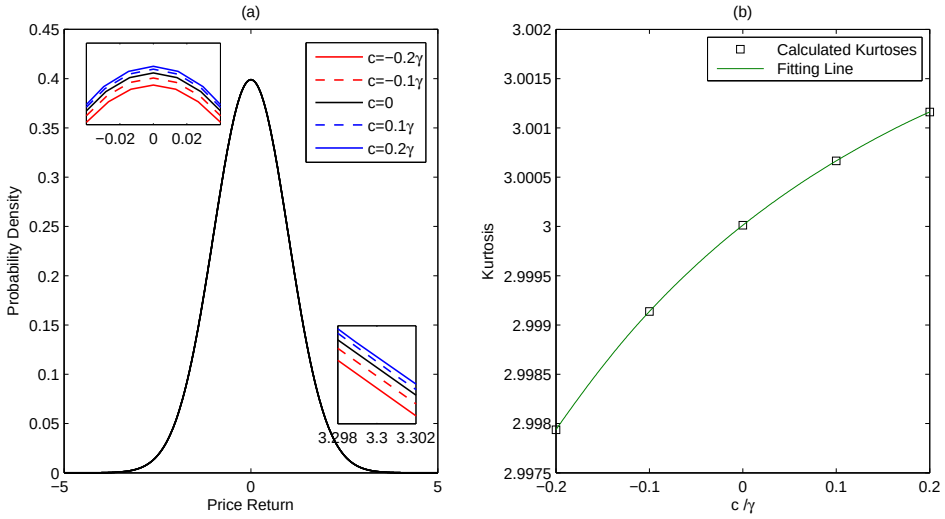

Figure 2.10: (a) The probability distributions (of ground states) for liquid market with different c. The results have been normalized to that of the same volatility as $\sigma^2 = 1$. The distribution for $c = 0$ (black) is a rigorous Gaussian while the others are Gaussian-like. (b) The corresponding kurtoses of the liquid market model with $c \in [-0.2, 0.2]$.

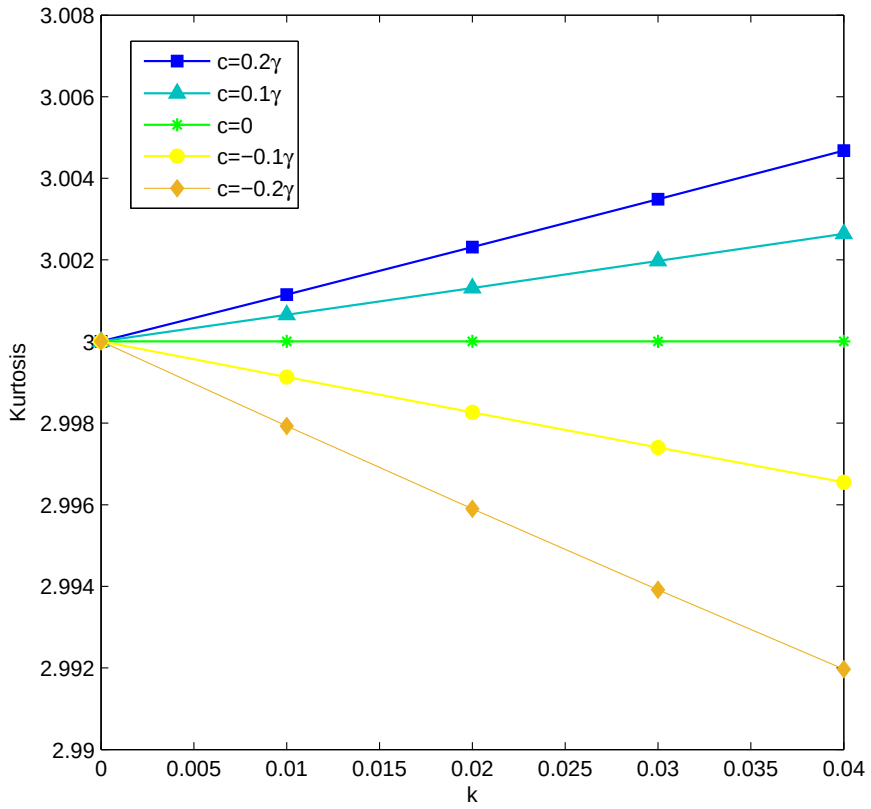

Figure 2.11: Relation of the kurtoses of modeled distributions and k value for liquid market.

closer to the statistic characters of real data as the price return in real stock market performs a leptokurtic distribution [*Johnson et al.*, 2003] with kurtosis larger than 3. It is demonstrated that the introduction of a negative quartic perturbation improves the modeling result. Thus we find that the risk aversion plays an important role for the stylized facts of stock price.

Although the risk aversion term (quartic term) depends on both k and c, resulted from the assumption for the symmetry of contrarians' and trend followers' "risk aversion effect", it is more reasonable to take $-kc$ as a whole. Our before mentioned assumption of the identical risk aversion effect for contrarians and trend followers (i.e. $k = b_{TF}/a_{TF} = b_{CT}/a_{CT}$) may confuse the analysis of the modeling results. In liquid market, $-kc$ must be negative to describe risk aversion because it should be opposite to the main behavior - positive quadratic term. We can put positive c as a special case for negative quartic term. We can also say that the leptokurtic distributions of price return may partially be attributed to the weaker collective risk aversion of trend followers than that of contrarians (and also that of market makers if it is considered).

We can further check the role of k as the only variable in the risk aversion term. k is defined as the measurement of "risk aversion effect", which together with the instantaneous price return $r(t)$ determines the shrinkage percentage for the new orders expected to be submitted regardless of risk aversion. $k \leq 1/r^2$ is requested by its financial definition. In the above assumed condition that $\{\gamma = 1,\ c/\gamma \in [-0.2, 0.2]\}$, the probability approaches zero before $r = 5$, thus it is safe for us to choose $k \leq 0.04$ to maintain the financial constrain of k. The narrow range of k strictly constrained by its financial definition results in the seemingly insignificant difference in the final probability distribution. Although the probability distributions modeled for liquid market perform similarly, the kurtosis dependency of the distribution on k shown in Figure 2.11 indicates that kurtosis increases with the increase of k for positive c while decreases for negative c. This is consistent with the analysis of c in the last paragraph that 1) a negative quartic perturbation with larger absolute values give better modeling results of the stock market, and 2) the

negative perturbation is caused by the relatively weaker collective risk aversion (not the ordering behavior itself) of trend followers than that of contrarians.

2.4.3 Error analysis of numerical solutions

In order to solve the time-independent SE, i.e. the eigen equation of energy, we apply finite difference method (FDM) and obtain the eigen vectors from Matlab. According to Appendix A, we calculate the eigen vectors of the matrix as

$$H = \frac{\hbar^2}{2m}\frac{1}{\Delta x^2}\begin{pmatrix} 2 & -1 & 0 & \cdots & 0 \\ -1 & 2 & -1 & \ddots & \vdots \\ 0 & -1 & 2 & \ddots & 0 \\ \vdots & \ddots & \ddots & \ddots & -1 \\ 0 & \cdots & 0 & -1 & 2 \end{pmatrix} + \begin{pmatrix} V_1 & 0 & \cdots & \cdots & 0 \\ 0 & V_2 & \ddots & \ddots & \vdots \\ \vdots & \ddots & \ddots & \ddots & \vdots \\ \vdots & \ddots & \ddots & \ddots & 0 \\ 0 & \cdots & \cdots & 0 & V_N \end{pmatrix}. \tag{2.38}$$

In the numerical calculation, as the boundary is set zero, the space should be carefully chosen to guarantee the continuity at the boundary. The space step Δx must be small enough to ensure the accuracy of the results but not too small to waste computing resource.

We test the Matlab code for harmonic oscillator since the corresponding exact solution is accessible. For the Hamiltonian with $V_i = \frac{1}{2}m\omega^2 x_i^2$, we have the exact probability density of the ground state as

$$\rho(x)_{exact} = |\psi_0(x)|^2 = \frac{\alpha}{\sqrt{\pi}}\exp(-\alpha^2 x^2) \tag{2.39}$$

with $\alpha = \sqrt{m\omega/\hbar}$. We compare the numerical solutions with the exact one by defining the maximum error as

$$||e|| = \max_{i=1,2,\ldots,N}\{|\rho(x_i)_{numerical} - \rho(x_i)_{exact}|\}, \tag{2.40}$$

where N is the number of lattice, $\rho(x_i)_{numerical}$ is the value of probability density at x_i from the numerical solution and $\rho(x_i)_{exact}$ is from the exact solution.

It is shown in Table 2.1 and Table 2.2 that appropriate Δx can save the calculation time and guarantee the precision at the same time. For $\omega = 1$, we can choose the value of Δx between 0.01 and 0.05 since $\Delta x < 0.01$ becomes time consuming while $\Delta x > 0.05$ brings larger numerical error. In our numerical calculations, we take $\Delta = 0.005$. In addition, for the same space lattice, the results for $\omega = 10$ have larger errors than $\omega = 1$. This is because the former solutions are concentrated in a smaller space, resulting that the space lattice must be shrunk to keep the precision.

Table 2.1: Some examples of numerical errors and the corresponding elapsed time for $\omega = 1$, $x \in [-5, 5]$, where $\hbar = m = 1$ has been assumed. The elapsed time represents the time that need for Matlab to calculate the eigen systems with matrix size N, where $N = 10/\Delta x + 1$.

$\omega = 1$, $x \in [-5, 5]$		
Δx	$\|\|e\|\|$	Elapsed Time (s)
0.0005	1.113×10^{-8}	122.542
0.001	4.424×10^{-8}	16.655
0.005	1.102×10^{-6}	0.382
0.01	4.408×10^{-6}	0.075
0.05	1.103×10^{-4}	0.004

Table 2.2: Some examples of numerical errors and the corresponding elapsed time for $\omega = 10$, where the other parameter setting is the same with Table 2.1.

$\omega = 10$, $x \in [-5, 5]$		
Δx	$\|\|e\|\|$	Elapsed Time (s)
0.0005	3.484×10^{-7}	123.764
0.001	1.394×10^{-6}	16.780
0.005	3.485×10^{-5}	0.352
0.01	1.394×10^{-4}	0.072
0.05	3.507×10^{-3}	0.003

Chapter 3

Stationary Modeling Results

In this chapter, we make use of the quantum model proposed in Chapter 2 to fit real data from stock market, by adjusting the values of parameters γ, c and k in the model potential. We study the three market environments respectively. As the real markets are always efficient, they are market maker dominant. We can use the data directly for the modeling. However, there is no specific real market dominated by the trend followers. But it is believed that for some time period, any real market may unfortunately dominated by trend followers even though the period would be short. Thus we propose a data filtering method to produce a artificial trend follower dominant market, followed by data analysis with our quantum model.

3.1 Data

According to our model, the differences of the statistical behaviors of price return for different markets can be modeled by the variable parameters in the potential. Adjusting the parameters of the potential in the quantum model, we can reproduce the probability distributions of price return for different market data. Our study focus on the general stylized facts in the stock markets. Without loss of generality, we study index instead of a single stock. We downloaded the data from the website of Yahoo Finance (https://finance.yahoo.com/). What we will use in the chapter and next chapter about

volatility clustering modeling are daily data of Nikkei 225, SSE Composite Index and S&P 500, as well as monthly data of Nikkei 225 for studying the effect of data frequency. Nikkei 225, also called Nikkei index, or Nikkei Stock Average, is a stock market index for the Tokyo Stock Exchange. It has been calculated daily by the Nihon Keizai Shimbun newspaper since 1950. It is a price-weighted index with unit yen, and the components are reviewed once a year. Currently, the Nikkei is the most widely quoted average of Japanese equities. It began to be calculated on September 7, 1950, retroactively calculated back to May 16, 1949. Since January 2010 the index is updated every 15 seconds during trading sessions. SSE Composite Index is a stock market index of all stocks, including A shares and B shares, that are traded at the Shanghai Stock Exchange in China. S&P 500 which is an abbreviation of Standard & Poor's 500 is an American stock market index based on the market capitalizations of 500 large companies having common stock listed on the NYSE or NASDAQ.

Table 3.1 lists the data that will be used in this study. The time periods of the data for different markets are selected consistent because it can make the comparison of the environments for different markets more reasonable and convenient. The data information contains the date, the corresponding open price, the highest and lowest price, the closing price, and the trading volume. In this dissertation, we take the closing price with its data as the historical price series for the indices.

Table 3.1: The list of indices used in this study.

	Frequency	Period (MM/DD/YYYY)	Number
Nikkei 225	Month	1/4/1996 - 6/6/2016	1061
Nikkei 225	Day	1/4/1996 - 6/1/2016	5026
SSE Composite Index	Day	1/4/1996 - 6/1/2016	5184
S&P 500	Day	1/4/1996 - 6/1/2016	5138

For the time series of a market index with the time interval Δt, such as one day for daily data and one month for monthly data in this study, the index return of the jth tick, $r_j = (p_j - p_{j-1})/p_{j-1}$, can be regarded as the instantaneous price return of the quantum

model with $dt = 1$ tick.

According to the description of our quantum model for the stock price, at each time tick, the price return is essentially a wave packet than a single point. The historical data comes from the measuring results, which can not be used directly for the verification of the wave function obtained from the quantum model. We have to deal with large numbers of data for a time period, compare their statistical characters with the wave function, and adjust the parameters of the potential to evaluate the quantum model. Thus two assumptions about the market should be stated: 1) the stock market environments for sample data are stationary, and 2) the sample data can be used statistically as the complete set of possible measuring values of the stock price.

3.2 Liquid markets

It has been mentioned that the real stock markets are liquid most of the time, thus the statistical results of full sample data are supposed to be consistent with that of liquid market environment in our model. As the effect of parameters c and k on the PDF is small and has been discussed in Chapter 2 (see Figure 2.10 and 2.11 in Chapter 2), we will keep them constant and study the dependency of different indices on parameter γ.

We adjust γ for the monthly and daily data of Nikkei 225 (Table 3.1) respectively in Figure 3.1, using the ground states of the quantum oscillators. The parameter setting of $\{c = 0.2\gamma$ and $k = 1\}$ has been assumed to declare a liquid market.

The monthly sample data can be well fitted by the wave function of ground state with $\gamma = 2.05 \times 10^4$, where the standard deviation of the modeled PDF is guaranteed as that of the data. Although the theoretical PDF is smooth, the statistical distribution of sample data fluctuates along the Gaussian-like distribution. It can be attributed to the fact that the potential of the market is not rigorously time independent since the data sample covers a long period.

On the other hand, the daily data is fitted by the wave function of ground state with

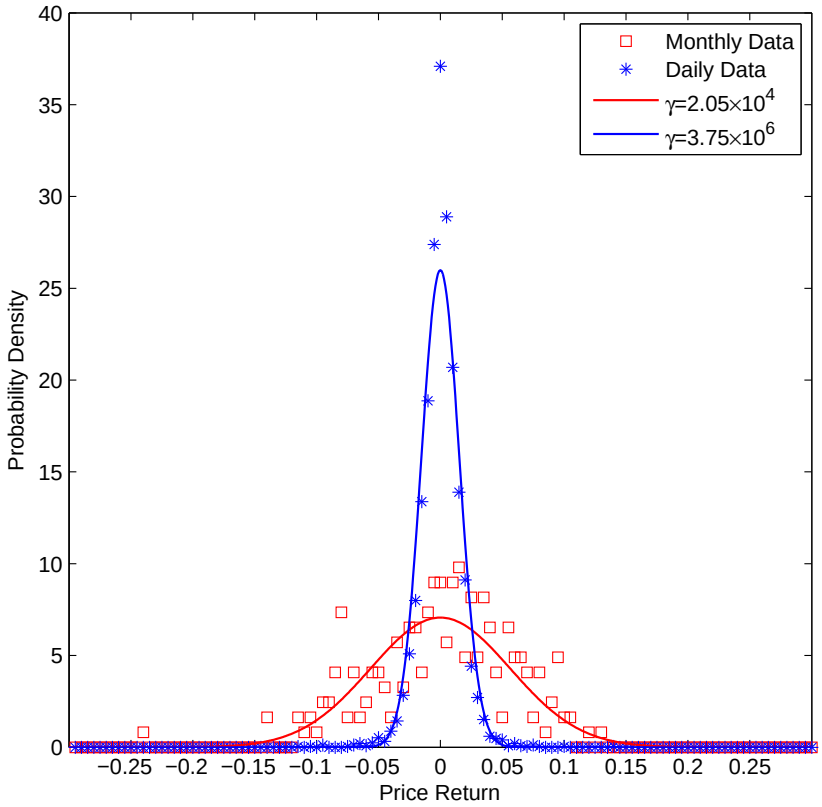

Figure 3.1: Fitting of the quantum anharmonic oscillator at ground state to the monthly (January 4, 1996 - June 6, 2016) and daily (January 4, 1996 - June 1, 2016) Nikkei225 Index, by adjusting γ. Other parameters have been assumed as $c = 0.2\gamma$ and $k = 1$. The theoretical distributions are scaled to have the same standard deviations with the corresponding sample data.

$\gamma = 3.75 \times 10^6$. But it is not difficult for us to find that the fitting result is not as good as the monthly one since the PDF of data has sharper peak than the model. As the daily data covers the same time period as the monthly one, the failure can not be attributed to market differences. We then have to reconsider the feasibility of applying the ground state alone. It is possible that more modes other than ground state are existed. We have questioned the use of ground state alone in the last chapter, and stated the dominant role of it in "quantum stock price" with the recognition of excited states although rarely happen. Based on this idea, it is understandable that when the sample data is recorded more frequently, the stock price would be more possibly to be measured at its excited states. As the daily sample is of high frequency than the monthly one, larger portion of the data may correspond to the states other than the ground one. It indicates that the wave function of ground state alone is incapable of modeling the sample data with high frequency, such as the daily data in this study.

As it is supposed that a portion of the data was recorded when the stock price is at the excited states, we can define a mixed-state probability density function as

$$|\Psi(r)|^2 = \frac{1}{\Omega} \sum_{n=0}^{N} \omega_n |\psi_n(r)|^2, \tag{3.1}$$

where n represents the energy level, ω_n is the weight of the nth state proportional to the time that the stock stays in the nth excited state, $\Omega = \sum_{n=0}^{N} \omega_n$, and $|\psi_n(r)|^2$ is the probability density function of the nth energy level. Although it is not easy to precisely determined the weights of different states for a given data sample, we can just screen the weights to improve the modeling result. A fitting result with $\{\omega_0 = 1,\ \omega_n = 0.005$ for $n = 1, 2, \ldots, 10$ and $\omega_n = 0$ for $n > 10\}$ is plotted by the solid purple line in Figure 3.2. The weight for the ground state is set much heavier than the other states due to the assumption that the excited states are much unstable than the ground state, which means most of the data is from n_0. The adjusted γ equals 1.80×10^7. Although the weights of the excited states are small, it is shown that the modeling can be improved considerably.

Of course different weight settings can be tried and more excited stated can be taken into account. More precise parameter settings need the extension of the stationary model to a dynamical one, which will be discussed in Chapter 4.

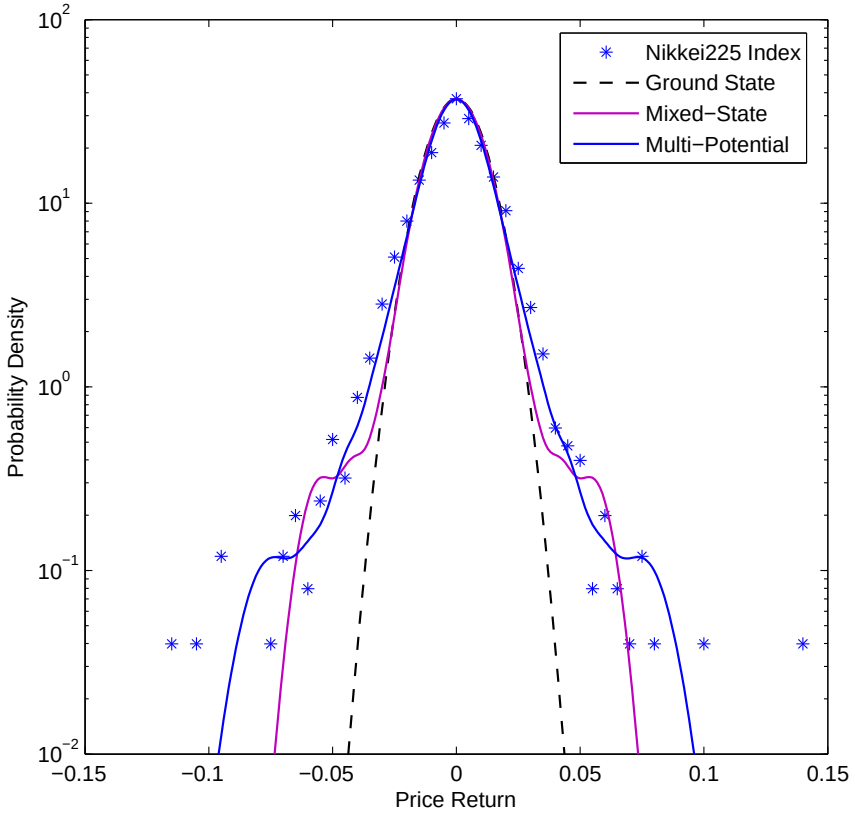

Figure 3.2: Fitting of the quantum anharmonic oscillator at mixed-state to the daily Nikkei225 Index. The dashed black line is the probability distribution described by the ground state of the quantum model ($\gamma = 1.55 \times 10^7$); the solid purple line is a mixed-state distribution of Eq. (3.1) with $\omega_0 = 1$ and $\omega_n = 0.005, n = 1, 2, ..., 10$ ($\gamma = 1.80 \times 10^7$); the solid blue line is the combination of two mixed-state distributions with the same parameter settings except for $\gamma_A = 4.55 \times 10^7$ and $\gamma_B = 5.20 \times 10^6$ respectively.

Comparing the fitted values of γ for the monthly data (2.05×10^4) and daily data (3.75×10^6 and 1.80×10^7), we can see that their potential strengths are quite different although for the same time period in the same market. This difference comes from the assumption that the potential describing the market environment is invariant. As the real market environment should have changed with time, especially for the data covers the period as long as 20 years, the fitted parameter is the average value. For the monthly

data, a great number of detailed environment information that is related to strong external force measured by γ was missed.

More precisely speaking, γ is of different values for different time. For a short time, there is no enough data for us to do statistics and determine the values of parameters. However, the modeling result can be further improved by the consideration of heterogeneous potentials. Although it is not easy to determine the parameter setting for each small time period, we can predict that the parameter set $\{\gamma_i\}$ can capture the statistical characters of data sample more perfectly than a single γ. We use a simple case with two γ, denoted γ_A and γ_B respectively. The weights of these two γ are set equal and for each γ excited states are considered as Eq. (3.1). The multi-potential probability density function can then be described as

$$|\widetilde{\Psi}(r)|^2 = \frac{1}{2\Omega^A}\sum_{n=0}^{10}\omega_n^A|\psi_n^A(r)|^2 + \frac{1}{2\Omega^B}\sum_{n=0}^{10}\omega_n^B|\psi_n^B(r)|^2, \tag{3.2}$$

where n still labels the energy level, ω_n^i is the weight for the nth energy state, $\Omega^i = \sum_{n=0}^{10}\omega_n^i$, and $\psi_n^i(r)$ is the corresponding wave function with $i = A(B)$ for $\gamma_A = 4.55\times10^7$ and $\gamma_B = 5.20\times10^6$. As the solid blue line shown in Figure 3.2, the multi-potential probability distribution fits the data better than the mixed-state one.

In order to make sure that if the modeling methods are universally applicable, we also use it to analyze to data from other markets, i.e. SSE Composite Index and S&P 500. The results are listed in Table 3.2 and 3.3 at the end of this chapter. It is shown that the statistics of the fitted probability distributions agree with Nikkei 225 on the relative appropriateness of the three modeling methods as: Multi-Potential Modeling > Mixed-State Modeling > Ground-State Modeling.

In summary, we have demonstrated that the quantum oscillator model is applicable to Nikkei 225. It uses wave function to describe the stock price instead of stochastic processes in classical modeling. Different from the models with classical mechanics such as Langevin equation, the noise term is not necessary for the fluctuation of stock price

in equilibrium. The state of stock price is quantized and the ground state is much stable than the excited states. Thus the stock price stays at the ground state most of the time, which is the reason that the wave function of ground state alone can and has been applied to describe the probability distributions of price return. This quantum model can satisfyingly model index data with low frequency. Applying the mixed-state modeling and multi-potential modeling method, the index data with high frequency can also be well fitted.

3.3 Illiquid markets

The mechanics of the stock price in real markets can be modeled by the liquid market with dominant market makers in our quantum oscillator model. According to the financial interpretation of the model potential, however, there should exist situations even for a short moment where the liquidity is not well maintained. In this section, we discussed the illiquid markets, saying contrarian dominant and trend follower dominant markets. It is the first piece of work that considers the overwhelming behaviors of contrarian trading or trend following, which rarely but are existed in the real markets.

For the CT dominant market, we give a briefly theoretical discuss. For the TF dominant market, we propose a data filtering method to produce a quasi-series of historical prices, and adjust the parameters in our model to fit them.

3.3.1 Contrarian dominant markets

As $|c| \ll \gamma$ corresponds to liquid market, the illiquid markets request not only $|c| > \gamma$ but also $|c|$ comparable to γ. Thus we calculate the PDFs of $\gamma \leq c \leq 5\gamma$ for CT dominant market, as shown in Figure 3.3.

It is found that the behaviors of contrarians have similar effect on the shape of PDF as that of market makers. But the large c can relatively increase the risk aversion term, which finally results in sharper peaks in the probability distribution. As shown in Figure

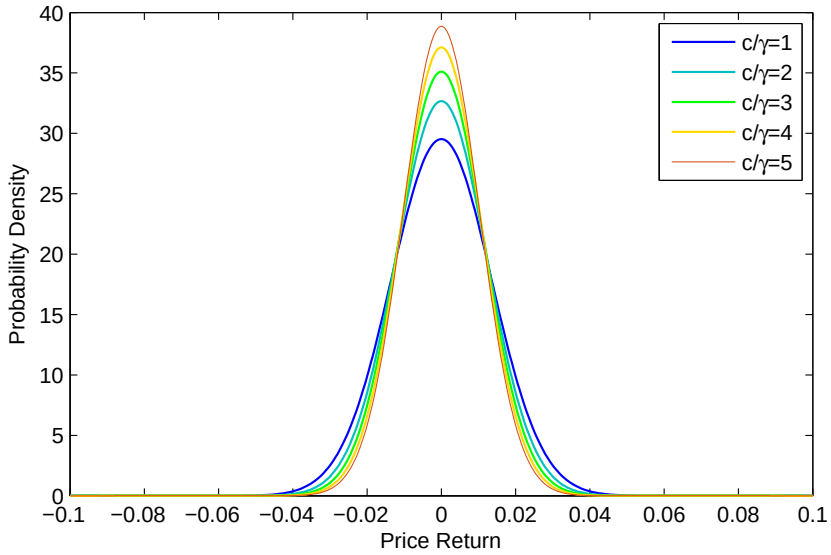

Figure 3.3: The modeling PDFs for the contrarian dominant markets with $c/\gamma = 1, 2, 3, 4, 5$ respectively. $\gamma = 3.75 \times 10^6$ and $k = 1$ is used according to the liquid market modeling result for Nikkei 225.

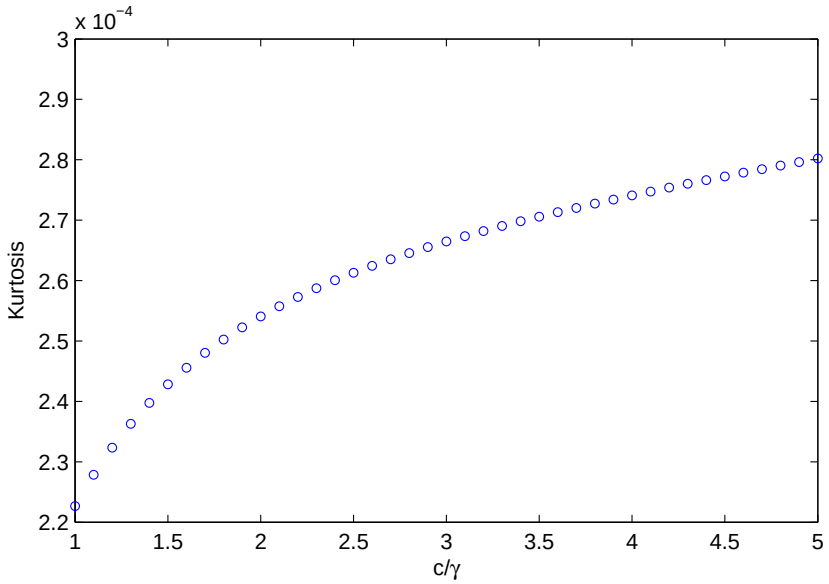

Figure 3.4: The relation of kurtosis and c/γ for contrarian dominant markets, where the value 3, i.e. the kurtosis of Gaussian distribution, has been subtracted for the vertical ordinate.

3.4, although the kurtosis is larger than 3, the difference is not significant. Therefore, we can not differentiate the environments of CT dominant market from the MM dominant one by adjusting the parameters of this quantum model to real market data.

3.3.2 Trend follower dominant markets

Trend follower dominant market as the other type of illiquid market represents the situations when the effect of TFs' behaviors is quite strong than the CTs' and even comparable to the MMs'.

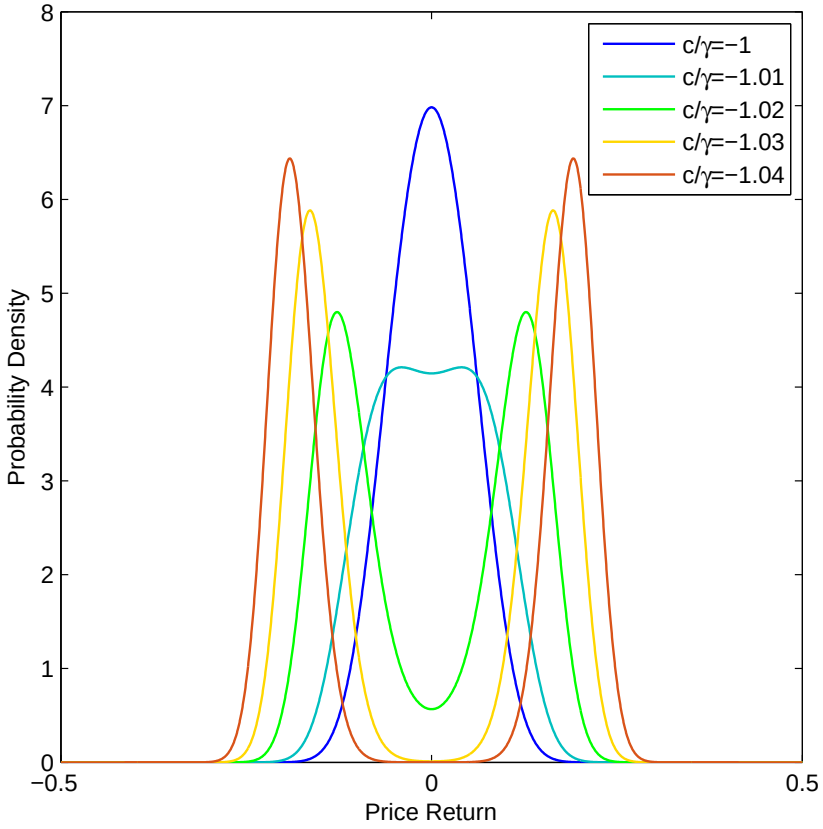

Figure 3.5: The PDFs calculated from the for trend following dominant markets with $c/\gamma = -1, -1.01, -1.02, -1.03, -1.04$ respectively, where $\gamma = 3.75 \times 10^6$ and $k = 1$.

Figure 3.5 shows that around $c/\gamma = -1$, the shape of PDF of the price return is much sensitive. When c becomes smaller than -1, causing the coefficient of the quadratic term in model potential, $(\gamma + c)/2$ turns to negative, the peak of the unimodal distribution

will collapse and two peaks locate symmetrically along the center instead. The well acknowledged Gaussian-like distribution turns to a bimodal distribution, where the two peaks mean the great possibility of the occurrence of crashes or bubbles.

In order to see if the bimodal PDF, which has not been studied in previous works, exists in real market, we have to deal with historical stock prices for TF dominant markets. Unfortunately, as the TF dominant environment rarely happened in the markets, there is no corresponding raw data. Thus we propose a data filtering method to obtain quasi-series of historical prices for TF dominant market.

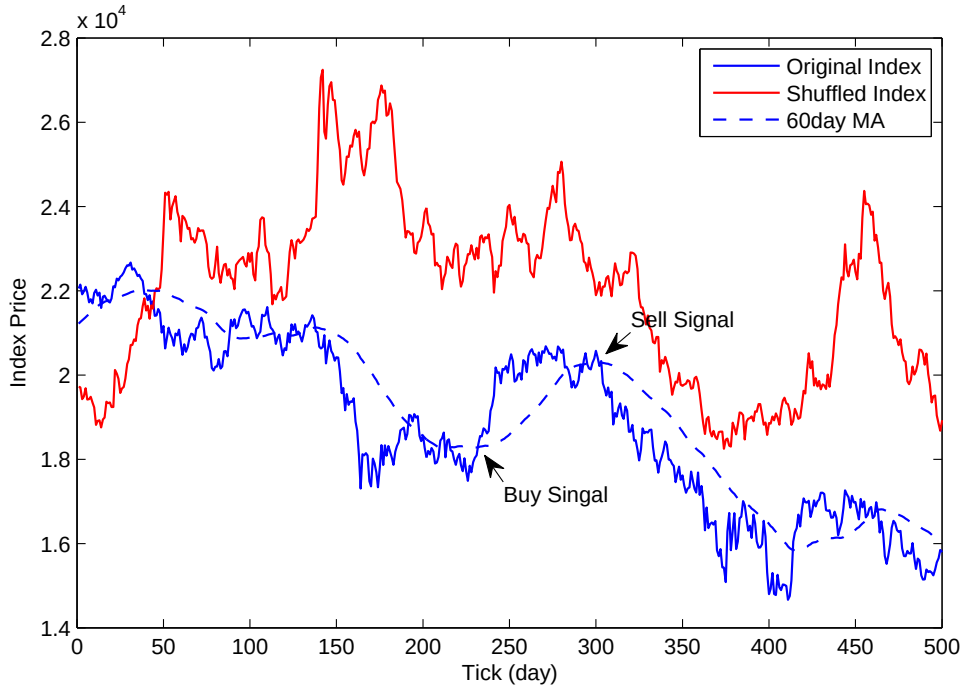

Figure 3.6: The time series of Nikkei225 daily data (from March 1, 1996 to February 29, 2016 with 4925 ticks, it is noted that only the first 500 ticks are showed in this figure to help distinct the price and MA line), the corresponding 60day MA, and an example of artificial price series obtained by shuffling the price returns of the original Nikkei 225 daily data where the initial price is set the same.

The key point of this method is moving average (MA), which has been used as a simple efficient tool for timing buy and sell signals. Making use of price series and MAs, the traders can figure out the beginning or the end of a trend in advance by following the Granville's rules [*Granville*, 1960]. There are 8 rules summarized for the prospective users.

For example, it can be considered a buy signal when the stock price passes upward through a flat or rising moving average line has been significantly declining, and conversely, if the stock price is passing downward though a flat or declining moving average line after a rising, it is a good time to sell (Figure 3.6). The other rules are more complicated and more difficult to grasp, however all of they tell us that it is never too much to focus on the crossovers of the moving average line and its corresponding stock prices.

Based on the consideration that the trend followers become extraordinarily active around the crossovers, we use the price returns of the crossovers to draw a probability distribution of trend following dominant market.

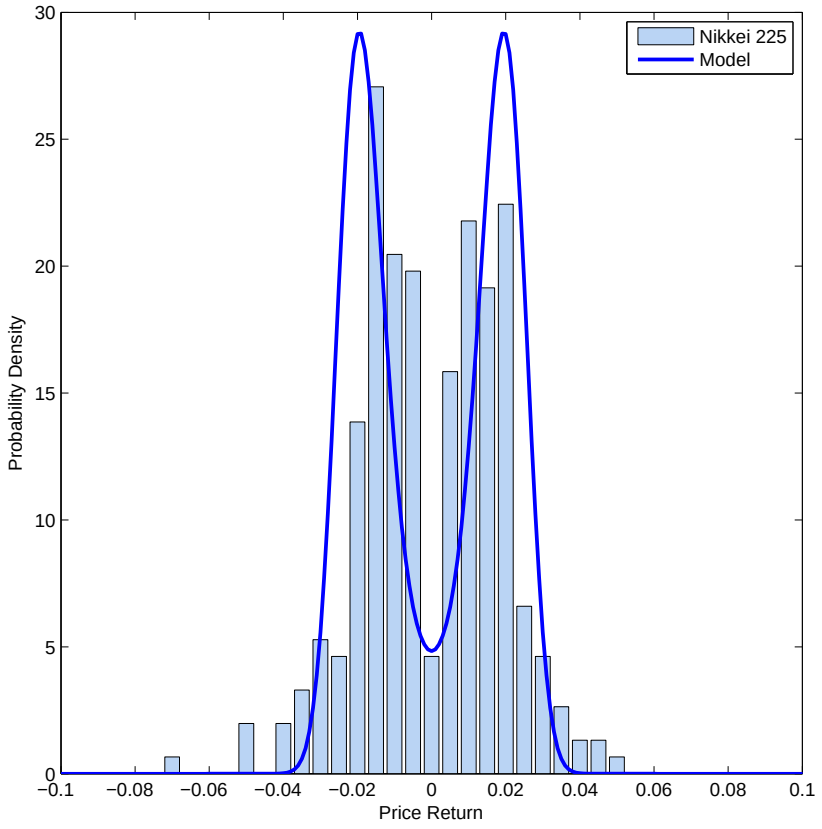

Figure 3.7: The probability distributions of the price return for the trend following dominant market extracted from the data in Figure 3.6 and the scaled model results with the same volatility ($\sigma = 0.0190$). The Scaled parameters are: $\gamma = 2.4 \times 10^{11}$, $c = -1.00047\gamma$, $k = 1$. The kurtosis are 2.9378 and 1.4453 respectively.

Figure 3.7 shows that our quantum model can describe the trend following dominant

market well. The scaled parameter c has the compatible absolute value with γ, which means that the trend following is strong but not enough to overwhelm the market makers. This is reasonable because we just coarsely consider the crossovers of 60 MA and price line as the ticks when the trend followers are active, while in reality the traders use MA of different lengths and the full Graville's rules require further analysis more than the simple crossovers. Thus the data sample we picked out inevitably contains some impurities and of course there was some other data missed. The data analysis and the quantum model consistently give us the result of a market with strong but not that strong trend following.

In order to make sure that the filtered price series maintained its original characters different from artificial random series, we will apply the filtering method to some random price series and compare the results with that for the real series. We randomly shuffled the price returns of the original data represented solid blue line 100 times, producing 100 sets of artificial price series like the line solid red line in Figure 3.6. The PDFs of the full series, no matter for the shuffled ones or the original data, is the same. Applying the data filtering method to the original and the 100 shuffled price series respectively, we obtain 101 sets of quasi-series of price return for TF dominant market. Figure 3.8 shows the statistical characters of quasi-series.

It can be seen that the standard deviations and kurtoses for the shuffled series are clustered at a distance away from that for the original data. We can believe that there exists some trends in the stock price that is different from random series.

Similar trends can also be observed in SSE Composite Index and S&P 500 as Figure 3.9 and Figure 3.10. The quasi-series produced from the data filtering method based on Granville's rules is demonstrated reliable.

Applying the data filtering method to SSE Composite Index and S&P500, similar bimodal distributions can be obtained. We adjusted the parameters to fit the two sets of quasi-series. It is shown that the overwhelming trend following would give rise to bubbles or crashes.

In addition, we checked the distributions of filtered data using MA with different

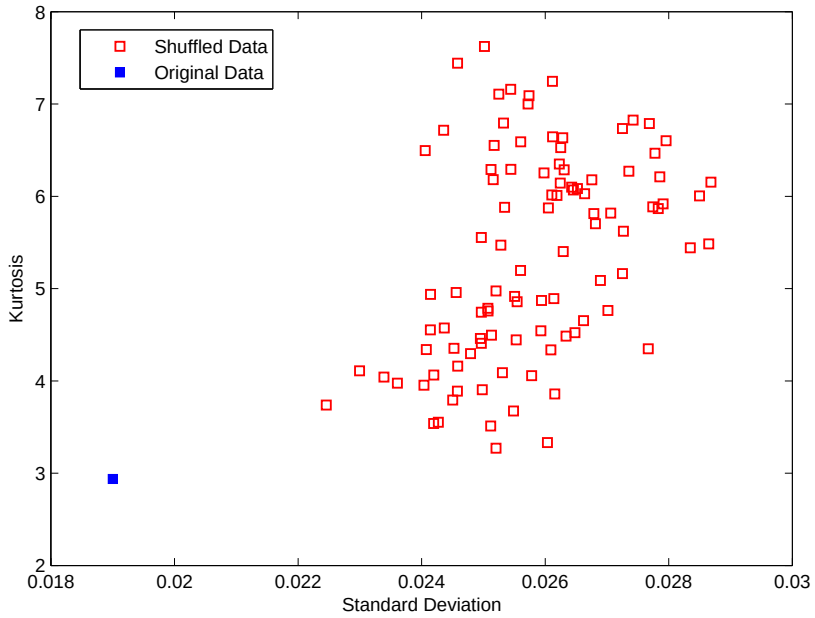

Figure 3.8: The standard deviations and kurtoses of the PDFs for TF dominant market extracted from 100 shuffled price series and the original Nikkei225 daily data (from March 1, 1996 to February 29, 2016).

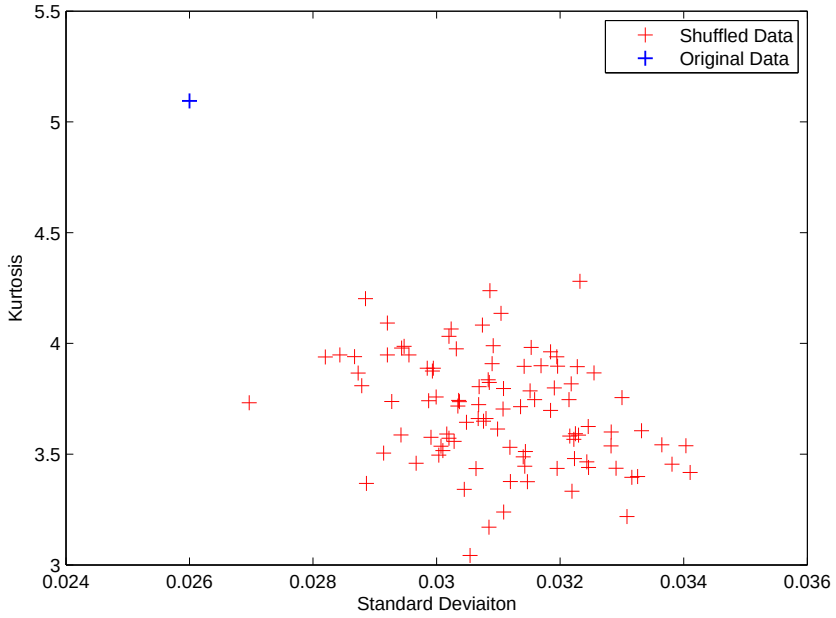

Figure 3.9: The standard deviations and kurtoses of the PDFs for TF dominant market extracted from 100 shuffled price series and the original SSE Composite Index, where MA= 60 days has been used.

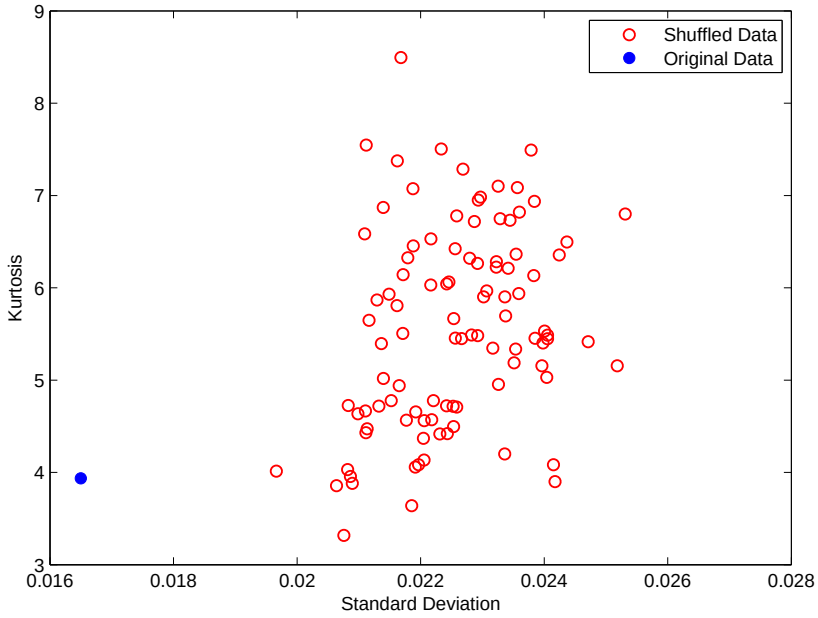

Figure 3.10: The standard deviations and kurtoses of the PDFs for TF dominant market extracted from 100 shuffled price series and the original S&P 500, where MA= 60 days has been used.

lengths of MA term. As shown in Figure 3.13, short-term MAs (such as those with the length of MA term shorter than 5 days) can not successfully help to acquire quasi-series for TF dominant market. It indicates that short-term MAs are rarely utilized by the chartists in market. In our calculation, MAs with term longer than 5 days are able to give bimodal distributions. Moreover, there is no clear dependency of the PDF with lengths of MA term for those long-term MAs.

The standard deviations of the filtered data with different lengths of MA term and for different markets are listed in Figure 3.14. If we consider the standard deviation of the filtered data as a measurement of the utilization frequency, the periodic changes of the standard deviation for a certain market data can be take as the result of the chartists' preference on the length of MA term. The blue squares, corresponding to Nikkei 225, have the largest number around MA= $10, 100, 180, ...$ days. It indicates that these MAs are more frequently referred by the participants in Nikkei 225. Similar preferences can also be observed in SSE Composite Index and S&P 500. It is noted that there is no

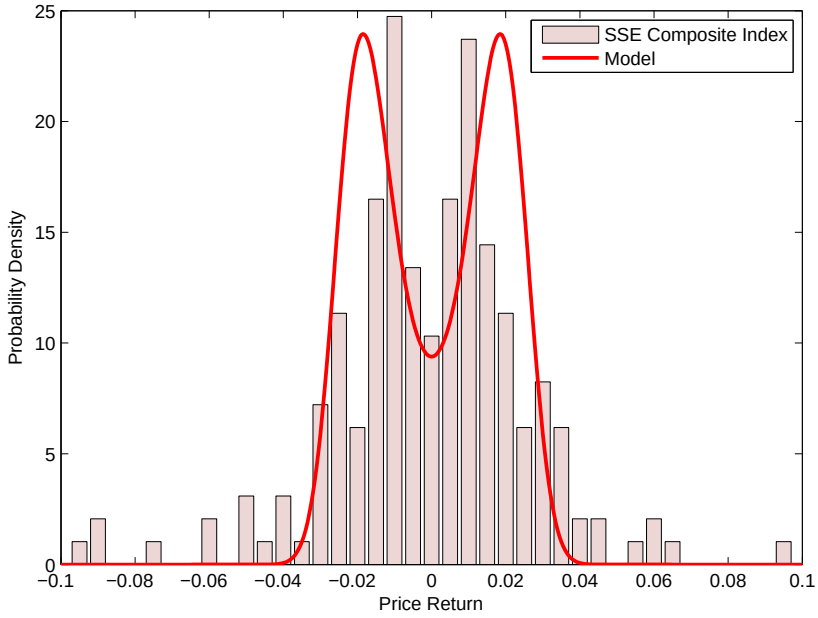

Figure 3.11: The histogram of price turn of SSE Composite Index for TF dominant environment and the fitted model results, where the quasi-series is extracted from daily SSE Composite Index, January 4, 1996 to June 1, 2016. The fitted parameters are: $\gamma = 1.4 \times 10^{11}$, $c = -1.00048\gamma$ with $k = 1$. The standard deviations and kurtoses are 0.0260 and 5.0947 for the data, while 0.0181 and 1.6451 for the model.

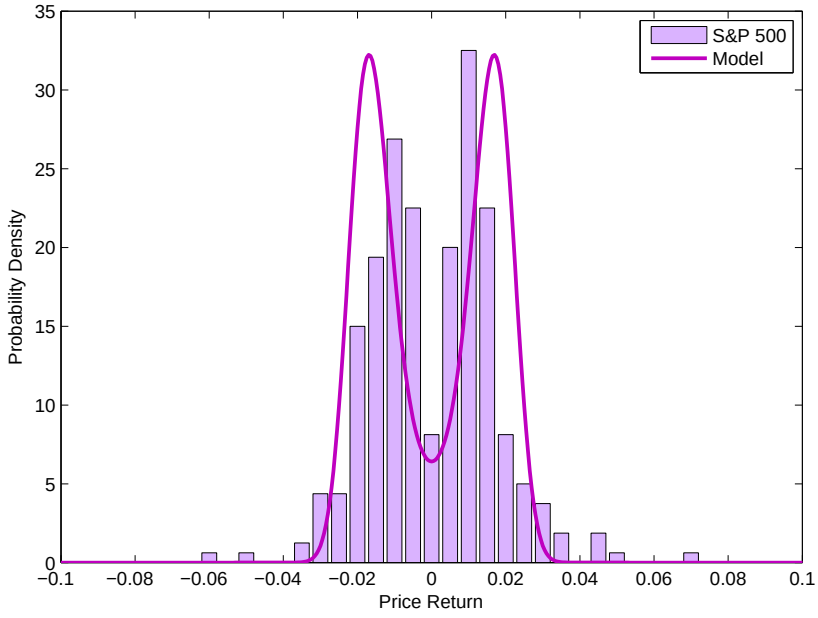

Figure 3.12: The histogram of price turn of S&P 500 for TF dominant environment and the fitted model results with the same volatility ($\sigma = 0.0165$). The quasi-series is extracted from daily S&P 500, January 4, 1996 to June 1, 2016. The fitted parameters are: $\gamma = 4.9 \times 10^{11}$, $c = -1.00036\gamma$, $k = 1$. The kurtosis are 3.9351 and 1.4787 respectively.

linear relation of their preference and the length of MA. However, it can be seen from the figure that long-term MAs are more preferable in Nikkei 225 and S&P 500 than in SSE Composite Index.

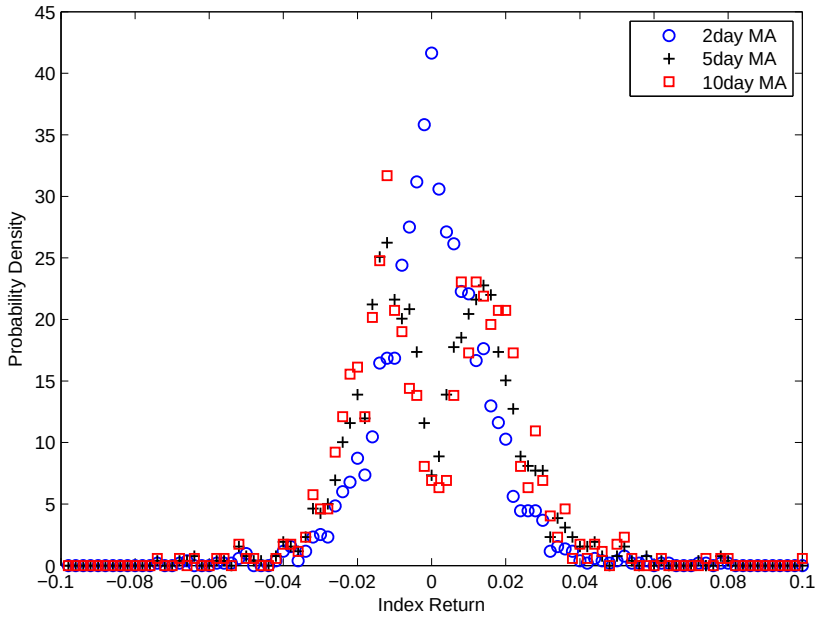

Figure 3.13: Probability distributions of filtered Nikkei 225 daily data according to different lengths of MA term.

The filtered data we obtain from 60day MA although can be used to represent the TF dominant market, there must contains some impurity. But as it does not make any qualitative difference in our study, we can just use the results with no more detailed analysis.

3.4 Summary

In this chapter, stationary models with wave function description are analyzed for the study of leptokurtic distributions of price return.

Based on the anharmonic oscillator with financial interpretation, we found that the sharp peaks and heavy tails of the probability distributions can be attributed to the mixed energy levels and multi-potentials of the stock. It can give satisfying modeling results of

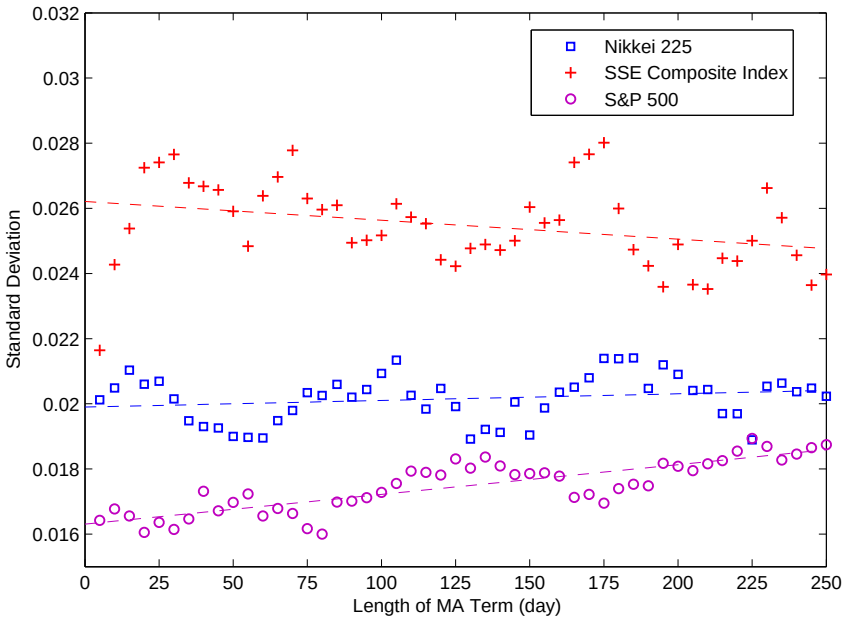

Figure 3.14: Standard deviations of the filtered data for Nikkei 225, SSE Composite Index and S&P 500 respectively.

return distributions for the liquid markets. The quantum model is good at describing the probability distributions because it can give a PDF directly without doing statistics on simulated time series.

In addition, the model makes it possible to study the extreme markets such as trend following dominant markets.

Table 3.2: The modeling results of different market indices using different modeling method. γ is determined by satisfying fitting of the peaks of distributions (referring to Figure 3.2).

Market Indices	Data		Ground-state M.			Mixed-state M.			Multi-potential M.			
	σ_D	κ_D	γ	σ_{M1}	κ_{M1}	γ	σ_{M2}	κ_{M2}	γ_1	γ_2	σ_{M3}	κ_{M3}
Nikkei 225	0.0154	8.34	1.55×10^7	0.0108	3.0006	1.80×10^7	0.0128	6.69	4.55×10^7	5.20×10^6	0.0143	8.34
SSE Composite Index	0.0171	7.96	3.45×10^7	0.0088	3.0008	3.55×10^7	0.0108	6.68	8.10×10^7	1.25×10^7	0.0117	7.96
S&P 500	0.0123	10.76	4.55×10^7	0.0082	3.0009	5.55×10^7	0.0096	6.67	3.25×10^8	5.08×10^6	0.0132	10.76

Table 3.3: The modeling results of different market indexes using different modeling method. γ is adjusted to ensure the consistence of the value of standard deviation σ.

Market Indices	Data		Ground-State M.		Mixed-State M.		Multi-Potential M.		
	σ	κ_D	γ	κ_{M1}	γ	κ_{M2}	γ_1	γ_2	κ_{M3}
Nikkei 225	0.0154	8.34	3.75×10^6	3.0003	8.50×10^6	6.69	3.40×10^7	3.88×10^6	8.34
SSE Composite Index	0.0171	7.96	2.44×10^6	3.0003	5.65×10^6	6.70	1.75×10^7	2.73×10^6	7.96
S&P 500	0.0123	10.76	9.10×10^6	3.0005	2.10×10^7	6.69	4.32×10^8	6.75×10^6	10.76

Chapter 4

Dynamical Quantum Modeling

4.1 Expected time series of price return and volatility

It has been demonstrated that for any instant time, the state of a stock price can be theoretically described by a wave function instead of a single observed value. However, the stylized facts that we observed from the markets are based on the large number of time series, which is in fact the measured values of stock prices but not the wave functions. Thus in oder to guarantee the verifiability, it seems not appropriate to apply the wave function itself to model the dynamics of stock price. In addition, reviews on quantum correlation indicate that physicists concern more about the correlations between operators or wave functions, which have nothing to do with the correlations of measurements. Fortunately, the wave function, as a full description of quantum state, provides us the information of theoretical expectations of all observables. If the stylized facts are maintained in the expectations, i.e. the averaged time series, it becomes possible to recover the facts in quantum models.

We firstly prove that the stylized facts, especially leptokurtic distributions and volatility clustering, are maintained in the averaged time series of price return. It is not possible to acquire time series of price return from the "paralleled world" since we have not found the way back in time. We can make use of the simulated time series instead of "paralleled

ones". The well studied GARCH (generalized autoregressive conditionally heteroscedastic) models will be applied in this study. As we focus on the volatility clustering in this chapter, it is sufficient to only work on the autocorrelations of return and volatility for the averaged time series.

A GARCH(p,q) process can be expressed as [*Francq and Zakoian*, 2010]

$$\begin{cases} \epsilon_t = \sigma_t \eta_t \\ \sigma_t^2 = \omega + \sum_{i=1}^{q} \alpha_i \epsilon_{t-i}^2 + \sum_{j=1}^{p} \beta_j \sigma_{t-j}^2, \end{cases} \tag{4.1}$$

where $\{\eta_t\}$ is an i.i.d sequence with distribution η. As we concern only leptokurtic distributions and qualitative description of volatility clustering, the specific version of the processes as GARCH(1,1) is qualified in this study:

$$\begin{cases} \epsilon_t = \sigma_t \eta_t \\ \sigma_t^2 = \omega + \alpha \epsilon_{t-1}^2 + \beta \sigma_{t-1}^2, \end{cases} \tag{4.2}$$

where η is taken as normal distribution $\mathcal{N}(0,1)$ with

$$\begin{aligned} &\langle \eta_t \rangle = 0, \quad \langle \eta_t \eta_{t'} \rangle = \delta_{tt'}; \\ &\langle \eta_t^2 \rangle = 1, \quad \langle \eta_t^4 \rangle = 3. \end{aligned} \tag{4.3}$$

4.1.1 Artificial time series from GARCH

Three parameters ω, α and β need to be confirmed before GARCH(1,1) simulation. Estimating GARCH(1,1) with the daily Nikkei 225 from January 4, 1996 to June 22, 2017 including 5287 data, we obtain the parameters as

$$\{\omega = 4.95 \times 10^{-6}, \quad \alpha = 0.112, \quad \beta = 0.870.\} \tag{4.4}$$

Making use of (4.4), we obtain a set of artificial time series of price return having similar statistical characters and stylized facts with the data. The length of each time series is the same with the real data, where the first 1000 time steps in the simulation have been abandoned. The number of the set is M=5000, i.e. 5000 paralleled time series are produced. Both the averaged time series of price return and volatility should be calculated as

$$\begin{aligned} E\epsilon_t &= \frac{1}{N}\sum_{m=1}^{M}\epsilon_t^{(m)}; \\ E\sigma_t^2 &= \frac{1}{N}\sum_{m=1}^{M}\epsilon_t^{2(m)}, \end{aligned} \tag{4.5}$$

where m denotes the number for the paralleled time series, $M = 5000$, and volatility has been considered as instant squared return based on zero return.

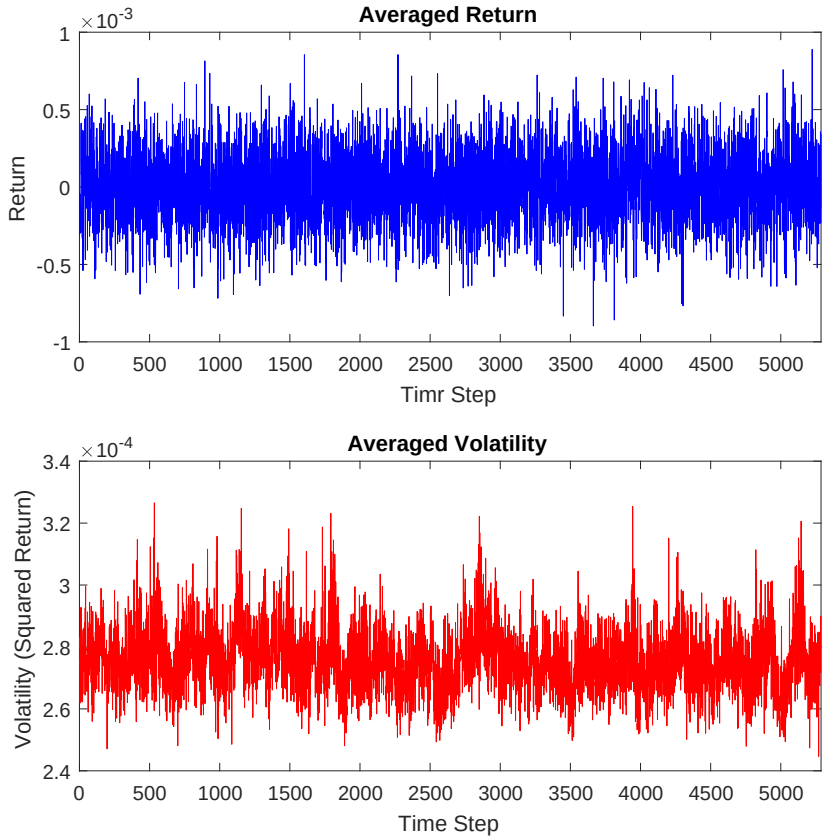

Figure 4.1: Averaged time series of price return and volatility produced from GARCH(1,1).

The averaged time series of artificial price return and volatility we obtained are shown in Figure 4.1. The averaged price return fluctuates around zero, and the averaged volatility fluctuates around a positive value. This positive value can be theoretically obtained as

$$\begin{aligned}\overline{\epsilon_t^2} =& \overline{\omega + \alpha\epsilon_{t-1}^2 + \beta\sigma_{t-1}^2} \\ =& \omega + (\alpha+\beta)\overline{\sigma_{t-1}^2} \\ =& \sum_{i=0}^{m-1}(\alpha+\beta)^i\omega + (\alpha+\beta)^m\overline{\sigma_{t-m}^2} \\ =& \frac{1-\gamma^m}{1-\gamma}\omega + \gamma^m\overline{\sigma_{t-m}^2},\end{aligned} \tag{4.6}$$

with $\gamma = \alpha + \beta$. The overline symbol $\overline{\ \cdot\ }$ represents calculating the average of the paralleled series for each time step. As GARCH models require $\alpha + \beta < 1$, when m is large enough, it is not difficult to obtain

$$\overline{\epsilon_t^2} \to \frac{\omega}{1-\gamma}. \tag{4.7}$$

For the parameter setting (4.4), the theoretical value of volatility in equilibrium is 2.75×10^{-4}, which is consistent with the numerical results in Figure 4.1.

Calculating the autocorrelations for the averaged time series of both return and volatility, it is found that the characters of the autocorrelations, i.e. zero autocorrelation of return and slow decaying autocorrelation of volatility, are maintained. Figure 4.2 exhibits the autocorrelations for randomly picked 5 time series and the averaged ones. The differences among these autocorrelations are caused by the randomness of the stochastic processes. It is not possible and necessary for us to quantify the exponents of the decays. However, It can be easily seen that beginning with the real data, we can recover the facts - no autocorrelation in return but slow decaying positive autocorrelation in volatility of return - with the artificial time series produced by the GARCH model and the corresponding averaged one.

As shown in Table 4.1, the averaged series is not suitable to be considered as an

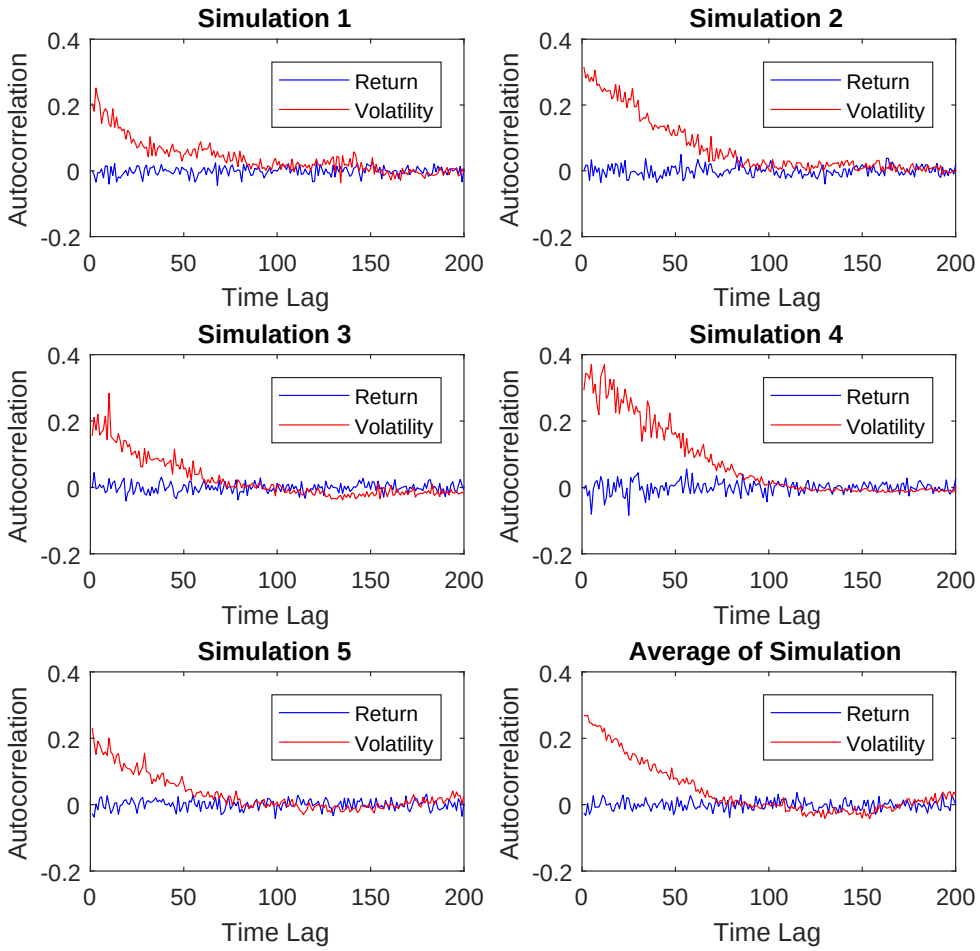

Figure 4.2: Autocorrelations of return and volatility calculated from the GARCH simulated time series and the corresponding averaged series in Figure 4.1. 5 of all the 5000 time series are randomly picked and plotted.

Table 4.1: The statistical characters of artificial time series of price return and the corresponding averaged one, compared with the real data. The average values are calculated from the averaged time series of return and volatility, not the average of the statistics.

	Mean	Variance	Skewness	Kurtosis
Simulation 1	-4.71×10^{-5}	2.05×10^{-4}	0.0640	4.76
Simulation 2	2.56×10^{-4}	2.31×10^{-4}	-0.137	5.54
Simulation 3	-5.30×10^{-5}	2.76×10^{-4}	-0.0823	5.63
Simulation 4	-3.52×10^{-4}	4.96×10^{-4}	-0.446	16.6
Simulation 5	-4.51×10^{-5}	2.43×10^{-4}	-0.0432	4.08
Averaged Return	5.08×10^{-7}	5.61×10^{-8}	0.0316	3.02
Averaged Volatility	2.76×10^{-4}	1.08×10^{-10}	0.501	3.88
Data	1.11×10^{-4}	2.32×10^{-4}	-0.134	8.51

artificial time series of price return or volatility since the fluctuation of return itself has been largely eliminated. In addition, the statistics of real data is not well fitted by that of the artificial series. We can attribute it to the defect of GARCH models, especially the simple GARCH(1,1) used here. The deviation of the autocorrelations for the averaged series from that for real data (Figure 4.3) also indicates the incapability of GARCH models. But as we only concern about volatility clustering in order to qualitatively prove the maintainability of it in the average of time series, we can ignore the defects of GARCH in this section.

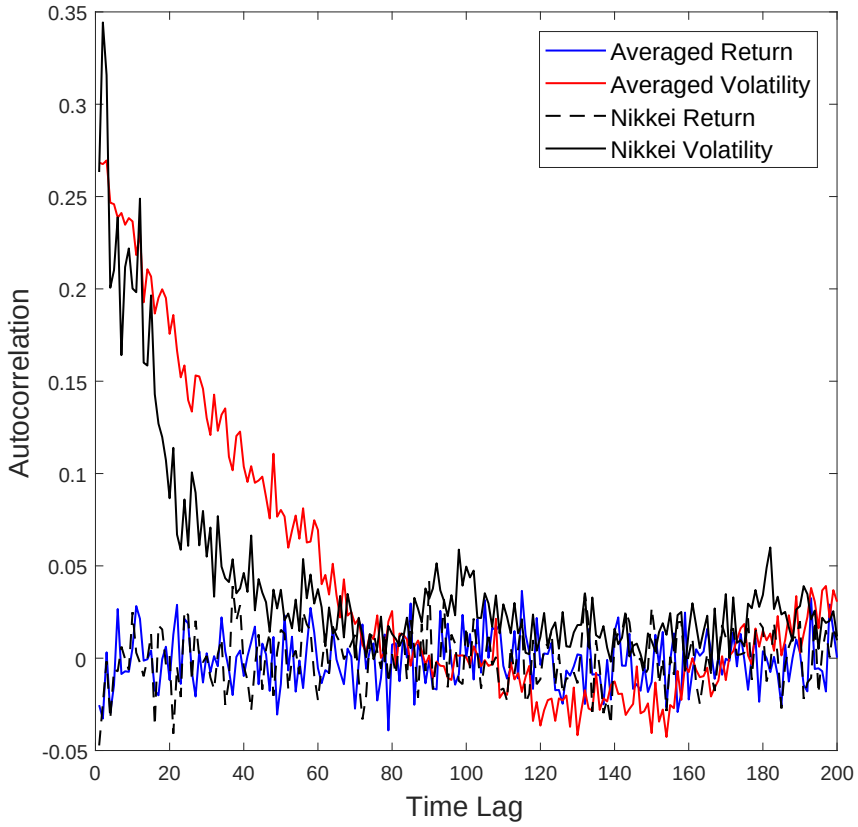

Figure 4.3: Autocorrelations of the price return and volatility for averaged GARCH simulations and real data.

4.1.2 Theoretical analysis

The conclusion that the characters of autocorrelations are maintained in the averaged GARCH series can also be proved theoretically. We use the formula of correlation function in statistical mechanics

$$C(t+\tau,t) = \langle X(t+\tau)X(t)\rangle - \langle X(t+\tau)\rangle\langle X(t)\rangle. \tag{4.8}$$

Firstly, it is not difficult to demonstrate that the autocorrelations of GARCH series are zero and the autocorrelations of the second order variables are positive.

Autocorrelation of ϵ_t (price return)

With the help of the relation that

$$\begin{cases} \langle \sigma_t \eta_{t+i}\rangle = \langle \sigma_t\rangle\langle \eta_{t+i}\rangle = 0, \quad i = 0,1,2,\ldots, \\ \langle \eta_t\rangle = 0, \end{cases} \tag{4.9}$$

we can obtain the autocorrelation of ϵ_t as

$$\begin{aligned} C_{\epsilon_t\epsilon_{t-n}} =& \langle \epsilon_t\epsilon_{t-n}\rangle - \langle \epsilon_t\rangle\langle \epsilon_{t-n}\rangle \\ =& \langle \sigma_t\sigma_{t-n}\eta_{t-n}\rangle\langle \eta_t\rangle - \langle \sigma_t\rangle\langle \eta_t\rangle\langle \sigma_{t-n}\rangle\langle \eta_{t-n}\rangle \\ =& 0. \end{aligned} \tag{4.10}$$

Autocorraltion of ϵ_t^2 (volatility)

Similarly, based on the relations

$$\langle \sigma_t^l \eta_{t+i}^k\rangle = \langle \sigma_t^l\rangle\langle \eta_{t+i}^k\rangle, \quad i = 0,1,2,\ldots, \quad l,k = 1,2,3,\ldots, \tag{4.11}$$

and

$$\langle \epsilon_t^2\rangle = \langle \sigma_t^2\eta_t^2\rangle = \langle \sigma_t^2\rangle\langle \eta_t^2\rangle = \langle \sigma_t^2\rangle, \tag{4.12}$$

together with Eq. (4.3), we obtain

$$\begin{aligned}
\langle \epsilon_t^2 \epsilon_{t-n}^2 \rangle =& \langle (\sigma_t \eta_t)^2 \cdot (\sigma_{t-n} \eta_{t-n})^2 \rangle = \langle \sigma_t^2 \sigma_{t-n}^2 \eta_{t-n}^2 \rangle \\
=& \langle (\omega + \alpha \epsilon_{t-1}^2 + \beta \sigma_{t-1}^2) \sigma_{t-n}^2 \eta_{t-n}^2 \rangle \\
=& \omega \langle \sigma_{t-n}^2 \rangle + (\alpha + \beta) \langle \sigma_{t-1}^2 \sigma_{t-n}^2 \eta_{t-n}^2 \rangle \\
=& \left[1 + (\alpha + \beta) \right] \omega \langle \sigma_{t-n}^2 \rangle + (\alpha + \beta)^2 \langle \sigma_{t-2}^2 \sigma_{t-n}^2 \eta_{t-n}^2 \rangle \\
=& \cdots \\
=& \sum_{i=0}^{n-2} (\alpha + \beta)^i \omega \langle \sigma_{t-n}^2 \rangle + (\alpha + \beta)^{n-1} \langle \epsilon_{t-(n-1)}^2 \epsilon_{t-n}^2 \rangle \\
=& \sum_{i=0}^{n-1} (\alpha + \beta)^i \omega \langle \sigma_{t-n}^2 \rangle + (\alpha + \beta)^{n-1} \left(3\alpha + \beta \right) \langle \sigma_{t-n}^4 \rangle,
\end{aligned} \tag{4.13}$$

with

$$\begin{aligned}
\langle \epsilon_t^2 \epsilon_{t-1}^2 \rangle =& \langle \sigma_t^2 \sigma_{t-1}^2 \eta_{t-1}^2 \rangle \\
=& \langle (\omega + \alpha \epsilon_{t-1}^2 + \beta \sigma_{t-1}^2) \sigma_{t-1}^2 \eta_{t-1}^2 \rangle \\
=& \omega \langle \sigma_{t-1}^2 \rangle + (3\alpha + \beta) \langle \sigma_{t-1}^4 \rangle.
\end{aligned} \tag{4.14}$$

At the same time,

$$\begin{aligned}
\langle \epsilon_t^2 \rangle \langle \epsilon_{t-n}^2 \rangle =& \langle \sigma_t^2 \rangle \langle \sigma_{t-n}^2 \rangle \\
=& \langle \omega + \alpha \epsilon_{t-1}^2 + \beta \sigma_{t-1}^2 \rangle \langle \sigma_{t-n}^2 \rangle \\
=& \omega \langle \sigma_{t-n}^2 \rangle + (\alpha + \beta) \langle \sigma_{t-1}^2 \rangle \langle \sigma_{t-n}^2 \rangle \\
=& \left[1 + (\alpha + \beta) \right] \omega \langle \sigma_{t-n}^2 \rangle + (\alpha + \beta)^2 \langle \sigma_{t-2}^2 \rangle \langle \sigma_{t-n}^2 \rangle \\
=& \cdots \\
=& \sum_{i=0}^{n-1} (\alpha + \beta)^i \omega \langle \sigma_{t-n}^2 \rangle + (\alpha + \beta)^n \langle \sigma_{t-n}^2 \rangle^2.
\end{aligned} \tag{4.15}$$

Then the autocorrelation of ϵ_t^2 can be easily to obtained as

$$\begin{aligned} C_{\epsilon_t^2\epsilon_{t-n}^2} =& \langle \epsilon_t^2 \epsilon_{t-n}^2 \rangle - \langle \epsilon_t^2 \rangle \langle \epsilon_{t-n}^2 \rangle \\ =& (\alpha+\beta)^{n-1} \left[(3\alpha+\beta)\langle \sigma_{t-n}^4 \rangle - (\alpha+\beta)\langle \sigma_{t-n}^2 \rangle^2 \right] \\ =& (\alpha+\beta)^{n-1} \left[(\alpha+\beta) \cdot Var(\sigma_{t-n}^2) + 2\alpha \langle \sigma_{t-n}^4 \rangle \right] \\ \propto& (\alpha+\beta)^n, \end{aligned} \tag{4.16}$$

where $Var(\sigma_{t-n}^2) = \langle \sigma_{t-n}^2 \sigma_{t-n}^2 \rangle - \langle \sigma_{t-n}^2 \rangle \langle \sigma_{t-n}^2 \rangle$ is the variance of $\{\sigma_{t-n}^2\}$.

Autocorrelation of $E\epsilon_t$ (expected price return)

We denote $E\epsilon_t$ the sequence calculated from averaging a great number of independent series ϵ_t with the same parameters. For any time t, $E\epsilon_t$ is the expected value of ϵ_t. If we have M (M is large enough) time series, the mth one is represented by $\epsilon_t^{(m)}$ with m the index numbered the time series. It is then known that the M numbers for the same time step are independent, thus

$$E\epsilon_t = \overline{\epsilon_t^{(m)}} = \overline{\sigma_t^{(m)} \eta_t^{(m)}} = \overline{\sigma_t^{(m)}} \cdot \overline{\eta_t^{(m)}} = 0, \tag{4.17}$$

where, $\overline{\quad\cdot\quad}$ means calculating the average according to index m. The sequence $E\epsilon_t$ is in fact constant 0. It is obvious that we have

$$C_{E\epsilon_t E\epsilon_{t-n}} = \langle E\epsilon_t \cdot E\epsilon_{t-n} \rangle - \langle E\epsilon_t \rangle \langle E\epsilon_{t-n} \rangle = 0. \tag{4.18}$$

Autocorrelation of $E\epsilon_t^2$ (expected volatility)

For time t, $E\epsilon_t^2$ denotes the average of $\epsilon_t^{2(m)}$ according to index m:

$$E\epsilon_t^2 = \overline{\epsilon_t^{2(m)}} = \overline{\sigma_t^{2(m)} \eta_t^{2(m)}} = \overline{\sigma_t^{2(m)}} \cdot \overline{\eta_t^{2(m)}} = \overline{\sigma_t^{2(m)}}. \tag{4.19}$$

After calculations

$$\begin{aligned}\langle E\epsilon_t^2 \cdot E\epsilon_{t-n}^2\rangle =&\langle\overline{\sigma_t^2}\cdot\overline{\sigma_{t-n}^2}\rangle\\ =&\omega\langle\overline{\sigma_{t-n}^2}\rangle+(\alpha+\beta)\langle\overline{\sigma_{t-1}^2}\cdot\overline{\sigma_{t-n}^2}\rangle\\ =&\left[1+(\alpha+\beta)\right]\omega\langle\overline{\sigma_{t-n}^2}\rangle+(\alpha+\beta)^2\langle\overline{\sigma_{t-2}^2}\cdot\overline{\sigma_{t-n}^2}\rangle\\ =&\cdots\\ =&\sum_{i=0}^{n-1}(\alpha+\beta)^i\omega\langle\overline{\sigma_{t-n}^2}\rangle+(\alpha+\beta)^n\langle(\overline{\sigma_{t-n}^2})^2\rangle,\end{aligned}\tag{4.20}$$

and

$$\begin{aligned}\langle E\epsilon_t^2\rangle\langle E\epsilon_{t-n}^2\rangle =&\langle\overline{\sigma_t^2}\rangle\langle\overline{\sigma_{t-n}^2}\rangle\\ =&\omega\langle\overline{\sigma_{t-n}^2}\rangle+(\alpha+\beta)\langle\overline{\sigma_{t-1}^2}\rangle\langle\overline{\sigma_{t-n}^2}\rangle\\ =&\left[1+(\alpha+\beta)\right]\omega\langle\overline{\sigma_{t-n}^2}\rangle+(\alpha+\beta)^2\langle\overline{\sigma_{t-2}^2}\rangle\langle\overline{\sigma_{t-n}^2}\rangle\\ =&\cdots\\ =&\sum_{i=0}^{n-1}(\alpha+\beta)^i\omega\langle\overline{\sigma_{t-n}^2}\rangle+(\alpha+\beta)^n\langle\overline{\sigma_{t-n}^2}\rangle^2,\end{aligned}\tag{4.21}$$

we have the autocorrelation of expected volatility

$$\begin{aligned}C_{E\epsilon_t^2 E\epsilon_{t-n}^2} =&\langle E\epsilon_t^2\cdot E\epsilon_{t-n}^2\rangle-\langle E\epsilon_t^2\rangle\langle E\epsilon_{t-n}^2\rangle\\ =&(\alpha+\beta)^n\left\{\langle(\overline{\sigma_{t-n}^2})^2\rangle-\langle\overline{\sigma_{t-n}^2}\rangle^2\right\}\\ =&(\alpha+\beta)^n\cdot Var(\overline{\sigma_{t-n}^2})\\ \propto&(\alpha+\beta)^n.\end{aligned}\tag{4.22}$$

The consistence of Eq. (4.22) with Eq. (4.16) indicates that the autocorrelations are maintained in the expected (or averaged) time series. Thus it is demonstrated that we can study volatility clustering in quantum description with "expected time series" of squared return (volatility).

4.2 Trading volume as a measurement of energy

As shown in the stationary modeling of the liquid markets in Chapter 3, although the quartic term in the potential results in probability distributions of price return with larger kurtosis, it is not the major attribution of the leptokurtic distributions of a long time series of price return. In another way, the difference between the wave functions of a harmonic oscillator and the corresponding anharmonic one (at the same energy level) can be neglected in the dynamical modeling. Thus, in order to simplify the computation, we apply the potential of harmonic oscillator to study the changes of probability distributions. As the PDFs for all the energy levels are symmetric along $x = 0$, it is obvious that no matter how the probability distribution changes, the expected return is constant zero. This indicates that there is no autocorrelation of the return. Then we focus on the time series of expected volatility in this chapter.

The changes of probability density function can be represented by the dynamics of energy, since there is a correspondence between the PDF and energy. Moreover, the PDF (or energy) is determined by two factors - the parameters of the potential and the energy level at which the stock price stays, which will be discussed separately.

Then what is the financial correspondence of energy in the stock market? Meng et al. suggested trading volume as a representation of energy for a single stock [*Meng et al.*, 2016]. Trading volume seems a prospective measurement of the "energy" for a stock. Before dynamical modeling of energy, we need to study the statistical characters of the trading volume and its relation to price return in advance.

We deal with the attainable data for Nikkei 225, which covers the daily close price and recorded trading volume from March 17, 2003 to June 22, 2017. The date is not always successive due to some missing of the corresponding trading volume. There includes data for 3474 days. Figure 4.4 plots the time series of price return and the corresponding trading volume. It is noted that trading volume is detrended for autocorrelation analysis with the help of normalized trading volume:

$$\begin{aligned}\hat{V}_{t,k} =& \frac{V_t - \mu_{V;t,k}}{\sigma_{V;t,k}},\\ \mu_{V;t,k} =& \frac{1}{k}\sum_{i=0}^{k-1} V_{t-i},\\ \sigma_{V;t,k} =& \sqrt{\frac{1}{k}\sum_{i=0}^{k-1}(V_{t-i} - \mu_{V;t,k})^2}.\end{aligned} \tag{4.23}$$

The detrended trading volume can then be expressed as

$$\widetilde{V}_{t,k} = \sigma_V \hat{V}_{t,k} + \mu_V, \tag{4.24}$$

where μ_V and σ_V are the mean and standard deviation of the full series of trading volume.

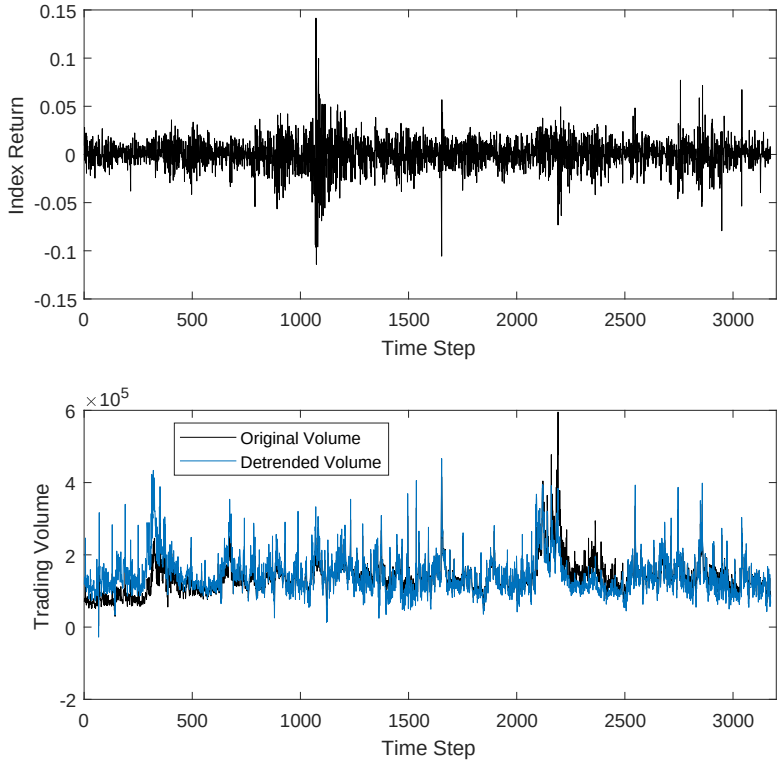

Figure 4.4: The time series of price return and trading volume. The trading volume has been detrended according to Eq. (4.23) and Eq. (4.24) with the detrending window $k = 300$.

Figure 4.5, the scatter figure of the normalized trading volume and price return, shows that the data points clustered in obvious different pattern around low volumes and high volumes. It is shown that for low volumes, the price return tends to fluctuate with small volatility, while more data points would emerge far from zero return for high volumes. Figure 4.6 gives the probability distributions of the price return for different volume ranges, which together with the corresponding statistics shown in Table 4.2 indicates that the probability distributions of price return for large volume tend to be more like multimodal ones. It is consistent with our discussion in Chapter 3, where the PDFs for excited states are multimodal and larger energy has more peaks.

Figure 4.5: Scatter plot of the normalized trading volume and corresponding index return.

Thus it is reasonable for us to assume a linear relation between trading volume of a stock and its energy in the quantum model. We can consider the trading volume as a measurement of energy.

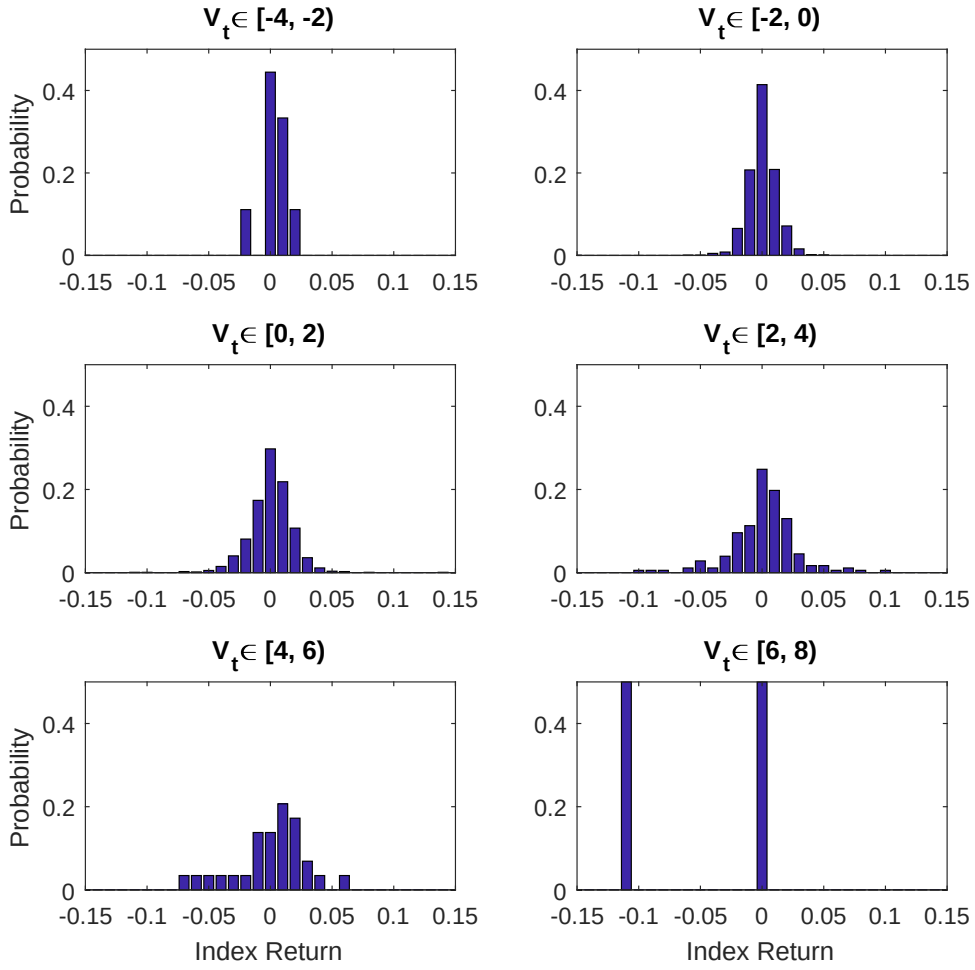

Figure 4.6: Probability distributions of price return for different normalized trading volume ranges.

Table 4.2: Statistics of the price returns for different normalized trading volume ranges as in Figure 4.6. The skewness and kurtosis are missing for $\hat{V}_t \in [6, 8)$ because the data sample is too few to be calculated.

$\hat{V}_t$	Mean	Std	Skewness	Kurtosis
$[-4, -2)$	0.00334	0.0103	-0.641	1.98
$[-2, 0)$	0.000146	0.0113	-0.109	4.64
$[0, 2)$	0.000516	0.0176	-0.117	9.65
$[2, 4)$	0.00106	0.0266	-0.251	5.86
$[4, 6)$	0.000128	0.0290	-0.775	3.25
$[6, 8)$	-0.0509	0.0772	-	-
Full Data	0.000307	0.0153	-0.278	10.9

4.3 Dynamics of energy level

We firstly assume the external potential form is kept, which means the dynamics of probability distribution is caused only by the changes of energy level.

4.3.1 Relation of trading volume and expected volatility

As shown in the last section, we use the dynamics of trading volume to represent the dynamics of energy, which provides a corresponding time series of expected volatility.

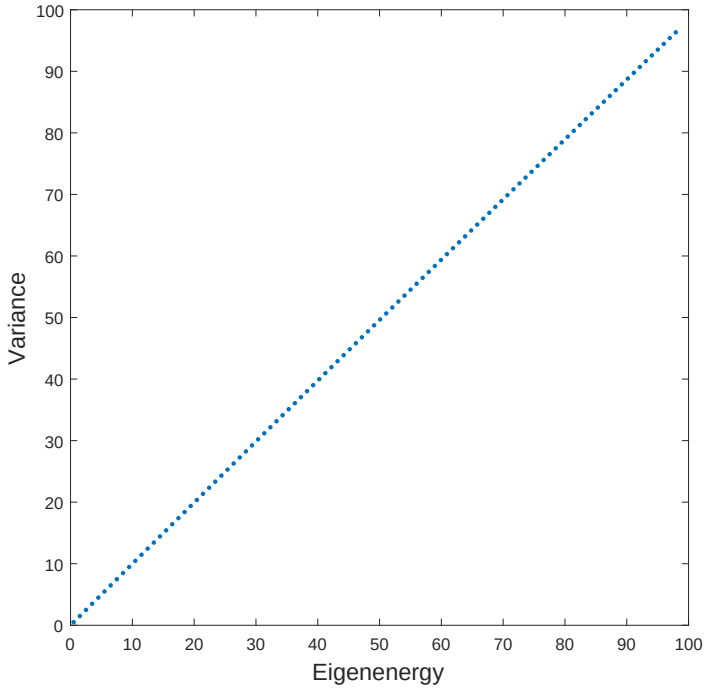

Figure 4.7: Linear relation between the eigen energies and corresponding variance. Harmonic oscillator with unit $\hbar$, m and $\omega_0 = 1$ has been applied.

According to the wave functions of harmonic oscillator, there is a linear relation between energy and variance, i.e. expected volatility, as shown in Figure 4.7. The relation is calculated from

$$\begin{aligned} E(r^2;t) &= \langle \psi_n(r;t)|r^2|\psi_n(r;t)\rangle; \\ E_n &= \frac{1}{2}\hbar\omega_0. \end{aligned} \tag{4.25}$$

In other words, the autocorrelation of the expected volatility would coincide with that of the trading volume. This means in the energy level modeling, the autocorrelation of volatility (squared return) is approximated by that of trading volume. It is partly reasonable because the positive correlation between conditional volatility and volume has been found [*Gallant et al.*, 1992].

4.4 2-Level modeling

As the trading volume is approximately continuous while the energy level or corresponding eigen energy is discrete, it is more reasonable not to use the volume directly for the modeling of energy level. Moreover, in the real market, the autocorrelation of volume and that of volatility is not the same, which is deviated from result of direct application of trading volume as energy level discussed in the last section. Then we assume that maybe classifying the volumes into several countable energy levels is more appropriate.

We can begin this kind of modeling from the simplest case, where only two different energy levels are considered. As an example, we use $\hat{V}_c = 2$ as the critical normalized volume to help divide the data into two groups. The price return with normalized volume less than $\hat{V}_c$ is at the lower level, while the price return with normalized volume more than $\hat{V}_c$ is at the higher level (refer to Figure 4.5).

Figure 4.8 shows the probability distributions of price return for Level 1 and Level 2 respectively. It can be seen from the figure that the PDF of Level 1 is more similar to the squared modulus of wave function of ground state, while the PDF of Level 2 is mixed with that of excited states (higher energy levels).

After labeling the energy level for each price return, we can obtain the corresponding time series of energy level as Figure 4.9 from the original data. We can see that some obvious clustering of energy level. Then it is not surprising to find that the autocorrelation of energy level is positive and decays slowly. It is shown in Figure 4.10 that the memory of the artificial energy level is shorter than the original volume and close to that of squared

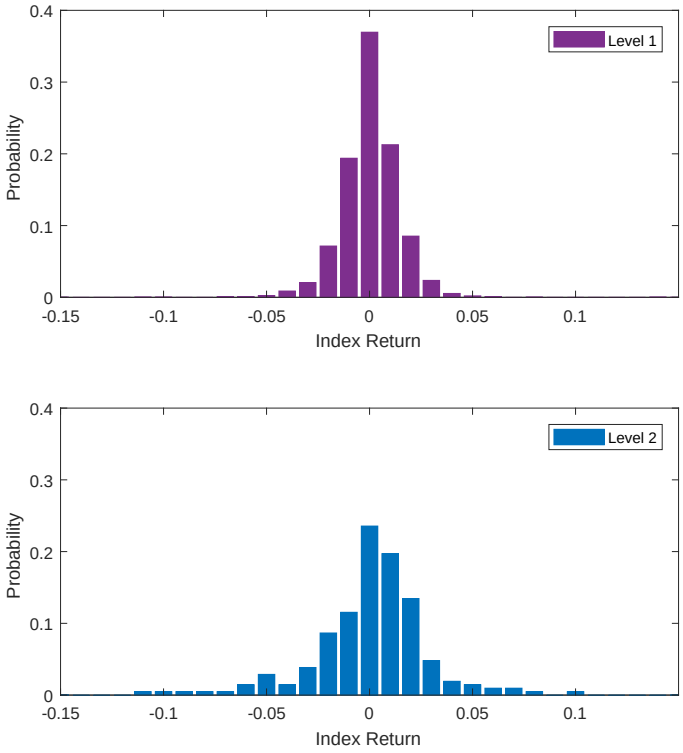

Figure 4.8: Probability distributions of daily Nikkei 225 return for the two different energy levels respectively, where $\hat{V}_c = 2$ has been assumed.

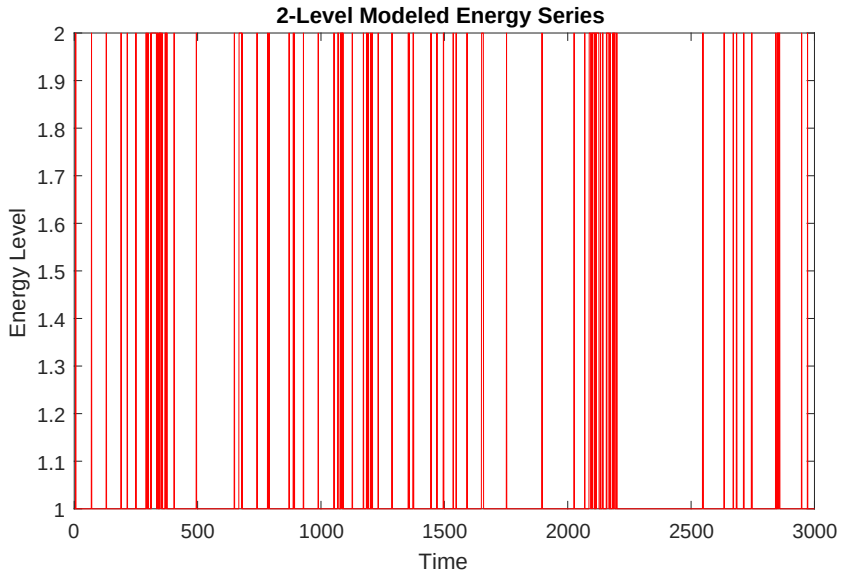

Figure 4.9: Time series of energy level obtained from trading volume history for Nikkei 225. $\hat{V}_c = 2$ has been used to label the level.

return. It indicates that it may exists only few energy levels with different shapes of PDF in the real market. The deviation of the autocorrelation of trading volume from the volatility may be attributed to the neglect of potential change, which will be discussed in the next section about dynamics of potential.

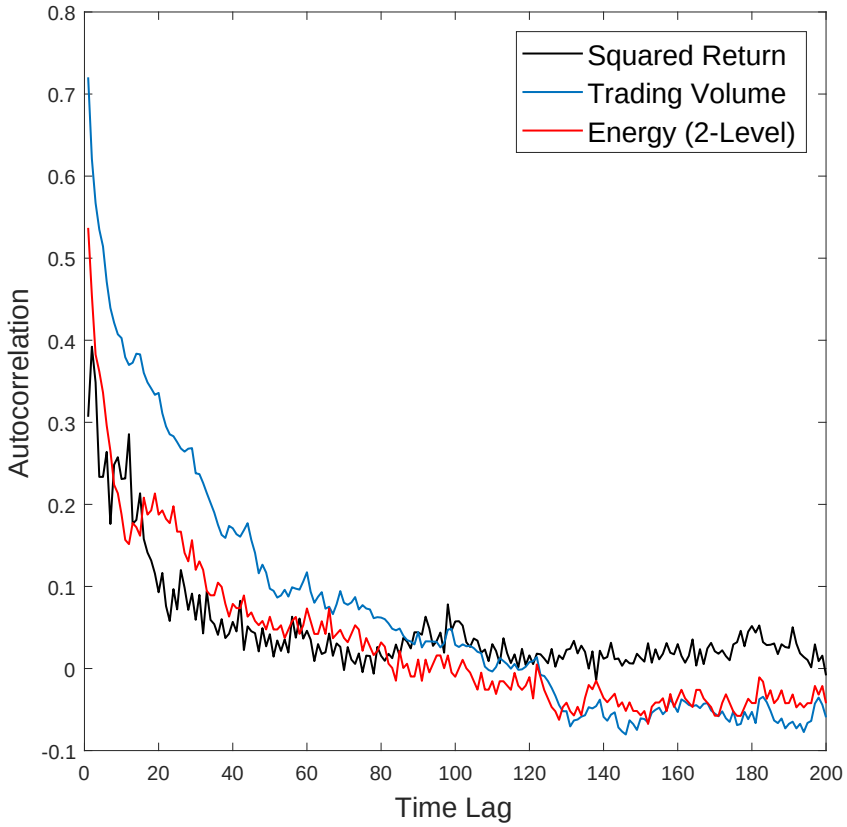

Figure 4.10: Autocorrelations of squared return, trading volume and the energy level series obtained from the trading volume.

In a summary, the dynamical modeling of energy level demonstrates that there exist excited energy levels with multimodal PDFs in the stock market. And these high energy levels are scarcely observed. The positively linear relation of the energy (level) and corresponding variance explains the positive correlation between volume and conditional volatility [*Gallant et al.*, 1992]. The deviation of the autocorrelation of volume from volatility indicates that other dynamics such as the dynamics of potential should be considered. In addition, the recovery of volatility clustering can be realized by modeling

the dynamics of energy level.

4.5 Dynamics of potential

According to dynamical modeling of energy level in the last section, it is necessary for us to discuss the contribution of the changing potential to the autocorrelation of volatility. It is convenient for us to consider only ground states of harmonic oscillators, based on the reasons that 1) it has been proved in the previous chapters that the stock markets stay at the ground states most of the time, and 2) excited states are rare as stated in the last section.

For a harmonic oscillator with potential

$$V(r) = \frac{1}{2}\omega_0^2 r^2, \tag{4.26}$$

the PDF for ground state is

$$p(\omega_0, r) = |\psi_0(\omega_0, r)|^2 = \sqrt{\frac{\omega_0}{\pi}} \exp\left(-\omega_0 r^2\right), \tag{4.27}$$

with eigen energy

$$E_0 = \frac{1}{2}\omega_0, \tag{4.28}$$

where $m = 1$ and $\hbar = 1$ have been assumed, and ω_0^2 corresponds to $\gamma + c$ in the model potential Eq. (2.33). It is found that Eq. (4.27) is a normal distribution $\mathcal{N}(\mu, \sigma^2)$ with

$$\mu = 0, \qquad \sigma^2 = 1/2\omega_0. \tag{4.29}$$

4.5.1 GARCH-like modeling

Eq. (4.29) indicates that the dynamics of potential is mathematically the same thing with the dynamics of conditional volatility, one of the best known model is GARCH.

Thus GARCH can be considered a special case of our model. And similar models, which can be named GARCH-like models can be proposed. One of the possible difference is that the dependence on squared return is not necessary to be predefined. Moreover, as the quantum models deal with expectation rather than random variables, we cannot and need not to give simulated time series of price.

4.5.2 Trading volume modeling

It is known that estimation of GARCH models concerns only stock price, while another quantity, trading volume we proposed in this quantum model is rarely considered. Then here we will give a quantum modeling of the dynamics of potential with trading volume.

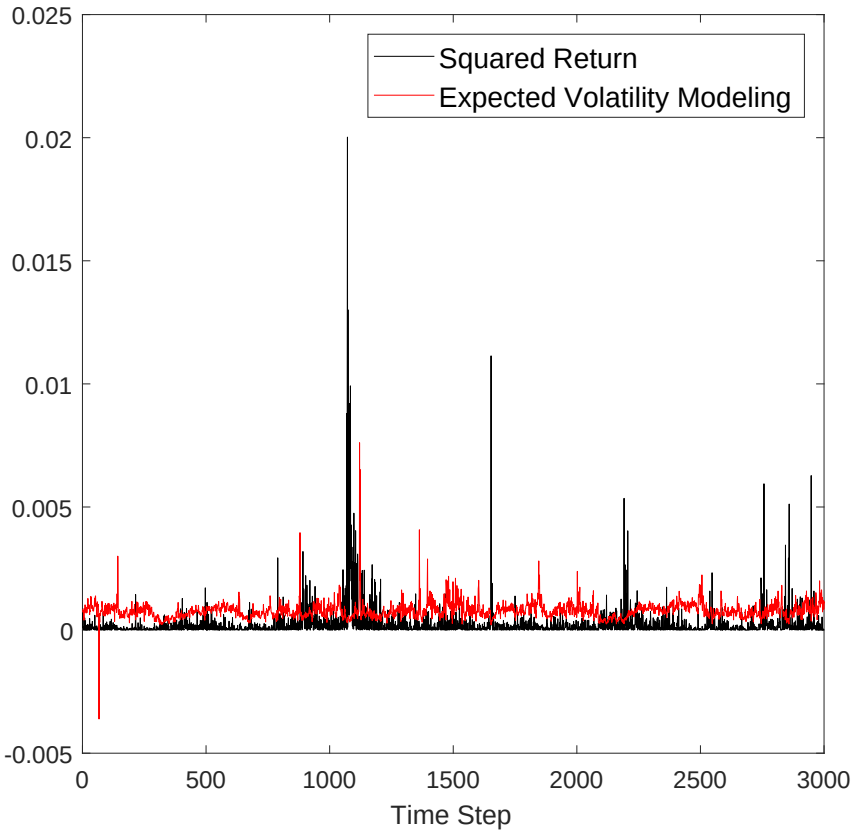

Figure 4.11: Time series of expected volatility compared with the squared return of real data. The data sample is from Nikkei 225 illustrated at the beginning of this chapter. In order to make the expected volatility shares the same order with data, we have applied $\sigma^2 = 100/E_0$.

Making use of Eq. (4.28) and Eq. (4.29), we can analytically obtain the relation of ground state energy and variance:

$$\sigma^2 \quad \sim \quad \frac{1}{E_0}. \tag{4.30}$$

From this relation and the time series of trading volume from the real market, we can model the time series of expected volatility as Figure 4.11. The modeled time series agrees with the theoretical results that the expected volatility would fluctuate around a positive value. A deficiency of the modeled time series is that there may exist singularity with negative value, which should not emerge. The expected volatility of the 67th time step in the figure is the only one in our modeling. It is caused by the detrending process of the volume. However, this kind of singularity would not affect the autocorrelation.

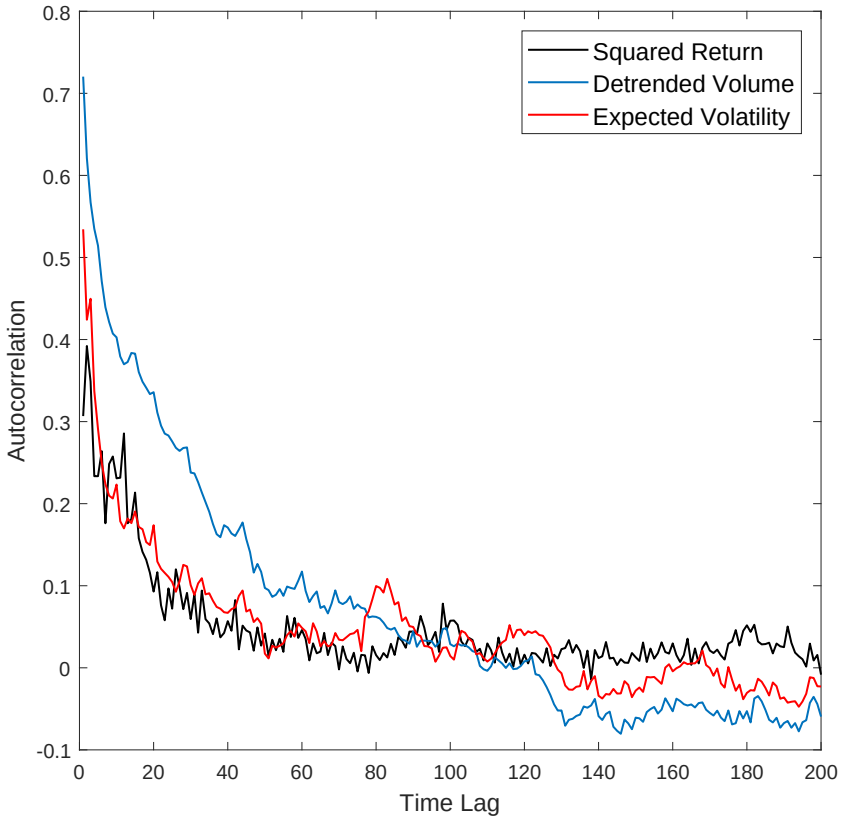

Figure 4.12: Autocorrelations of squared return and the expected volatility modeled by trading volume. The autocorrelation of volume itself is also displayed.

Then the calculated autocorrelation of expected volatility is plotted in Figure 4.12. It is shown that the autocorrelation of squared return can also be perfectly fitted in the model involving changes of potential. In other words, for a certain energy level, the dynamics of potential maybe the cause of volatility clustering in price return. The data of trading volume can help us to recover the autocorrelation of squared return (volatility) in our quantum model.

It is noted that a quantitative relation between trading volume and expected volatility is firstly proposed as Eq. (4.30). It indicates that the autocorrelation of expected volatility is no longer the same with that of volume. Instead, the reciprocal relation indicates to a negative correlation of volume and volatility, which is contradict with the stylized fact - positive volume/volatility correlation. This can be explained by the work done by Meng et al. [*Meng et al.*, 2015].

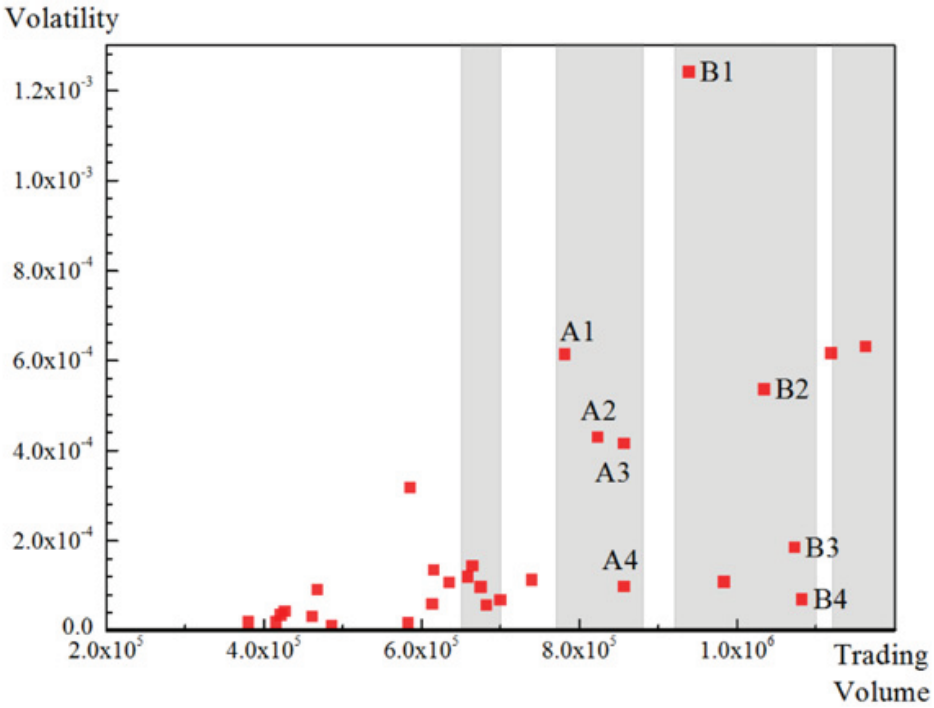

Figure 4.13: Volatility as a function of trading volume E. Data are extracted from the daily lines of Ping An Bank Co., Ltd (No. 000001) in Shenzhen Stock Exchange from Jan. 14 to Feb. 28, 2013. [*Meng et al.*, 2015]

Figure 4.13 is the volatility/volume correlation they obtained from real single stock. In their study, they found that although there is a positive correlation of volatility and

energy band (energy level), the volatility and energy is negatively correlated in the band (level). It is just consistent with our modeling if we combine the dynamics of energy level and that of potential together.

4.6 Summary

In this chapter, we extended the stationary quantum model in Chapter 2 and 3 to a dynamical one. As quantum models give up the random variables used in stochastic modeling, we study the autocorrelation of expected volatility and return series.

We successfully recovered the autocorrelation of return volatility, i.e. volatility clustering, by taking trading volume into account, which has rarely done in previous works. The dynamics of volatility have been attributed to that of potential itself and energy level. The existence of energy levels agrees with the data analysis in the stationary modeling in Chapter 3. The modeling of energy level results in positive volume/volatility correlation based on the assumption of discrete energy and multimodal distributions, while the modeling of potential results in negative volume/volatility correlation based on continuous energy and unimodal distributions. It is believed that a combination of these two modeling method would be more reasonable. In addition, quantitative relations of volume (energy level) and expected volatility are proposed, which contributes to robustness of stylized fact - positive correlation between volatility and volume.

Chapter 5

Conclusions and Future Works

5.1 Conclusions

This dissertation is a presentation of the author's Ph.D studies on the quantum approaches to the modeling of stock markets. Although there have been numerous works on the financial markets, quantum application to finance brings novel ideas into the fundamental mechanics in markets. As the financial markets are driven by human whose behaviors are unpredictable, the classical models that based on the determinate theories are in fact not the best choice for the study of finance. Quantum finance is a young field but has achieved significant results by applying different theories from quantum mechanics. With the assumption that the dynamics of stock price is not like a motion of a classical particle but more similar to a quantum "particle", we use wave function instead of actual number to describe the fluctuation of stock price.

A appropriate Hamiltonian, consisting of the intrinsic kinetic operator and a external potential operator, is then the key for this kind of models. Some previous works applied the potential of fundamental quantum physical systems, such as the square well [*Ataullah et al.*, 2009] and the harmonic oscillator [*Ye and Huang*, 2008; *Zhang and Huang*, 2010; *Cotfas*, 2013; *Meng et al.*, 2015], directly for the modeling of stock price. However, the lack of financial interpretation of the potential results in the disability of looking into the

microscopic structure of markets. In order to overcome this shortcoming, we proposed a financially interpretable potential for the stock price based on the dynamics of excess order in the market. We derived a oscillator potential, including a quartic term that measures the risk averse behavior of the market participants, as well as a quadratic term which describes an elastic force towards zero return. It is demonstrated that the probability distributions of the price return for Nikkei 225, SSE Composite Index and S&P 500 can be well modeled. The introduction of the risk aversion term can somehow help reproduce the leptokurtic of the distribution. The main reason of the sharp peak and heavy tails can be attributed to the existence of excited states of the stock price, whose PDFs are of multimodal distributions. It is one of the most important contributions since there had been no such kind of discussion before. The differences of the modeling results for Nikkei 225, SSE Composite Index and S&P 500 are reflected by the parameters in the Hamiltonian. The utilization of wave functions ensure the possibility to describe probability without noise term which had been indispensable for classical modeling. The quantum description shed some light on the nature of stock price. It means that the stock price may be essentially indeterminate, since the microscopic structure and dynamics of the market are controlled by the behavior of human who behave (make decisions) probabilistically.

One more achievement of the stationary modeling is that our quantum model can be applied not only to the efficient markets (liquid markets), but also to other extreme markets (illiquid markets) such as contrarian dominant markets and trend following dominant markets. In order to verify the theoretical results of TFDM, we proposed a data filtering method based on Granville's rules to obtain object data. It is found that the probability distributions of price return collapse in the center, and instead two peaks emerge at the both sides of zero return symmetrically. It indicates the tendency to have crashes or bubbles, caused by the trend following behavior of the traders. In addition, the study of the data filtering method help us understand some universal behaving patterns of the traders. For example, traders in SSE Composite Index pay more attentions to the short

term MAs than those in Nikkei 225 and S&P 500.

In the modeling of volatility clustering, the quantum model was extended to a dynamic version. The positive autocorrelation of squared return is considered as a quantitative representation of volatility clustering. As quantum models provide PDFs instead of random variables, expected time series of price return and volatility were introduced for the autocorrelation study. Based on previous studies and data analysis of Nikkei 225, we proposed trading volume as a measurement of energy. Then the dynamics of volume can be modeled by energy level or potential respectively. The positive and slow decaying autocorrelation of volatility can be recovered by each type of the dynamical modeling. One of the conclusions of stationary modeling that the excited energy levels exist but rarely emerge is confirmed. Moreover, quantitative relations of volume and volatility were derived for different modeling methods - positive volume/volatility correlation for energy level modeling and negative volume/volatility correlation for potential modeling.

Our quantum modeling exhibits many characters and advantages. Compared to the classical models, 1) The fluctuation of stock price is naturally existed in our model, which can be explained without noise simulation; 2) The PDFs can be modeled without producing time series; 3) Energy level as a new concept for the stock markets are applied. Compared to previous quantum models, 1) Oscillator potentials are financially derived; 2) A anharmonic term of the potential has been discussed; 3) The existence of high energy levels (multimodal distributions) has been discussed; 4) The dynamics of energy (wave function) including energy level and potential is studied to recover volatility clustering; 5) Volume/energy correspondence and volume/volatility are discussed.

5.2 Future works

Based on the results and conclusions of the quantum models we proposed, a large number of studies can be taken into progress of my future research. According to the main two parts of this thesis, the future works can be proceeded by:

- Optimizing the dynamical models by combining the energy level modeling and potential modeling together.
- Proposing a quantitative method to predict probability distributions of price return by combining the stationary and dynamical modeling results.
- Further studying volume/volatility correlation and other stylized facts such as leverage effect with quantum models
- Trying quantum version of agent-based models.

Appendix A

Numerical Solutions for Schrodinger Equation

It is known that Schrodinger equation (SE), which is essentially a linear partial differential equation and also a diffusion equation, fully describes the state of a quantum system. However, the partial differential equation can only be analytically solved for several systems with simple Hamiltonians, such as free particle and harmonic oscillator. Fortunately, nowadays we can theoretically obtain the solutions of much more equations with the help of computer and numerical algorithm.

In order to model the dynamics of stock price, we have to deal with SEs for different Hamiltonians. Thus we take use of Finite Difference Method (FDM) to numerically solve the SE. Further more, the numerical solutions is convenient for further analysis and comparison of real data. FDM is based on taylor series,

$$\begin{aligned} f(x-h) &= f(x) - hf'(x) + \frac{h^2}{2}f''(x) + \mathcal{O}(h^3); \\ f(x+h) &= f(x) + hf'(x) + \frac{h^2}{2}f''(x) + \mathcal{O}(h^3), \end{aligned} \tag{A.1}$$

where $f(x)$ is a real or complex-valued function and h is a real or complex number. If h is small enough, the first order derivative and second order derivative of function $f(x)$

can be approximated as

$$f'(x) = \frac{1}{2h}[f(x+h) - f(x-h)] + \mathcal{O}(h^2), \tag{A.2}$$

and

$$f''(x) = \frac{1}{h^2}[f(x-h) - 2f(x) + f(x+h)] + \mathcal{O}(h^2), \tag{A.3}$$

which is called centered difference.

A.1 Eigen equation of energy

In the stationary modeling, we need the wave functions of stock price with a time-independent potential. The time-independent SE, i.e. eigen equation of energy

$$\left[-\frac{\hbar^2}{2m}\frac{d^2}{dx^2} + V(x)\right]\psi(x) = E\psi(x) \tag{A.4}$$

is satisfied by any point $x_i (i = 1, 2, 3, ..., N)$, where x is divided into N continuous small parts during the possible range. We use ψ_i and V_i to represent $\psi(x_i)$ and $V(x_i)$ in the following text.

Taking use of Eq. (A.3), the second order derivative can be approximated as

$$\psi_i'' = \frac{1}{\Delta x^2}(\psi_{i-1} - 2\psi_i + \psi_{i+1}), \tag{A.5}$$

where Δx is the step size with the value of $\Delta x = x_{i+1} - x_i = x_i - x_{i-1}$. Eq. (A.4) for x_i can then be written in a numerical form as

$$-\frac{\hbar^2}{2m}\frac{1}{\Delta x^2}(\psi_{i-1} + \psi_{i+1}) + \left[\frac{\hbar^2}{2m}\frac{2}{\Delta x^2} + V_i\right]\psi_i = E\psi_i. \tag{A.6}$$

Denoting the vector form of the wave function as $\Psi = \begin{pmatrix} \psi_1 & \psi_2 & \cdots & \psi_N \end{pmatrix}^T$, the numerical form Eq. (A.6) for all the positions $x_i (i = 1, 2, 3, ..., N)$ can then be transformed

into matrix representation

$$H\Psi = E\Psi, \tag{A.7}$$

with

$$\begin{aligned} H &= K + V \\ &= \frac{\hbar^2}{2m}\frac{1}{\Delta x^2}\begin{pmatrix} 2 & -1 & 0 & \cdots & 0 \\ -1 & 2 & -1 & \ddots & \vdots \\ 0 & -1 & 2 & \ddots & 0 \\ \vdots & \ddots & \ddots & \ddots & -1 \\ 0 & \cdots & 0 & -1 & 2 \end{pmatrix} + \begin{pmatrix} V_1 & 0 & \cdots & \cdots & 0 \\ 0 & V_2 & \ddots & \ddots & \vdots \\ \vdots & \ddots & \ddots & \ddots & \vdots \\ \vdots & \ddots & \ddots & \ddots & 0 \\ 0 & \cdots & \cdots & 0 & V_N \end{pmatrix} \end{aligned} \tag{A.8}$$

i.e. $\{H_{i,i} = \frac{\hbar^2}{m}\frac{1}{\Delta x^2} + V_{i,i}$, $H_{i,i\pm1} = -\frac{\hbar^2}{2m}\frac{1}{\Delta x^2}$, $H_{i,j} = 0$ for other elements$\}$. The eigenvectors Ψ_n of the matrix equation are the wave functions corresponding to different energy levels E_n.

The Matlab code is written as follows, where the constants can be adjusted when necessary.

```
%% This piece of code is written to solve the time-independent Schrodinger equation with
    finite difference method.
close all
clc
clear all

%% Assign constants and parameters
% The variable step_size is the distance between each position.
% The variable number_of_data_points gives the total number of data points in the system.
% The system spans from x = -step_size*(number_of_data_points-1)/2 to x = step_size*(
    number_of_data_points-1)/2.
step_size = 0.005;
number_of_data_points = 2001;
```

```
x_positions = linspace(-step_size*(number_of_data_points-1)/2,step_size*(
    number_of_data_points-1)/2,number_of_data_points);

% The variable hbar and the mass of the electron are set to one by default (Hartree Units).
% You can change them to their SI values, but you will have to adjust step_size accordingly.
% gamma, k and c are the parameters measure the potential of the
% Hamiltonian, which can be set as different values for different markets.
hbar = 1;
mass = 1;
gamma=1;
k=0.01;
c=0.2;  % the values of gamma, k and c can be changed accroding to your model setting.

%% Calculate Hamiltonian Matrix
% This section uses the finite difference method to calculate the Hamiltonian matrix.

% Kinetic energy matrix
kinetic = zeros(number_of_data_points);
for i = 1:number_of_data_points
    kinetic(i,i) = 2;
    if i > 1
        kinetic(i, i-1) = -1;
        kinetic(i-1, i) = -1;
    end
end
kinetic_multiplier = hbar^2/(2*mass*step_size^2);
kinetic = kinetic * kinetic_multiplier ;

% Potential energy matrix
potential = zeros(number_of_data_points);
```

```
for  i  = 1:number_of_data_points
        potential(i,i) = gamma*(0.5*(1+c)*x_positions(i)^2-0.25*k*c*x_positions(i)^4);
end

% Hamiltonian matrix
hamiltonian = kinetic + potential;

%% Calculate the eigenvectors and the corresponding probability distribution functions
[eigenvectors, eigenvalues] = eig(hamiltonian); % the eigensystems of the Hamiltonian
    matrix

% The ground state
ground_state= eigenvectors(:,1).*eigenvectors(:,1);
ground_state_probability=ground_state/sum(ground_state*step_size); % normalization of
    probability desity to ensure the total probability be 1

% The first four excited energy state. Of course you can obtain any state by similar lines.
first_state = eigenvectors(:,2).*eigenvectors(:,2); % +eigenvalues(2,2)*ones(
    number_of_data_points,1)
first_state_probability = first_state/sum(first_state*step_size);

second_state = eigenvectors(:,3).*eigenvectors(:,3) ;
second_state_probability=second_state/sum(second_state*step_size);

third_state = eigenvectors(:,4).*eigenvectors(:,4);
third_state_probability =third_state/sum(third_state*step_size);

forth_state = eigenvectors(:,5).*eigenvectors(:,5);
forth_state_probability =forth_state/sum(forth_state*step_size);

```

```
68 fifth_state  = eigenvectors(:,6).*eigenvectors(:,6);
69 fifth_state_probability = fifth_state /sum(fifth_state*step_size);
70
71 %% Plot the probability distribution functions
72 % The probability distributions are plot around the corresponding energy
73 % levels for clear comparision. Theoretically you can have
74 % "number_of_data_points" eigenvectors, but you only interested in the
75 % first several ones. The PDF of the ground state which is Gaussian-like is
76 % the most important one.
77 figure;
78 plot(x_positions, ground_state_probability + +eigenvalues(1,1)*ones(
       number_of_data_points,1), 'b', 'LineWidth', 2);
79 hold on;
80 plot(x_positions, first_state_probability + eigenvalues(2,2)*ones(number_of_data_points
       ,1), 'g', 'LineWidth', 2);
81 hold on;
82 plot(x_positions, second_state_probability + eigenvalues(3,3)*ones(number_of_data_points
       ,1), 'r', 'LineWidth', 2);
83 hold on;
84 plot(x_positions, third_state_probability + eigenvalues(4,4)*ones(number_of_data_points
       ,1), 'c', 'LineWidth', 2);
85 hold on;
86 plot(x_positions, forth_state_probability + eigenvalues(5,5)*ones(number_of_data_points
       ,1), 'm', 'LineWidth', 2);
87 hold on;
88 plot(x_positions, fifth_state_probability + eigenvalues(6,6)*ones(number_of_data_points
       ,1), 'k', 'LineWidth', 2);
89 hold on;
90 plot(x_positions, diag(potential), '--k');
91 ylim ([0,10]);
```

```
92 legend('Ground State', 'First Excited State', 'Second Excited State', 'Third Excited State',
       'Forth Excited State', 'Fifth Excited State', 'Potential');
93 xlabel('Position');
94 ylabel('Probability distributions around different energy levels');
```

A.2 Dynamics of wave function

```
1  % Model quantum harmonic oscillator with periodic perturbation
2  % (Crank-Nicolson)
3  close all
4  clc
5  clear all
6
7  % Initialize the numerical paramters
8  Nx = 1001; % number of grid points
9  delta_x=0.01;  % grid size
10 x=-delta_x*(Nx-1)/2:delta_x:delta_x*(Nx-1)/2;
11 x=x';
12 j0=(Nx+1)/2; % the number order of the space center
13 delta_t=0.0001; % time step
14 Nt=100; % number of ticks
15 t=1:Nt;
16
17
18 % Initialize the physical parameters
19 hbar=1;
20 omega=1;
21 m=1;
22 alpha=sqrt(m*omega/hbar);
```

```
23
24 % Set the initial wave function
25 psi0=sqrt(alpha)/(pi^(0.25))*exp(-1/2*(alpha^2)*x.^2);
26
27 % The Hamiltonian operator matrix
28 H = zeros(Nx);
29 coeff = -hbar^2/(2*m*delta_x^2);
30 v0=m*omega^2*x.^2;
31 for j=2:(Nx-1)
32     H(j,j-1) = coeff;
33     H(j,j) = -2*coeff+v0(j);
34     H(j,j+1) = coeff;
35 end
36 % First and last rows for periodic boundary conditions
37 H(1,Nx) = coeff; H(1,1) = -2*coeff+v0(1); H(1,2) = coeff;
38 H(Nx,Nx-1) = coeff; H(Nx,Nx) = -2*coeff+v0(Nx); H(Nx,1) = coeff;
39
40 %% Compute the system with (periodic) perturbation
41 V=x.^2; % form of the perturbation
42 tic
43 CN = ( inv(eye(Nx) + 0.5i*delta_t/hbar*H) * (eye(Nx) - 0.5i*delta_t/hbar*H) );
44 equi = input('Enter number of time steps for the system to be stable:');
45 for n=2:equi
46     psi0= exp(-1i*V/hbar).*(CN*psi0);
47     p0=conj(psi0).*psi0;
48     plot(x,p0);
49     drawnow;
50 end
51 psi(:,1) =psi0;
52 psi2(:,1) =psi(:,1) .*conj(psi(:,1));
```

```
53 p(1)=sum(conj(psi(:,1)).*psi(:,1))*delta_x;
54 p(1)=p(1)*conj(p(1));
55 px(1)=sum(conj(psi(:,1)).*x.^4.*psi(:,1))*delta_x;
56 px(1)=px(1)*conj(px(1));
57 px2(1)=sum(conj(psi(:,1)).*x.^2.*psi(:,1))*delta_x;
58 px2(1)=px2(1)*conj(px2(1));
59
60 tick=input('Enter the time steps for one tick:');
61 for n=2:Nt
62     psi_temp=psi(:,n-1);
63     for count=1:tick
64         psi_temp=exp(-1i*V/hbar).*(CN*psi_temp);
65     end
66     psi(:,n)=psi_temp;
67     psi2(:,n)=psi(:,n).*conj(psi(:,n));
68     p(n)=sum(conj(psi(:,1)).*psi(:,n))*delta_x;
69     p(n)=p(n)*conj(p(n));
70     px(n)=sum(conj(psi(:,1)).*x.^4.*psi(:,n))*delta_x;
71     px(n)=px(n)*conj(px(n));
72     px2(n)=sum(conj(psi(:,1)).*x.^2.*psi(:,n))*delta_x;
73     px2(n)=px2(n)*conj(px2(n));
74     if rem(n,10)==0
75         toc
76     end
77 end
78
79 %%
80 % Check the unitary
81 A=delta_x*sum(psi2);
82
```

```
figure(2);
subplot(211);
for n=1:Nt
%       if rem(n,100)==0
            plot(x,psi2(:,n));
            hold on;
%       end
end
% subplot(212);
% plot(x,psi2(:,1),x,psi2(:,tau-1),x,psi2(:,tau+1),x,psi2(:,Nt));

for n=1:Nt
    C(n)=sum(p(1:n))/n;
    Cx(n)=sum(px(1:n))/n;
    Cx2(n)=sum(px2(1:n))/n;
end
figure(3);
subplot(221);
plot(t,p);
xlabel('t'); ylabel('|<psi(t)|psi(0)>|^2');
subplot(223);
loglog(t,C);
xlabel('t'); ylabel('C(t)');
 title ('Correlation function of time');
subplot(222);
loglog(t,Cx/Cx(1));
xlabel('t'); ylabel('Cx(t)');
 title ('Correlation function for x');
subplot(224);
loglog(t,Cx2/Cx2(1));
```

```
113 xlabel('t'); ylabel('Cx2(t)');
114  title ('Correlation␣function␣for␣x^2');
115
116 figure(4);
117 subplot(311);
118 plot(t,p);
119 xlabel('t'); ylabel('|<psi(t)|psi(0)>|^2');
120 subplot(312);
121 plot(t,px);
122 xlabel('t'); ylabel('px(t)');
123 subplot(313);
124 plot(t,px2);
125 xlabel('t'); ylabel('px2(t)');
126
127 % check the kurtosis of  final  PDF
128 final_mean=sum(psi2(:,Nt).*x*delta_x);
129 final_var=sum(psi2(:,Nt).*(x-final_mean).^2*delta_x);
130 final_std=sqrt(final_var);
131 final_quar=sum(psi2(:,Nt).*(x-final_mean).^4*delta_x);
132 final_kur=final_quar/(final_var)^2;
133
134 %
135 % figure(4);
136 % plot(x,V);
```

Appendix B

Probability Distribution for Classical Oscillators

B.1 Harmonic oscillators

We consider a classical harmonic oscillator moving under a force which depends on the oscillator's position x and a constant k

$$F(x) = -kx \tag{B.1}$$

$$V(x) = \frac{1}{2}kx^2 \tag{B.2}$$

where $x = 0$ is the equilibrium position at which the force is 0 and $k > 0$. Taking use of Newton's second law, the dynamical equation of the system is

$$\ddot{x} + \frac{k}{m}x = 0 \tag{B.3}$$

where m is the mass of the oscillator. The solution for the differential equation Eq. (B.3) can be easily obtained as

$$x(t) = A\cos(\omega t + \phi) \tag{B.4}$$

where $\omega = \sqrt{k/m}$ and A, ϕ are constants. Eq. (B.4) tells us that the motion is periodic with period $T = 2\pi/\omega$, amplitude A and initial phase ϕ.

We put the oscillator in a black box. Then every time when we want to observe the oscillator and check the position of its mass, we must open the box. If we observe the oscillator enough times with the same time interval and count the numbers it is observed for each position interval dx, a probability density distribution can be achieved. Denote the probability density at position x as $p(x)$, then it is reasonable to consider

$$P(x - \frac{\varepsilon}{2} \sim x + \frac{\varepsilon}{2}) = \int_{x-\frac{\varepsilon}{2}}^{x+\frac{\varepsilon}{2}} p(x)dx = 2 \cdot \frac{\varepsilon/v(x)}{T} \tag{B.5}$$

where ε is infinitesimal, $v(x)$ is the absolute velocity of the mass at position x. The relationship of absolute velocity and position can be calculated from Eq. (B.4) as

$$\begin{aligned} v(t) = \frac{dx(t)}{dt} &= A\omega \sin(\omega t + \phi) \\ v^2 + (\omega x)^2 &= A^2 \\ v &= \sqrt{A^2 - \omega^2 x^2} \end{aligned}$$

then

$$p(x) = \frac{2}{vT} = \frac{1}{\pi\sqrt{(A/\omega)^2 - x^2}} \tag{B.6}$$

We can also solve Eq. (B.3) numerically using finite difference schemes

$$\begin{cases} \dot{x}_{n+1} = v_{n+1} = \frac{x_{n+1} - x_n}{\Delta t} \\ \ddot{x}_n = \dot{v}_n = \frac{v_{n+1} - v_n}{\Delta t} \end{cases} \tag{B.7}$$

then Eq. (B.3) can be written into numerical form as

$$\frac{v_{n+1} - v_n}{\Delta t} + \omega^2 x_n = 0$$

which gives the recursive equation for the value of positions x_n with the same time step

Δt:

$$\begin{cases} v_{n+1} = v_n - \omega^2 \Delta t x_n \\ x_{n+1} = x_n + v_{n+1} \Delta t \end{cases} \tag{B.8}$$

In the numerical calculation, in addition to the intrinsic parameter ω, the motion also depends on the initial condition with known position x_1 and velocity v_1. Then taking use of Eq. (B.8), we can easily calculate the corresponding position and velocity (x_n and v_n) at any time with n time steps.

B.2 Anharmonic oscillators

In stead of the potential $V(x) = \frac{1}{2}kx^2$ in harmonic oscillator, here we begin to study anharmonic oscillators with potential

$$V(x) = \frac{k_1}{2}x^2 + \frac{k_2}{4}x^4 \tag{B.9}$$

where $k_1 > 0$. The corresponding Newton's equation is

$$\ddot{x} + \frac{k_1}{m}x + \frac{k_2}{m}x^3 = 0 \tag{B.10}$$

with m as the mass of the anharmonic oscillator.

We solve Eq.(B.10) numerically by using:

$$\begin{cases} \dot{x}_{n+1} = v_{n+1} = \frac{x_{n+1} - x_n}{\Delta t} \\ \ddot{x}_n = \dot{v}_n = \frac{v_{n+1} - v_n}{\Delta t} \end{cases} \Rightarrow \begin{cases} v_{n+1} = v_n - (\frac{k_1}{m}x_n + \frac{k_2}{m}x_n^3)\Delta t \\ x_{n+1} = x_n + v_{n+1}\Delta t \end{cases} \tag{B.11}$$

Eq. (B.11) shares similar form with Eq. (B.8) except for the second term in the velocity recursion because of the different potential force.

We firstly consider the potentials with positive square term, i.e. $k_1 > 0$. Figure B.1 shows the potentials and position functions for three potentials with the same $k_1 = 1$, but

different k_2.

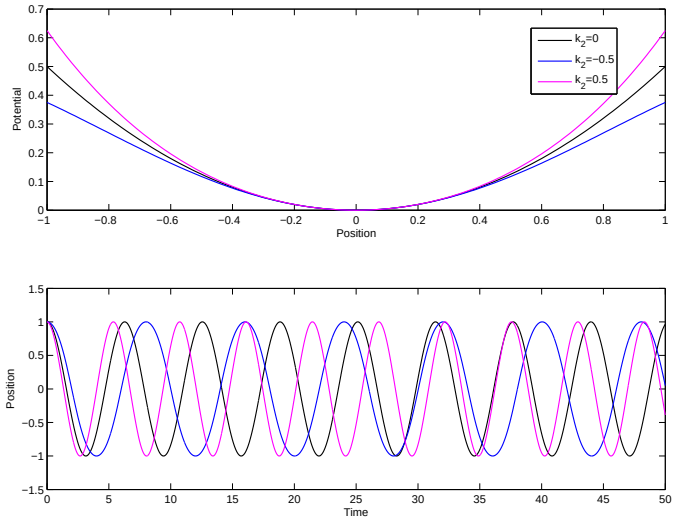

Figure B.1: Position Functions for Potentials with Positive Square Term

In fact when $k_2 < 0$ and the absolute value of k_2 is large enough, the potential would inverse at the two sides of the horizontal axis. However, in order to use this analysis in our market model, where $|k_2|$ should not to be too large, so we constrain the energy of the oscillator to keep it stay inside of the potential well. In our calculation, we set the initial position of the oscillator is $x_1 = 1$ while the initial velocity is $v_1 = 0$. We can see from Figure B.1 that a appropriate quartic term in addition to a positive square term potential only affect the motion os the oscillator quantitively. Given a suitable initial energy to the oscillator, its motion will always be periodic.

Figure B.2 gives the classical probability density for the above potentials according to the probability density defined by Eq. (B.6).

What about if $k_1 < 0$? Figure B.3 demonstrate three potentials with respectively no quartic term, positive one and negative one. Similarly to the positive square discussion, the absolute value of k_1 is set equal to 1, i.e. $k_1 = -1$. The black, blue and magenta line in Figure B.3 represent the potential with $k_2 = 0$, $k_2 = -0.5$, $k_2 = 0.5$ respectively. It is obvious that a "oscillator" with negative square potential would run along either side of the axis until it meets a wall (a excluded situation is staying still at $x = 0$). And

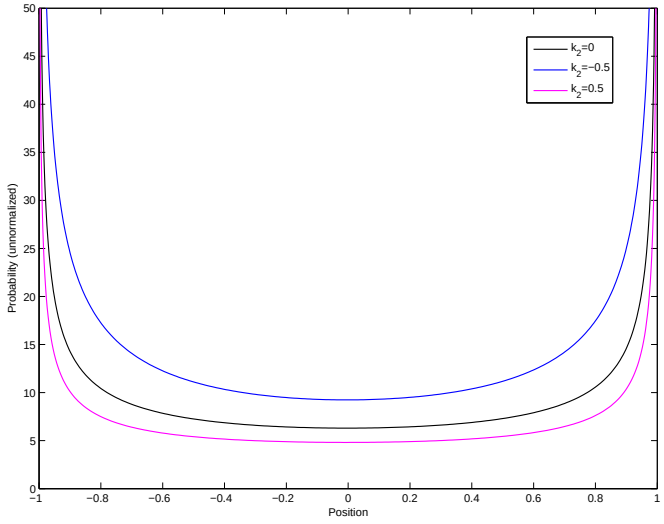

Figure B.2: Classical Probability Distributions for Potentials with $k_1 > 0$

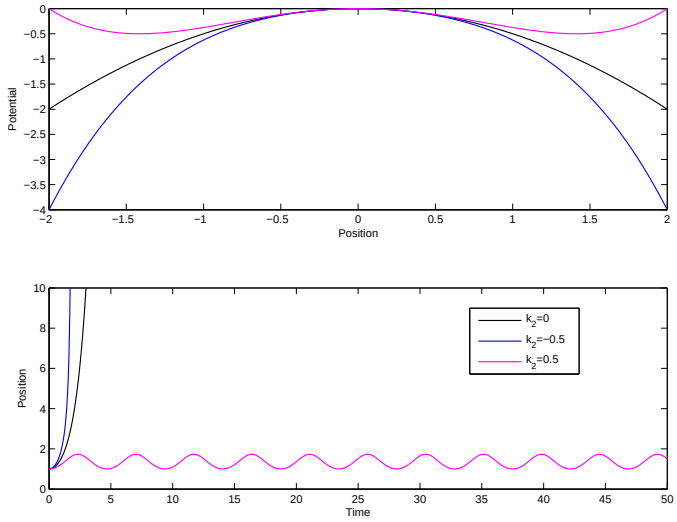

Figure B.3: Position Functions for Potentials with Negative Square Term

a negative k_2 would just accelerate the progress. A wall is needed for the probability analysis, which is not included in our study.

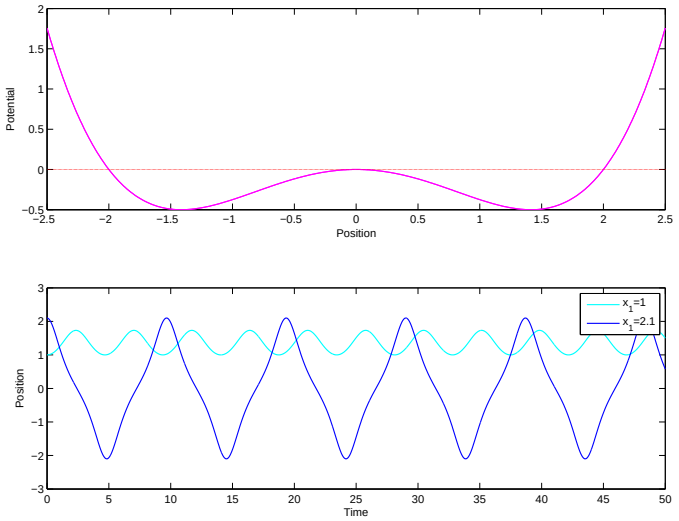

Figure B.4: Position Functions for Potentials with $k_1 < 0$ and $k_2 > 0$

However, when $k_2 > 0$ (the magenta line), the position function becomes periodic again. Given the form of potential, the motion will be determined by the initial condition. Figure B.4 shows two results with different initial conditions, where the potential is the same as the magenta line in Figure B.3. The initial velocity is the same 0, but the initial position for the cyan is $x_1 = 0$ while the blue one is $x_1 = 2.1$.

We can see from the potential figure that the oscillating mode can be classified into two kinds, where the specific conditions ($x_1 = 0$ and $x_1 = \pm 2$ is out of our consideration when the "oscillator" would stay still at the equilibrium position $x = 0$). The oscillating mode is similar to $x_1 = 1$ (cyan) for $x_1 \in (-2, 0) \cup (-2, 0)$ while like $x_1 = 2.1$ (blue) for $(x_1 < -2) \cup (x_1 > 2)$. The "probability density" for these two modes is showed in Figure B.5.

It can be seen from Figure B.5 that the first mode (cyan) is in fact the similar with that of positive k_1 because both of them are describing a particle in a parabolic or a parabolic-like well. For the second mode, the "oscillator" moves through a potential barrier from one well to another. So there exists a small hill in the middle of the "probability"

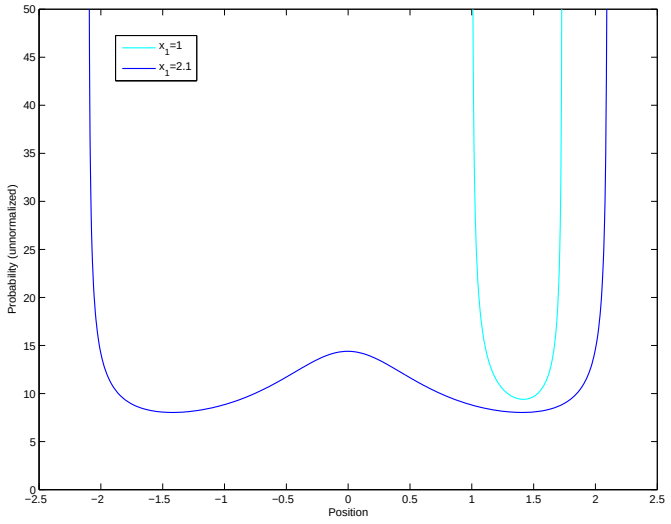

Figure B.5: Classical Probability Distributions for Potentials with $k_1 < 0$

density distribution.

References

Ataullah, A., I. Davidson, and M. Tippett (2009), A wave function for stock market returns, *Physica A*, *388*, 455–461, doi:10.1016/j.physa.2008.10.035.

Baaquie, B. E. (2004), *Quantum Finance*, Cambridge University Press, Cambridge.

Bachelier, L. (1964), *The random character of stock market prices*, MIT Press, Cambridge.

Bouchaud, J.-P., and R. Cont (1998), A langevin approach to stock market fluctuations and crashes, *The European Physical Journal B*, *6*, 543–550.

Buchanan, M. (2013), What has econophysics ever done for us?, *Nature Physics*, *9*, 317.

Caccioli, F., and M. Marsili (2010), Information efficiency and financial stability, *Economics: The Open-Access, Open-Assessment E-Journal*, *4*(2010-20), 1–20, doi: 10.5018/economics-ejournal.ja.2010-20.

Cassagnes, A., Y. Chen, and H. Ohashi (2014), Path integral pricing of outside barrier asian options, *Physica A*, *394*, 266–276, doi:10.1016/j.physa.2013.09.067.

Challet, D., and M. Marsili (1999), Phase transition and symmetry breaking in the minority game, *Physical Review E*, *60*(6), 6271–6274.

Challet, D., and M. Marsili (2003), Criticality and market efficiency in a simple realistic model of the stock market, *Physical Review E*, *68*, 036,132.

Challet, D., and Y.-C. Zhang (1997), Emergence of cooperation and organization in an evolutionary game, *Physica A*, *246*, 407–418, doi:10.1016/S0378-4371(97)00419-6.

Challet, D., and Y.-C. Zhang (1998), On the minority game: Analytical and numerical studies, *Physica A*, *256*, 514–532, doi:10.1016/S0378-4371(98)00260-X.

Challet, D., M. Marsili, and Y.-C. Zhang (2001), Minority games and stylized facts, *Physica A*, *299*, 228–233, doi:10.1016/S0378-4371(01)00300-4.

Challet, D., M. Marsili, and Y.-C. Zhang (2005), *Minority Games: interacting agents in financial markets*, Oxford University Press, Oxford.

Cont, R. (2001), Empirical properties of asset returns: stylized facts and statistical issues, *Quantitative Finance*, *1*, 223–236, doi:10.1080/713665670.

Cont, R. (2007), *Long Memory in Economics*, 289-309 pp., Springer, Berlin.

Cotfas, L.-A. (2013), A finite-dimensional quantum model for the stock market, *Physica A*, *392*, 371–380, doi:10.1016/j.physa.2012.09.010.

Daly, J., M. Crane, and H. Ruskin (2008), Random matrix theory filters in portfolio optimisation - a stability and risk assessment, *Physica A*, *387*, 4248–4260, doi:10.1016/j.physa.2008.02.045.

Farmer, J. D., M. Shubik, and E. Smith (2005), Is economics the next physical science?, *Physics Today*, *58*(9), 37–42, doi:10.1063/1.2117821.

Francq, C., and J.-M. Zakoian (2010), *GARCH Models*, John Wiley & Sons Ltd, Chichester, United Kingdom.

Gallant, A. R., P. E. Rossi, and G. Tauchen (1992), Stock prices and volume, *The Review of Financial Studies*, *5*, 199–242, doi:10.1093/rfs/5.2.199.

Gopikrishnan, P., V. Plerou, L. A. N. Amaral, M. Meyer, and H. E. Stanley (1999), Scaling of the distribution of fluctuations of financial market indices, *Quantitative Finance*, *60*(5), 5305–5316.

Granville, J. E. (1960), *A Strategy of Daily Stock Market Timing for Maximum Profit*, Prentice-Hall.

Haven, E., and A. Khrennikov (2013), *Quantum Social Science*, Cambridge University Press, Cambridge.

Huang, J. (2015), Experimental econophysics: Complexity, self-organization, and emergent properties, *Physics Reports*, *564*, 1–55, doi:10.1016/j.physrep.2014.11.005.

Johnson, N. F., P. Jefferies, and P. M. Hui (2003), *Financial Market Complexity*, Oxford University Press, New York.

Khrennikov, A. (2010), *Ubiquitous Quantum Structure: From Phychology to Finance*, Springer, Berlin.

LeVeque, R. J. (2007), *Finite Difference Methods for Ordinary and Partial Differential Equations: Steady-State and Time-Dependent Problems*, SIAM, Philadelphia.

Lillo, F., and R. N. Mantegna (2003), Power-law relaxation in a complex system: Omori law after a financial market crash, *Physical Review E*, *68*, 016,119, doi: 10.1103/PhysRevE.68.016119.

Linetsky, V. (1998), The path integral approach to financial modeling and options pricing, *Computational Economics*, *11*, 129–163.

Liu, Y., P. Gopikrishnan, P. Cizeau, M. Meyer, C.-K. Peng, and H. E. Stanley (1999), Statistical properties of the volatility of price fluctuations, *Physical Review E*, *60*(2), 1390–1400.

Mandelbrot, B. B. (1963), The variation of certain speculative prices, *The Journal of Business*, *36*(4), 394–419.

Mantegna, R. N. (2005), Presentation of the english translation of ettore majorana's paper: The value of statistical laws in physics and social sciences, *Quantitative Finance*, *5*(2), 133–140, doi:10.1080/14697680500148174.

Mantegna, R. N., and H. E. Stanley (1995), Scaling behavior in the dynamics of an economic index, *Nature*, *376*(6), 46–49.

Mantegna, R. N., and H. E. Stanley (1999), *An Introduction to Econophysics: Correlations and Complexity in Finance*, Cambridge University Press, Cambridge.

Meng, X., J.-W. Zhang, J. Xu, and H. Guo (2015), Quantum spatial-periodic harmonic model for daily price-limited stock markets, *Physica A*, *438*, 154–160, doi:10.1016/j.physa.2015.06.041.

Meng, X., J.-W. Zhang, and H. Guo (2016), Quantum brownian motion model for the stock market, *Physica A*, *452*, 281–288, doi:10.1016/j.physa.2016.02.026.

Mizuno, T., H. Takayasu, and M. Takayasu (2007), Analysis of price diffusion in financial markets using puck model, *Physica A*, *382*, 187–192, doi:10.1016/j.physa.2007.02.049.

Ohnishi, T., T. Mizuno, K. Aihara, M. Takayasu, and H. Takayasu (2004), Statistical properties of moving average price in dollar-yen exchange rates, *Physica A*, *344*, 207–210, doi:10.1016/j.physa.2004.06.118.

Plerou, V., P. Gopikrishnan, L. A. N. Amaral, M. Meyer, and H. E. Stanley (1999), Scaling of the distribution of price fluctuations of individual companies, *Physical Review E*, *60*(6), 6519–6529.

Preis, T., J. J. Schneider, and H. E. Stanley (2011), Switching processes in financial markets, *PNAS*, *108*(19), 7674-7678.

Press, W. H., J. A. Teukolsky, W. T. Vetterling, and B. P. Flannery (2007), *Numerical Recipes: The Art of Scientific Computing*, Cambridge University Press, Cambridge.

Scalas, E. (2006), The application of continuous-time random walks in finance and economics, *Physica A*, *362*, 225–239, doi:10.1016/j.physa.2005.11.024.

Schaden, M. (2002), Quantum finance, *Physica A*, *316*, 511–538.

Sharifi, S., M. Crane, A. Shamaie, and H. Ruskin (2004), Random matrix theory for portfolio optimization: a stability approach, *Physica A*, *335*, 629–643, doi:10.1016/j.physa.2003.12.016.

Takayasu, M., T. Mizuno, and H. Takayasu (2006), Potential force observed in market dynamics, *Physica A*, *370*, 91–97, doi:10.1016/j.physa.2006.04.041.

Takayasu, M., T. Mizuno, and H. Takayasu (2007), Theoretical analysis of potential forces in markets, *Physica A*, *383*, 115–119, doi:10.1016/j.physa.2007.04.094.

Thurner, S., J. D. Farmer, and J. Geanakoplos (2010), Leverage causes fat tails and clustered volatility, *Quantitative Finance*, *12*(5), 695–707, doi:10.1080/14697688.2012.674301.

Ye, C., and J. Huang (2008), Non-classical oscillator model for persistent fluctuations in stock markets, *Physica A*, *387*, 1255–1263, doi:10.1016/j.physa.2007.10.050.

Zhang, C., and L. Huang (2010), A quantum model for the stock market, *Physica A*, *389*, 5769–5775, doi:10.1016/j.physa.2010.09.008.

Zhang, J., Y. Zhang, and H. Kleinert (2007), Power tails of index distributions in chinese stock market, *Physica A*, *377*, 166–172, doi:10.1016/j.physa.2006.11.012.